Australian Government
Department of Defence
Defence Science and
Technology Organisation

# Evaluation of Alternative Life Assessment Approaches Using P-3 SLAP Test Results

*David Mongru, Phil Jackson, Kai Maxfield and Chris Wallbrink*

**Air Vehicles Division**
**Defence Science and Technology Organisation**

DSTO-TR-2418

**ABSTRACT**

The effect of selecting different airworthiness standards and lifing methodologies on in-service structural life assessments is examined by using the full scale test results from the P-3 Service Life Assessment Program (P-3 SLAP). The effect on structural inspection thresholds and intervals is determined by applying the methods advanced by major international military and civilian airworthiness standards. Different life prediction models are also compared against the P-3 SLAP results and against results from DSTO coupon tests.

*Published by*

*Air Vehicles Division*
*DSTO Defence Science and Technology Organisation*
*506 Lorimer St*
*Fishermans Bend, Victoria 3207 Australia*

*Telephone: (03) 9626 7000*
*Fax: (03) 9626 7999*


*AR-014-780*
*June 2010*

**APPROVED FOR PUBLIC RELEASE**

# Evaluation of Alternative Life Assessment Approaches Using P-3 SLAP Test Results

## Executive Summary


The P-3 Service Life Assessment Program (P-3 SLAP) was an international program conducted between 1999 and 2004. Led by the United States Navy (USN), the program consisted of a series of full scale fatigue tests and analyses of the P-3 aircraft in order to determine the remaining structural life of the aircraft. Three other countries participated; Australia, Canada and The Netherlands. DSTO conducted the majority of the Australian technical activities including flight test loads measurement, wing teardown and an empennage full scale fatigue test. As well as these activities DSTO also conducted an interpretation of all the full scale test conducted under the SLAP and produced a Structural Management Plan consisting of the necessary inspections and component life limits for implementation by the RAAF.

The DSTO test interpretation process was developed to meet the requirements of FAR 25.571, the airworthiness standard selected for the in-service structural management of the RAAF P-3 fleet. The life assessment tools selected by DSTO were common to the other SLAP partners but the processes used to develop inspection intervals, life limits and Individual Aircraft Tracking algorithms were unique to DSTO, in part due to the airworthiness standard selected.

During the conduct of the DSTO empennage test an opportunity was taken, by applying an augmented loads sequence, to push the test as far as possible and gather failure data that would not otherwise be possible. At the same time it was known that this test loads augmentation would allow the test results to be used in a “Safe S-N” analysis as advocated by the UK MoD Def Stan 00-970, providing an opportunity for assessing an alternative approach to the airworthiness clearance of the empennage.

This report takes the idea of using the P-3 SLAP test results to evaluate alternative airworthiness standards further by also examining USN and USAF methodologies. The aim of this report is to make comparisons of the outcomes derived from the different approaches and comment on any differences and similarities. The comparisons, presented in terms of structural inspection thresholds and intervals for selected critical areas are of interest for both their differences and their similarities. The comparisons can help the RAAF Airworthiness Authority select the most appropriate methodologies for future life assessment tasks.

In the final sections of the report results from the life assessments tools used by DSTO in the SLAP test interpretation work are compared to results obtained from alternative models and to the results from a contemporary coupon test program.

# Authors

**David Mongru**
Air Vehicles Division

*Mr Mongru graduated from RMIT in 1990 with a Bachelor of Aerospace Engineering (Honours). He commenced work at DSTO in 1994 working on loads development and fatigue interpretation for the PC9 fatigue test. He joined the IFOSTP in 1996 performing fatigue analysis of critical components on the aft fuselage of the F/A-18. In 2001 he commenced work on the P-3 SLAP. His primary functions included fatigue test interpretation and provision of technical support to the P-3 empennage test. He is currently working in the airworthiness standards and fatigue mechanisms group.*

---

**Phil Jackson**
Air Vehicles Division

*Philip Jackson graduated from the Royal Melbourne Institute of Technology in 1981 with a Bachelor of Aeronautical Engineering (with Distinction). He spent the next 15 years as an engineering officer with the Royal Australian Air Force in both squadron and staff engineering posts specialising in aircraft structural integrity and fatigue management. In 1988 he completed a Masters of Science in Aerospace Vehicle Design at Cranfield Institute of Technology, UK and from 1991-94 was attached to the Canadian National Research Council, Ottawa, Canada as part of the F/A-18 International Follow-On Structural Test Project. He joined DSTO in 1997 and has been the technical and program lead for the DSTO contributions to the international P-3 Service Life Assessment Program (SLAP). He is currently Head, Helicopter and Transport Aircraft Structural Integrity in the Aircraft Structures Branch of Air Vehicles Division as well as leading the divisional research effort on airworthiness and aircraft design standards.*

---

**Kai Maxfield**
Air Vehicles Division

*Mr Maxfield graduated from RMIT in 2004 with a Bachelor of Aerospace Engineering (Honours). In August 2005 he commenced work with AeroStructures Technologies at DSTO. During this time he had been providing engineering support to the Air Vehicles Division of DSTO, primarily on the RAAF P-3 SLAP. In January 2007, Mr Maxfield joined the Air Vehicles Division, working on Airworthiness Standards and the P-3 SLAP. Since this time, he has also worked as test engineer for the F/A-18 FINAL testing. Mr Maxfield is currently the Australian Technical Representative for the RAF/RAAF C-130J-30 Full Scale Fatigue Test Programme at Marshall Aerospace, UK.*

---

**Chris Wallbrink**
Air Vehicles Division

*Chris Wallbrink graduated in 2005 with a PhD from Monash University in the department of Mechanical Engineering. He then held the position of research fellow at Monash University until the end of 2006 where his research interests included, modelling of fatigue crack growth, infrared NDT technologies and fibre optic corrosion detection devices. He joined DSTO in 2007 in the Air Vehicles Division and is currently conducting research into methods of fatigue crack growth modelling and airworthiness standards.*

---

# Contents

# Abbreviations

| | |
|---|---|
| **AC** | Advisory Circular |
| $\mathbf{a_{crit}}$ | Critical Crack Length |
| **AEB** | Age Exploration Bulletin |
| $\mathbf{a_{init}/a_i}$ | Initial Crack Length |
| $\mathbf{a_{NDI}}$ | Detectable Crack Length by Non Destructive Inspection |
| **AFGS** | Air Force Guide Specification |
| **AFH/AFHRS** | Airframe Hours |
| **BL** | Butt Line |
| **BuNo** | Bureau Number |
| **CA** | Constant Amplitude |
| **CAR** | Civil Air Regulations |
| **CG** | Crack Growth |
| **CGR** | Crack Growth Rates |
| **CI** | Crack Initiation |
| **Config** | Configuration |
| **DBI/SST** | Data-Base Interface/Spectra Sequencing Tool |
| **DCPD** | Direct Current Potential Drop |
| **Def Stan** | Defence Standard |
| **Dia.** | Diameter |
| **DLL** | Design Limit Load |
| **DoD** | Department of Defence |
| **DNH** | Dome Nut Hole |
| **DSTO** | Defence Science and Technology Organisation |
| **DTA** | Damage Tolerance Analysis |
| **EBA** | Effective Block Approach |
| **FAMS** | Fatigue Analysis of Metallic Structures |
| **FAR** | Federal Aviation Regulation |
| **FCA** | Fatigue Critical Area |
| **FEM** | Finite Element Method |
| **FMS** | Foreign Military Sales |
| **Freq** | Frequency |
| **FSFT** | Full-Scale Fatigue Test |
| **FS** | Fuselage Station |
| **HSS** | Horizontal Stabiliser Station |
| **IAT** | Individual Aircraft Tracking |
| **IAW** | In Accordance With |
| **Id** | Identity |
| **in** | Inches |
| **Init** | Initial |

| | |
|---|---|
| **JSSG** | Joint Service Specification Guide |
| **$K_N$** | Neuber Notch Factor |
| **$K_{N-TD}$** | Test Demonstrated Notch Factor |
| **ksi** | 1000 pounds per square inch |
| **$K_t$** | Stress Concentration Factor |
| **LH** | Left Hand |
| **LLTJ** | Low-Load Transfer Joint |
| **L-M** | Lockheed-Martin |
| **Max** | Maximum |
| **Mil-Spec** | Military Specification |
| **MPa** | Mega-pascal |
| **NLR** | National Aerospace Laboratory |
| **No.** | Number |
| **QF** | Quantitative Fractography |
| **RAAF** | Royal Australian Air Force |
| **RH** | Right Hand |
| **SFH/SFHRS** | Simulated Flight Hours |
| **SLAP** | Service Life Assessment Program |
| **SLR** | Stress-to-Load Ratio |
| **SMP** | Structural Management Plan |
| **S-N** | Stress-Life |
| **SRP** | Sustained Readiness Program |
| **TI** | Test Interpretation |
| **TL** | Total Life |
| **UK** | United Kingdom |
| **USA** | United States of America |
| **USAF** | United States Air Force |
| **USN** | United States Navy |
| **V-Stab** | Vertical Stabiliser |
| **WS** | Wing Station |

# 1. Introduction

The Royal Australian Air Force (RAAF) has operated the Lockheed-Martin (L-M) designed P-3 Orion maritime patrol aircraft for many years and in the 1990s, at the time of the formulation of the avionics update program for the aircraft that became Project AIR 5276, concern was expressed about the structural safe life limit then applied to the aircraft and the potential for life extension. In 1999 the Australian Department of Defence along with their counterparts in Canada and the Netherlands joined with the United States Navy (USN) to conduct the P-3 Service Life Assessment Program or P-3 SLAP. The program consisted of a number of full scale fatigue tests (FSFT) and accompanying analyses that would provide an updated fatigue assessment of the aircraft. The P-3 SLAP included full scale tests of the wing, fuselage and empennage at L-M in Marietta, Georgia, USA, a test of the main undercarriage at Vought, USA, and a full scale test of the empennage conducted at the Defence Science and Technology Organisation, (DSTO) in Melbourne, Australia. The two empennage tests resulted from the desire to test both a retired in-service article in its as-manufactured state as well as a recently-refurbished and modified structure. Test Interpretation (TI) was undertaken separately by the individual SLAP partners. The RAAF tasked DSTO to lead the Australian involvement in the P-3 SLAP and to undertake interpretation of the results of all the full scale tests in the program.

## 1.1 DSTO Test Interpretation

The P-3 aircraft was an evolution of the Lockheed Electra which had been designed and certified against Civil Air Regulations (CAR) 4b (the predecessor of Federal Aviation Regulation [FAR] 25). The structure was designed to a fail-safe philosophy, with some components such as the landing gear designed to safe life. As part of the P-3 SLAP, the RAAF elected to update the CAR 4b requirements for in-service management of the RAAF P-3 fleet with FAR 25.571 Amendment 25-95 which specified the conduct of a damage tolerance assessment.

DSTO conducted the test interpretation in accordance with the FAR 25.571 requirements and the guidance material from the accompanying Advisory Circular AC 25.571-1C. The TI methodology and results are given in [1]. The TI calculations were then used to develop in-service structural management instructions for the RAAF P-3 fleet consisting of inspection instructions and component life limits. The TI predictions were augmented by a probabilistic analysis of USN fleet data that had just become available as a result of inspections triggered by FSFT failures. The resulting structural management instructions were combined into a document called the Structural Management Plan (SMP) [3].

## 1.2 The Potential for a Comparison of Different Standards

During the preparation for the DSTO empennage test it was realised that augmented loading would be required in order to exercise the structure sufficiently to produce failures. It was also realised that the generation of any FSFT failure data would then also allow the empennage to be interpreted using the Defence Standard (Def Stan) 00-970 Safe S-N approach. Subsequent to the DSTO P-3 SLAP FAR 25.571 based TI work interest existed in the DSTO Airworthiness Standards and Fatigue Methods Task in conducting research to compare the

timing of the eventual fleet actions such as inspection thresholds and intervals resulting from the application of other international airworthiness standards and their associated lifing methodologies.

As a result, a number of critical locations from the P-3 SLAP wing and empennage tests were selected for the calculation and comparison of different airworthiness standards such as Def Stan 00-970 and the Joint Service Specification Guide JSSG 2006. This report presents those results. The aim of this report is to make comparisons of the outcomes derived from the different approaches and comment on any differences and similarities.

## 1.3 Airworthiness Standards Examined in this Comparison

The following airworthiness standards were selected and used in the comparison work.

(a) Def Stan 00-970. This UK Defence Design and Airworthiness Standard requires the calculation of a safe life for all fatigue critical locations and advocates the use of the Safe S-N methodology. Originally selected for a trial on the empennage, it was also able to be applied to the critical wing locations. The standard also gives guidance on how to calculate inspection intervals for inspectable locations post safe life.

(b) JSSG 2006. This US Department of Defence specification guide provides guidance on both the requirements for, and evaluation of, durability and damage tolerance. It includes both the United States Air Force (USAF) crack growth based approach that originated from the Air Force Guide Specification AFGS 87221 and Military Specification (Mil-Spec) 83444, as well as the USN Safe Life assessment approach. The USN approach had been broadly used by L-M in their P-3 SLAP TI work for the USN. Both approaches were selected for study in this report.

## 1.4 Probabilistic Analysis

Concurrent with DSTO's TI work, L-M also conducted interpretation of the P-3 SLAP results for their customer, the USN. As the USN had large numbers of high-life aircraft, their TI findings were very quickly converted into fleet wide inspections of the FSFT identified critical locations. Fleet findings (both cracked and uncracked aircraft) became available and this data was used subsequent to the initial DSTO TI analysis to corroborate or sometimes modify the original calculations of inspection threshold. The differences between predictions and fleet results reflect not only the assumptions and accuracy of the test and test interpretation programs in the areas of loads estimation, spectral content and crack growth tool predictions, but also the accuracy of some of the underlying assumptions of the methodology such as fatigue scatter.

## 1.5 Comparison of Lifing Methods

The life prediction method used in the P-3 SLAP TI work represents a "combined" approach to crack growth life prediction, ie the total crack growth life is a combination of a "crack initiation" and a crack growth life. Traditional strain-life and crack growth tools were used as will be explained in Section 2.4. The comparison against the Def Stan 00-970 advocated Safe S-

N approach presents an opportunity to compare the P-3 SLAP tools against this stress-life approach. Additionally, the experimental results from the P-3 SLAP tests also offered an opportunity to trial the recently developed DSTO Equivalent Block Approach (EBA) for P-3 type spectra. This is done in Section 8.

## 1.6 Post-Test Interpretation Coupon Tests

The P-3 SLAP TI process had also envisaged a post-interpretation set of coupon tests using the latest version of the fatigue spectra that were available. This was because the TI had proceeded using life and crack growth prediction tools that had been calibrated using early versions of both the FSFT and RAAF spectra. In some areas the load spectra had changed significantly and it was felt that the TI predictions needed to be confirmed by results from the latest spectra used in the analysis. This report also includes the results from that series of coupon tests run using the spectra from the TI. The experimental results are compared with the previously conducted (truly 'blind') predictions for RAAF usage.

# 2. Background to DSTO P-3 SLAP Test Interpretation

The P-3 SLAP consisted of a number of full scale tests conducted between 2001 and 2004. Test running was preceded by loads development, spectra development and test build up activities. All tests suffered failures from fatigue that resulted in TI work, fleet inspections and the development of new wing components with life improvements.

## 2.1 Wing and Fuselage Fatigue Test

The wing and fuselage FSFT, shown in Figure 1, was conducted by L-M at their facility in Marietta, Georgia using a USN 85th percentile spectrum. The FSFT article was a retired USN aircraft which had accrued 10,988 hours of nominally 85th percentile USN usage. Under the USN's fleet Sustained Readiness Program (SRP), numerous components on the left hand (LH) outer wing of the test article were replaced including most of the lower skin panels, front and rear spar webs and lower spar caps. The fuselage and the centre and right hand (RH) outer wings were left unmodified to represent the build state of the RAAF, Canadian and Dutch fleets. A total of 38,000 test hours was applied to the test article. A residual strength test was then conducted and the wing failed at an undiscovered fatigue crack in the centre wing area emanating from a fuel weep hole in a lower wing plank stringer (subsequently referred to as Fatigue Critical Area [FCA] 163).


*Figure 1: Wing/Fuselage Fatigue Test at L-M*

## 2.2 Empennage Testing

L-M also conducted a test of the empennage using the component from the same aircraft and applying the SRP modification to the tailplane (essentially replacing all tailplane skin structure). A total of 38000 hours of testing to the USN 85th percentile spectrum was applied to the test article, however due to schedule constraints certain 'abrupt' manoeuvre loads known to be very conservative in their calculation remained in the spectrum.

The structure tested by DSTO consisted of a retired USN empennage that had accumulated 13,289 actual flight hours and 13,112 landings and was of similar age and usage as aircraft in the RAAF fleet. The test article consisted of the aft fuselage behind the rear pressure bulkhead from fuselage station (FS) 1117 to FS 1259, the horizontal stabiliser (including the leading edges and elevators), the vertical stabiliser (including the leading edge) and the dorsal fin aft of FS 1117. The control surfaces were considered transition structure and the aft fuselage was attached to a section of the fuselage forward of the FS 1117 production splice that acted as a transition structure between the test article and the test rig. The empennage test rig at DSTO is shown in Figure 2.

Very early in the DSTO test program it was recognised that the stress levels in the empennage principal structural elements would mean that the test time needed to generate representative failures would be long. Increasing the spectrum load levels would reduce testing time and also allow exploration of the UK Def Stan 00-970 Safe S-N concept of variable scatter factor associated with different structural features. The test subsequently applied an aircraft usage based load spectrum for two lifetimes in order to expose any early failures resulting from design flaws, followed by the same load spectrum significantly augmented in load level but with the peak loads clipped to avoid unrepresentative yielding at critical locations. See [2].

The baseline testing phase consisted of 30,000 Simulated Flight Hours (SFH) of fatigue cycling, utilising a load spectrum that was representative of USN 85$^{th}$ percentile usage, designated as A041B. This spectrum was developed by L-M for their empennage test and was subsequently transformed for use on the Australian test rig with some additional modification of the abrupt manoeuvre loads in order to better match measured flight loads. For the fin, the loading was essentially identical in both tests. During this first phase of testing, the article exhibited a number of failures from poorly designed local details that had also been observed in service aircraft. Whilst this evidence gave comfort that the test was representative of in-service loading, no failures or crack growth was observed in the primary structural elements.

The first extended testing phase was then conducted, consisting of 15,000 SFH of testing under the augmented load designated as A041D. For the fin, the level of load increase or augmentation was 1.6 whilst the peak loads were clipped at 1.1 times the peak loads in the original A041B spectrum. At the conclusion of this phase of testing, there was still minimal fatigue damage observed in the primary structural elements.

*Figure 2: DSTO Empennage Fatigue Test*

A second phase of extended testing designated as damage tolerance testing was then undertaken also using the augmented A041D spectrum. Before cycling commenced artificial damage in the form of saw cuts was inserted into various primary structure elements aimed at gathering crack growth information to supplement the data that had already been obtained from the test. Almost immediately into the damage tolerance testing phase a natural fatigue failure occurred in hidden structure at the base of the RH Vertical Stabiliser (V-Stab) front spar cap and its associated doubler. This failure location was designated FCA811 and the subsequent test article teardown revealed that two cracks existed at this location. The crack that severed the front spar cap originated at a flange runout feature and was designated FCA811-2, whilst a second crack a few inches away, and itself almost at the point of failure originated at a fastener hole common to the spar cap and doubler and was designated as FCA811-1. Incidentally, FCA811-1 had been the original, analytically-predicted fatigue critical location for the fin front spar. The above failure resulted in the cessation of V-Stab, rudder and dorsal fin loading; however, cycling of the horizontal stabilisers and aft fuselage continued up until the end of the damage tolerance testing phase of 15,000 SFH.

Residual strength testing to design limit load (DLL) (which demonstrated the fail safe capacity of the degraded fin structure) and a full teardown and examination of the test article structure completed the test program. A summary of the defects detected throughout the fatigue test and during post-test teardown is in [2]. Apart from the fin front spar, significant failures were generated in the spars and stringers of the horizontal stabiliser, some of which were replicated in the L-M test.

## 2.3 Scope of DSTO Test Interpretation Work

Spectra applied to the SLAP tests were equivalent to USN 85th percentile 'severe' usage. RAAF usage was determined to be broadly similar to average USN usage, but significantly different to the 85th percentile spectrum developed for the tests. The differences were also highlighted by changes (generally refinements and improvements) in the aircraft external loads system throughout the P-3 program. As a result, the TI had to convert test results under the USN 85th percentile spectrum to RAAF average usage. RAAF average usage was also observed to differ between P-3C flying and AP-3C flying (the conversion involved an avionics update to the aircraft during the period 2000–2004) with the AP-3C usage calculated to be less severe.

To maintain commonality with the efforts of L-M and the other SLAP partners, data from L-M on the analysis of the wing/fuselage fatigue test (for which L-M had the lead) such as crack fractography, finite element method (FEM) based stress levels and stress intensity factors were used in the DSTO TI. For the DSTO empennage test, stress intensity values and strain/load relationships were calculated by DSTO.

## 2.4 Selection and Calibration of Lifing Tools

The tools used by all partners for their TI were also a product of early L-M testing and P-3 SLAP community consensus. The FAMS strain-life program [20] was selected for crack initiation calculations and FASTRAN 3.8 (with some modifications by L-M) was used for crack growth analysis.

Coupon tests undertaken by DSTO and others during the P-3 SLAP for tools calibration and verification included:

(a) Crack growth and fatigue life coupons run by L-M to investigate the effect on life of spectra clipping and truncation.
(b) Centre crack coupons run in Canada for L-M to support FASTRAN calibration.
(c) Crack growth and fatigue life coupons run by The Netherlands National Aerospace Laboratory (NLR) on behalf of all the P-3 SLAP FMS customers to investigate spectra differences.
(d) Coupons run at DSTO to augment the NLR coupons tests for additional FCA locations and other RAAF spectra.
(e) Coupons run at DSTO using constant amplitude loading to provide alternative material data to support FAMS calibration investigations.

The results of the NLR coupons tests are in [17] whilst the DSTO coupon tests are recorded in [21].

## 2.5 Follow-up Coupon Testing

Between the time that the FAMS and FASTRAN tools were initially calibrated and the DSTO TI was completed, the P-3 external loads system, the loads-to-stress relationships at FCAs and the content of the RAAF spectra had all undergone refinements within the P-3 SLAP. As a result, the original DSTO TI plan also envisaged an additional set of coupon tests run using the final TI loads spectra that would provide a post-TI check on the life predictions that were then being used in the SMP to make recommendations for the RAAF fleet management actions. This activity was called a 'close the circle' verification process and, after some delay, this test program was eventually carried out in 2008 and the results are given in Section 9.

# 3. P-3 Case Studies Critical Locations and Spectra

## 3.1 Critical Locations

The P-3 case studies will be conducted at a selected number of critical structural locations identified during the P-3 SLAP. The lower outer wing FCAs listed below were identified as significant as a result of cracks detected on the P-3 FSFT. Consequently, analysis of these locations was performed within the wing-fuselage TI report [1] and they will also be examined in this report.

- FCA301-WEB-4
- FCA351-CDN-2
- FCA352-PDN-1
- FCA375-PSS-2

Several empennage FCAs, listed below, were also selected for comparison. These locations were identified in the DSTO empennage TI report [2] as a result of significant cracking on the FSFT.

- FCA811-1
- FCA811-2
- FCA886

The location of each of these FCAs and the relevant full scale fatigue test results are presented in Appendix A. Significant amounts of fleet inspection data have been generated by the USN and other P-3 operators and are also included in the Appendix A. More information regarding the inspection programs that were (and continue to be) undertaken is included in [3]. The fleet inspection information was correct as of the time of the publication of [3] which was December 2006.

## 3.2 Wing Spectra

The sequence applied to the P-3 SLAP wing/fuselage test article is referred to as the FSFT spectrum in this report. This spectrum is representative of USN 85$^{th}$ percentile usage and was applied to the FSFT article for 38,000 SFHRS. RAAF spectra were generated for both P-3C and AP-3C usage. Both RAAF spectra represent average usage, with the P-3C spectrum representing RAAF flying between 1991 and 1999, and the AP-3C spectrum representing flying post the AIR 5276 Project avionics upgrade in circa 2000.

The wing stress sequences utilised in this report were created by different processes which are summarised below.

(a) All FSFT stress sequences at each wing FCA in Sections 4 to 9 were generated by L-M load sequence development software from USN 85th percentile mission criteria and using Phase IIB FEM-based stress-to-load ratios (SLRs). These FSFT sequences were also used in the DSTO wing/fuselage TI.

(b) The RAAF P-3C and AP-3C wing stress sequences in Sections 4 to 7 were generated using the P-3 SLAP Database Interface and Spectra Sequencing Tool (DBI/SST) [18], using RAAF mission criteria, the Phase IIC loads system and Phase IIB FEM SLRs. This is the case for all spectra except for the sequences used in the FAMS analysis at FCA301 where the Phase IIC loads system with revised touch-and-go criteria was utilised. The revised touch-and-go criteria were found to affect the FAMS analysis for FCAs inboard of WS 140 only. Crack growth analysis was not significantly affected. These RAAF spectra were used in the DSTO wing/fuselage TI and for the coupon tests of Section 9.

(c) The RAAF sequence used in Section 8.2 for both the coupon tests and the analysis work was created by L-M sequence development software and initial RAAF P-3C usage criteria using the Phase IIB loads system and Phase II FEM SLRs.

Further details regarding stress sequence generation may be found in [1], [17], [18] and [19].

## 3.3 Empennage Spectra

A number of empennage spectra were developed as part of the P-3 SLAP. The FSFT empennage stress sequences used in the TI and this report were created by factoring bending moments (generated from command actuator loads) by stress-to-load-ratios (SLRs) (generated from measured strain gauge data). Conversely, the RAAF P-3C and AP-3C empennage stress sequences used in the TI and this report were created using the P-3 SLAP Phase IIC loads system, Phase IIB FEM SLRs and the DBI/SST. Further details may be found in [2], [18] and [19].

## 3.4 Spectra Properties

Basic properties of the FSFT and RAAF spectra described above are presented in Table 1 (from [1] and [2]). Note the difference in landings between the P-3C and AP-3C spectra which reflects the more benign AP-3C spectra.

*Table 1: Basic Spectra Properties*

| Spectrum | Hours | No. of Missions | Total No. of Landings | No. of Touch & Go's | No. of Full Stop Landings | No. of Pressure Cycles |
|---|---|---|---|---|---|---|
| FSFT* | 15,000 | 4,401 | 23,660 | 14,767 | 8,893 | 7,165 |
| RAAF P-3C | 15,292 | 3,096 | 11,234 | 7,214 | 4,020 | 4,469 |
| RAAF AP-3C | 15,370 | 2,603 | 5,808 | 2,677 | 3,131 | 3,495 |

* Properties apply to wing and empennage FSFT spectra

Table 2 provides the properties of the FSFT and RAAF stress sequences for each FCA. Figure 3 to Figure 10 provide stress exceedence plots for each FCA. The sequence properties and the exceedence plots were taken from the TI reports of [1] and [2].

*Table 2: Stress Sequence Properties for each FCA*

| FCA | Spectrum | Maximum (psi) | Minimum (psi) | No. of Lines | Clipping Levels (psi) |
|---|---|---|---|---|---|
| 301 | FSFT | 31,160 | -5,518 | 878,810 | - |
| | RAAF - P-3C | 23,928 | -14,613 | 2,280,432 | - |
| | RAAF - AP-3C | 25,142 | -14,788 | 1,893,782 | - |
| 351 | FSFT | 25,587 | -12,882 | 864,482 | - |
| | RAAF - P-3C | 20,102 | -20,000 | 2,624,882 | -20,000 |
| | RAAF - AP-3C | 19,991 | -20,000 | 2,210,278 | -20,000 |
| 352 | FSFT | 26,511 | -11,368 | 863,768 | - |
| | RAAF - P-3C | 20,749 | -18,000 | 2,657,862 | -18,000 |
| | RAAF - AP-3C | 20,492 | -18,000 | 2,242,944 | -18,000 |
| 361* | FSFT | 24,106 | -14,255 | 845,248 | - |
| | RAAF - P-3C | 19,098 | -20,000 | 2,599,194 | -20,000 |
| | RAAF - AP-3C | 19,174 | -20,000 | 2,192,770 | -20,000 |
| 375 | FSFT | 25,702 | -8,954 | 824,112 | - |
| | RAAF - P-3C | 19,190 | -17,000 | 2,416,026 | -17,000 |
| | RAAF - AP-3C | 20,415 | -17,000 | 2,033,240 | -17,000 |
| 811-1 | FSFT - U041 | 25,453 | -23,560 | 438,980 | - |
| | FSFT - A041B | 25,295 | -23,412 | 438,980 | - |
| | FSFT - A041D | 27,828 | -25,756 | 438,980 | +27,828<br>-25,756 |
| | RAAF - P-3C | 21,411 | -19,833 | 701,260 | - |
| | RAAF - AP-3C | 21,304 | -19,735 | 539,372 | - |
| 811-2 | FSFT - U041 | 22,931 | -21,225 | 438,980 | - |
| | FSFT - A041B | 22,788 | -21,092 | 438,980 | - |
| | FSFT - A041D | 25,070 | -23,204 | 438,980 | +25,070<br>-23,204 |
| | RAAF - P-3C | 19,289 | -17,868 | 701,260 | - |
| | RAAF - AP-3C | 19,193 | -17,779 | 539,372 | - |
| 886 | FSFT - U041 | 10,232 | -5,720 | 647,210 | - |
| | FSFT - A041B | 10,232 | -5,718 | 704,478 | - |
| | FSFT - A041D | 15,351 | -9,149 | 423,716 | +15,351 |
| | RAAF - P-3C | 8,257 | -2,826 | 3,414,144 | - |
| | RAAF - AP-3C | 8,235 | -3,531 | 2,417,548 | - |

* Sequences for this FCA used in the EBA and coupon tests sections only

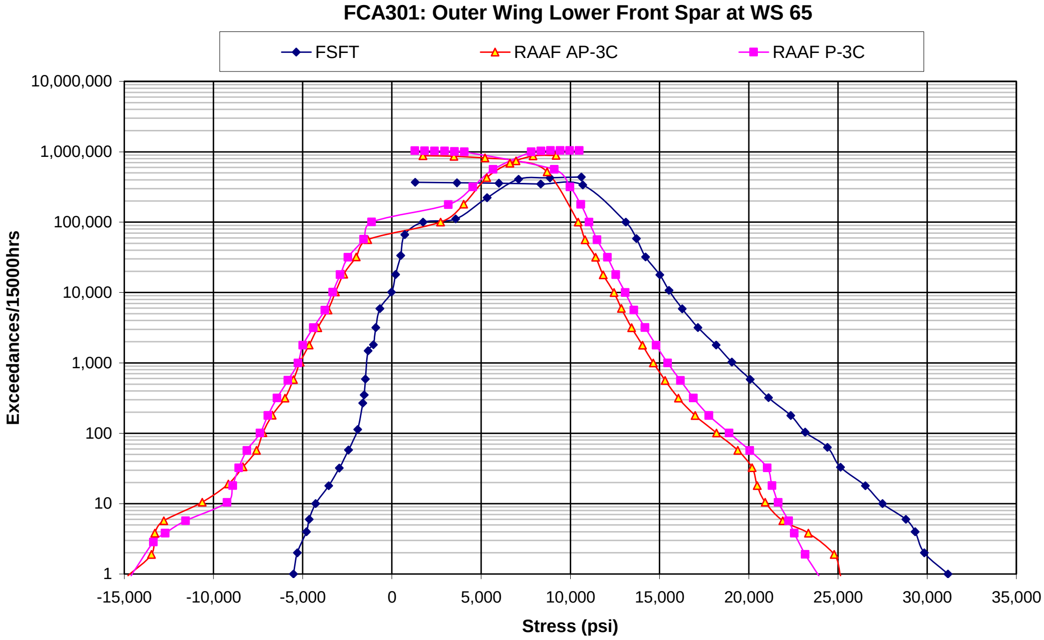


*Figure 3: Exceedance Curves for FCA301*

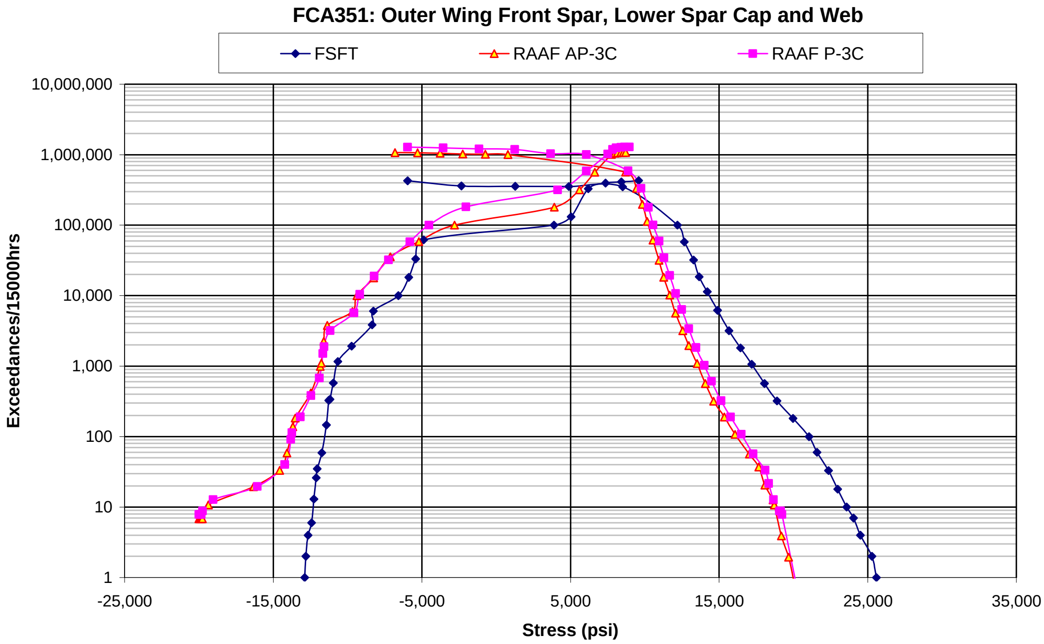


*Figure 4: Exceedance Curves for FCA351*

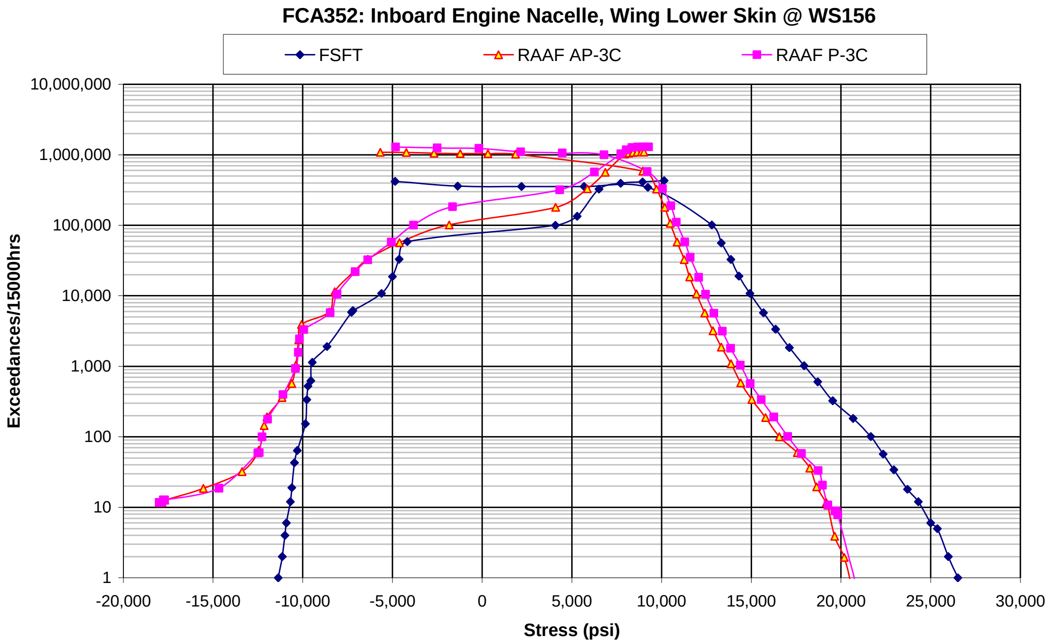


*Figure 5: Exceedance Curves for FCA352*

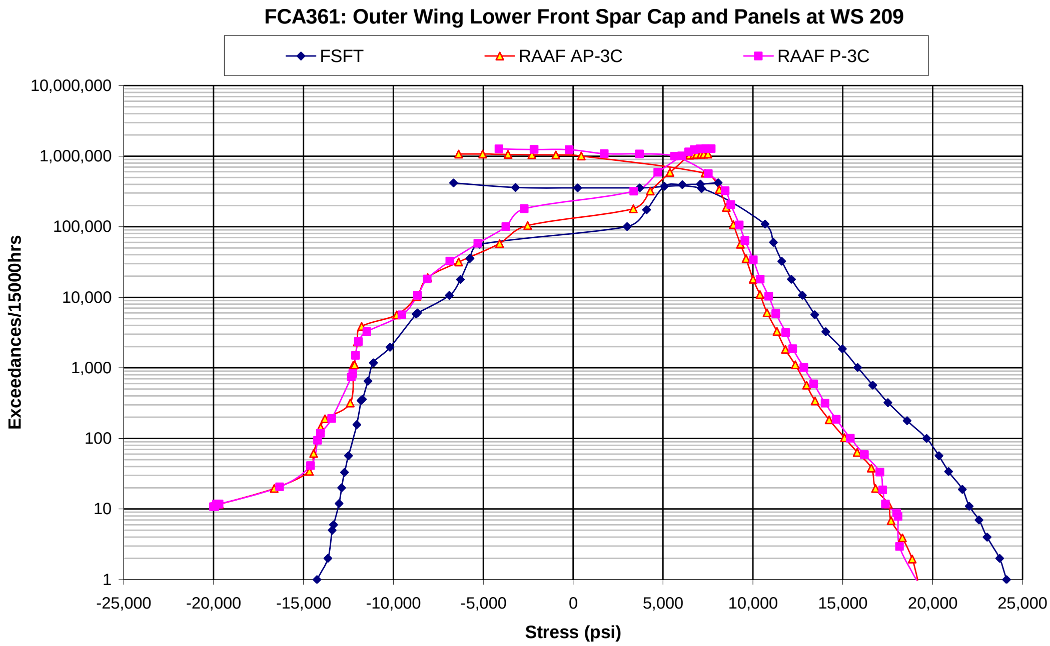


*Figure 6: Exceedance Curves for FCA361*

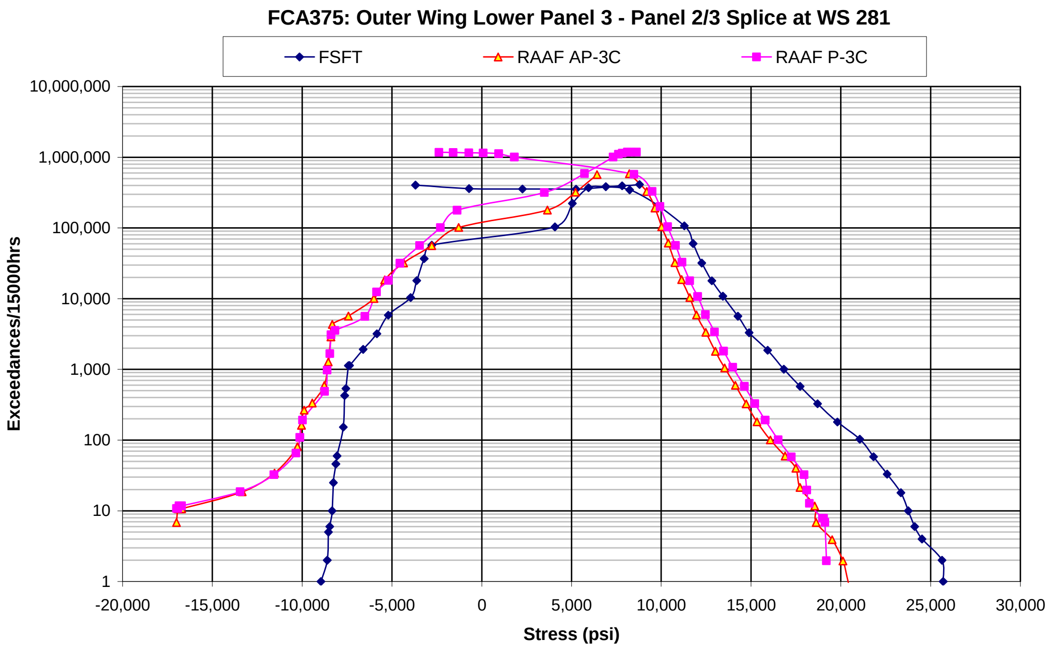


*Figure 7: Exceedance Curves for FCA375*

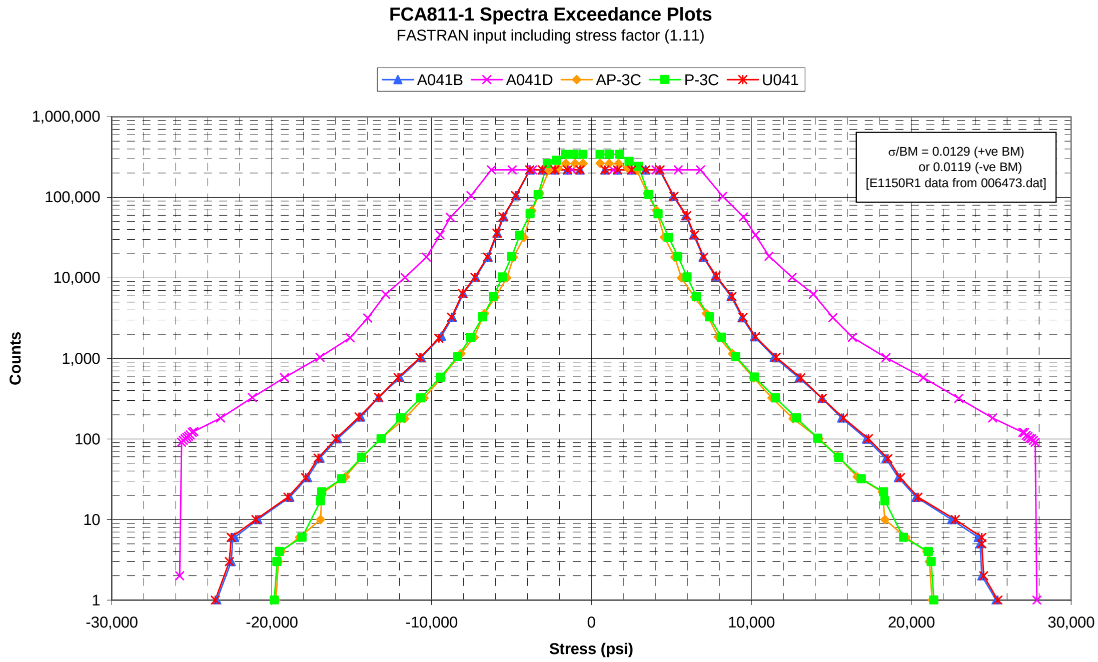


*Figure 8: Exceedance Curves for FCA811-1*

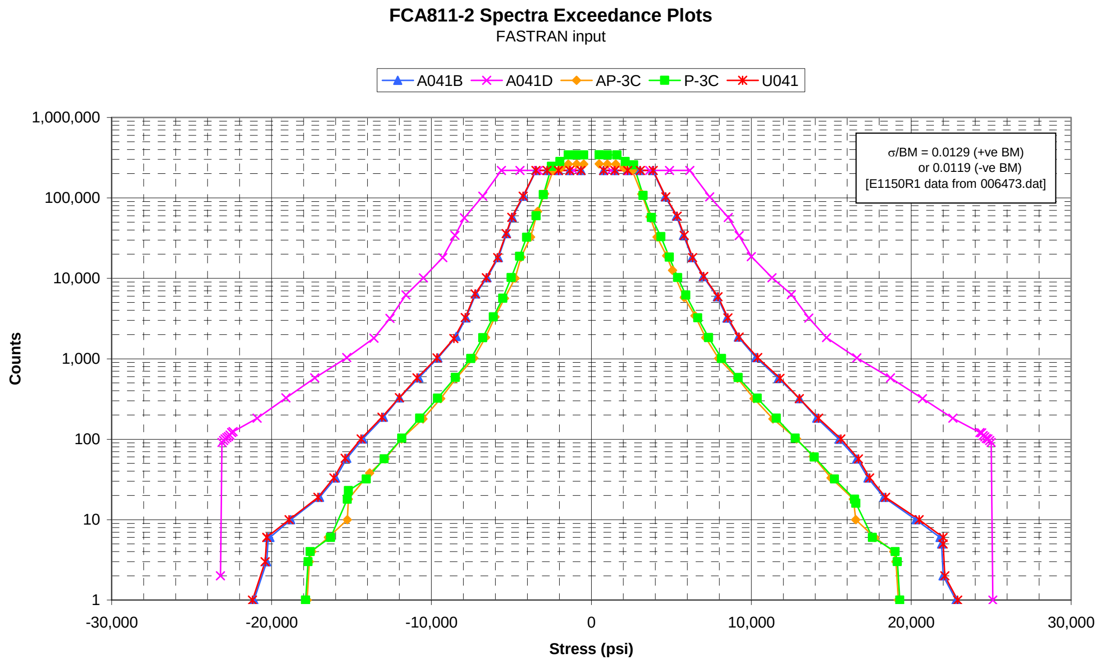


*Figure 9: Exceedance Curves for FCA811-2*

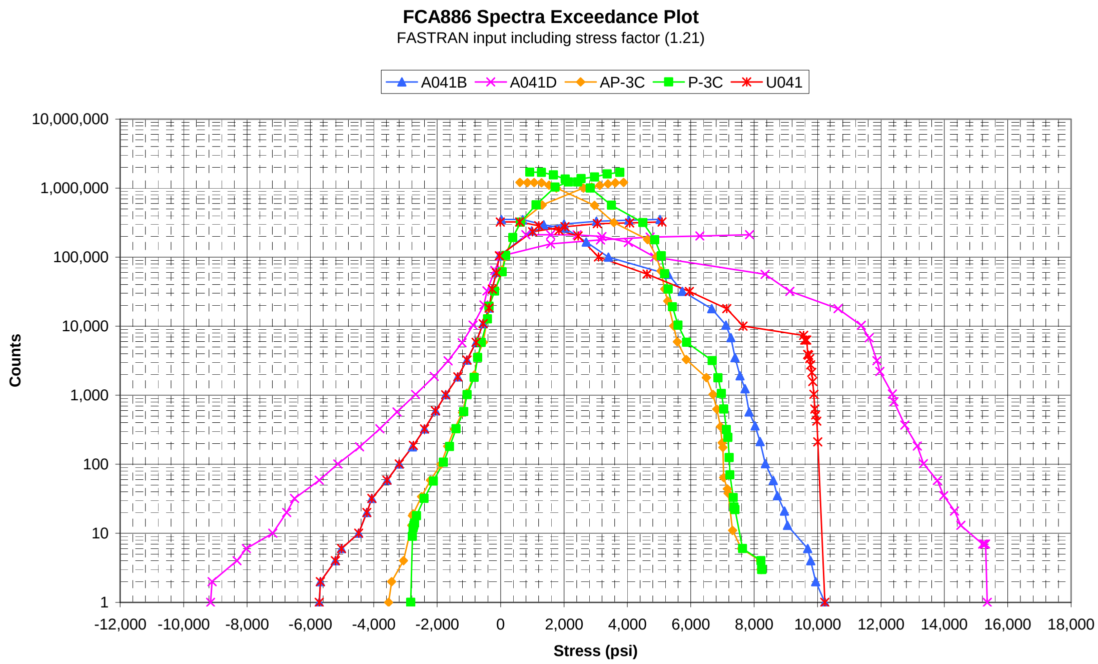


*Figure 10: Exceedance Curves for FCA886*

# 4. Test Interpretation Life Calculations Using FAR 25

## 4.1 FAR 25 Safe Life and Damage Tolerance Overview

The RAAF chose FAR 25.571[7], the successor of CAR 4b, as the airworthiness standard against which to interpret the P-3 SLAP test results and conduct the durability and damage tolerance evaluation of the structure from which a program containing the necessary structural inspection and modifications and/or replacements could be determined. Guidance on conducting the fatigue and damage tolerance analysis (DTA) was taken by DSTO from the applicable advisory circular, AC 25.571-1C [8]. The advisory circular provides options for the determination of inspection threshold (either by crack growth from a small initial size or the application of a factor, generally of about three, on demonstrated test life) as well as requirements for the treatment of fail-safe and non fail-safe structure. The method chosen for the DSTO analysis used the factored test demonstrated life approach and combined both fatigue life modelling (strain-life based crack ‘initiation’ to a nominal crack size of 0.050 inches (1.27mm)) and crack growth analysis (classical linear elastic fracture mechanics) in a ‘total life’ analysis method. Estimation of inspection intervals used the calculated crack growth period from detectable size to the maximum permissible size under the residual strength criterion divided by a suitable factor. The factor is not specified in [8] but a value of two was chosen in order to be consistent with equivalent US military standards. The method of conducting the durability and damage tolerance analysis and interpreting the test results is shown in Figure 11 and Figure 12.

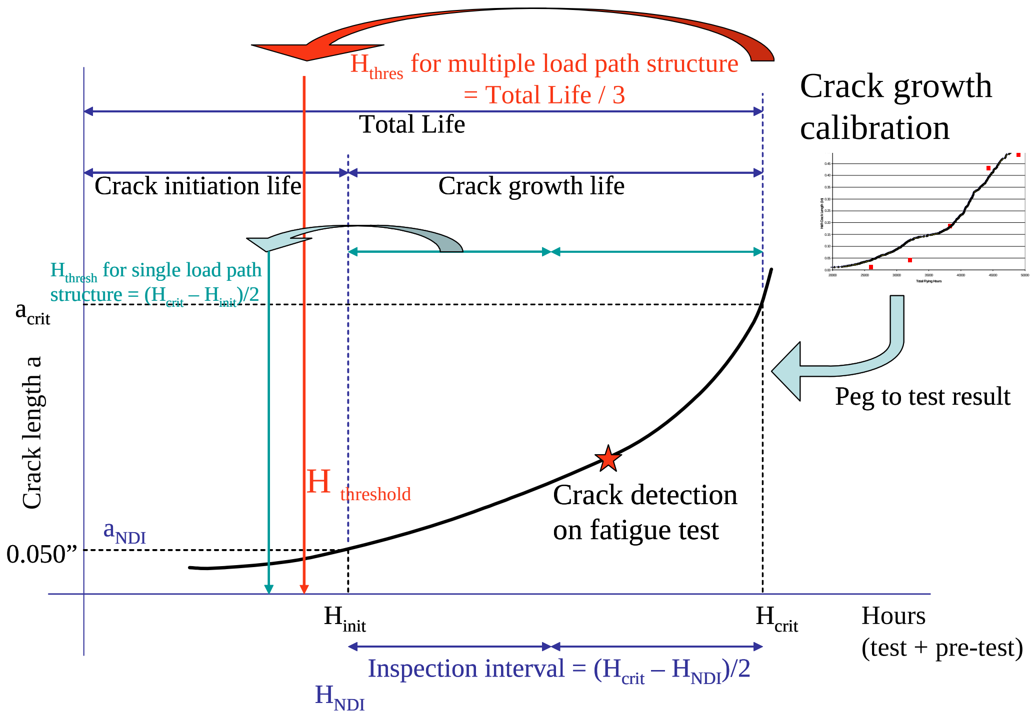


*Figure 11: Calculation of Inspection Intervals and Thresholds (from [1])*

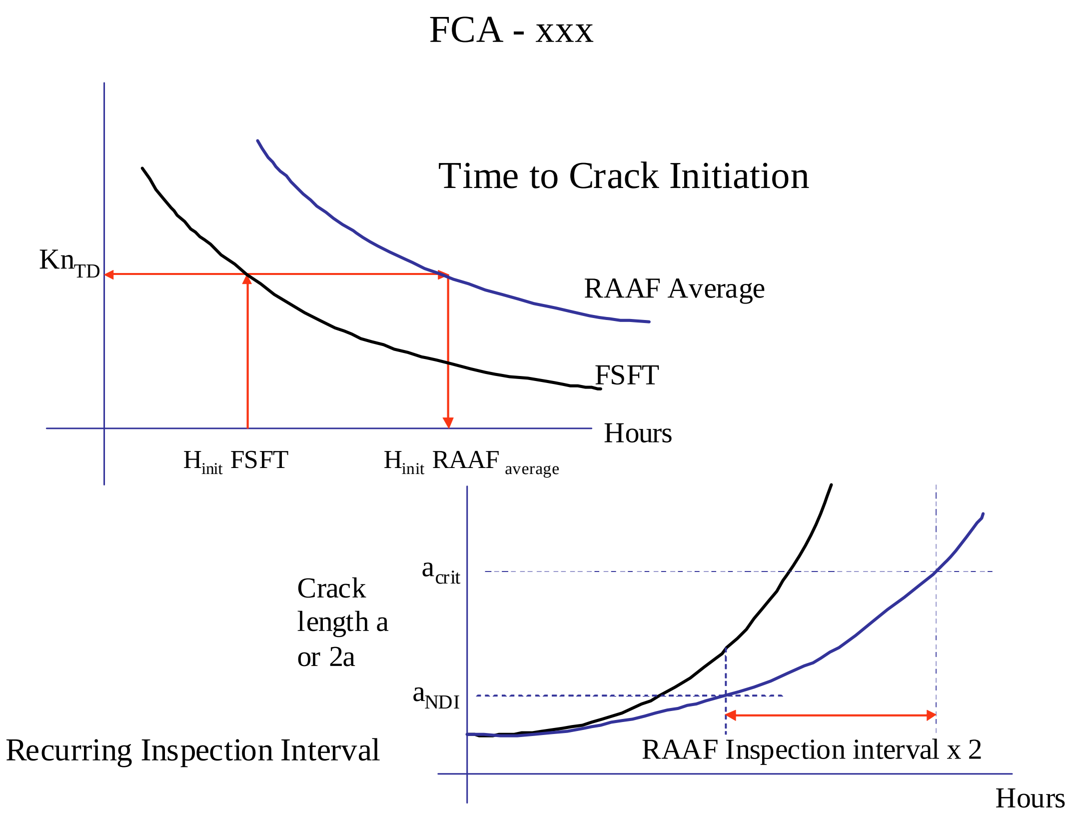


*Figure 12: Conversion of FSFT Test Lives to Lives under RAAF Spectra (from [1])*

### 4.1.1 Inspection Threshold and Safe Life

For the calculation of inspection threshold for multiple load path fail safe structure the test demonstrated life option from AC 25.571-1C (paragraph k.(1)(1)) was used with a factor of 3. For single load path or non-fail safe structure the AC 25.571-1C requires an inspection threshold based on crack growth from 'an initial flaw of maximum probable size'. Only one FCA was defined as non-fail safe structure in the DSTO TI. This location was FCA163 from which the wing test finally failed catastrophically under the residual strength load. In the DSTO TI process, the FAR 25-based calculated inspection threshold was called the Safe Life. The safe life was also used as the modification or replacement point for the component or structure in the subsequent SMP if inspection was not deemed viable.

### 4.1.2 Economic Threshold

As well as the inspection threshold determined from the AC 25.571-1C guidelines, the DSTO TI process also calculated an 'economic' threshold. The 'economic' inspection threshold is defined as the time to an inspectable crack size (hours to both 0.05″ and 0.12″ were calculated) divided by a factor of 2. This 'crack initiation' life was calculated using the FAMS program [5] and the factor of 2 represents an approximate 1/40 probability (assuming a standard deviation of 0.11). This threshold provided a value in airframe hours in which no more than one wing in the RAAF fleet of 20 aircraft could be expected to have a crack larger than 0.05 or 0.12″ and provided the RAAF an opportunity to set an inspection threshold that avoided large and difficult to repair cracks being found. In the development of the SMP this threshold

option was not taken up by the RAAF. However it is included here in order to provide a comparison with the AC 25.571-1C safe life approach.

### 4.1.3 Inspection Interval

The inspection interval was defined as the time from the inspectable crack size $a_{NDI}$ to component failure (at $a_{crit}$) divided by 2 to allow two opportunities of finding a crack prior to failure. This crack growth life was calculated utilising the FASTRAN program [5]. Two values of $a_{NDI}$ were used, 0.050″ and 0.12″, representing bolt hole eddy current and surface scan eddy current techniques respectively.

## 4.2 Results

A summary of the life calculations from the DSTO wing/fuselage and empennage TI reports [1,2] for the selected locations are provided in this section in Tables 3 to10. The results are presented exactly as they are presented in [1,2] and these references should be consulted for further explanation. As per Section 4.1, the total life (TL) can be re-calculated by adding the time to initiation $H_{init}$ (also labled $t_{init}$)at a=0.05″ to the crack growth life from $a_{NDI}$ = 0.050″ (labled as $t_{CG}$). The structural configuration of the RAAF fleet and the various fatigue tests were identical at the part number level of all critical locations, however for one empennage location, FCA 886, manufacturing tolerances produced a different radius at the critical detail for the DSTO empennage test and the L-M empennage test and so different test results eventuated.

### 4.2.1 FCA301-WEB-4

*Table 3: Summary of lives for FCA301-WEB-4*

| Factored AFHRS | | | | | | |
|---|---|---|---|---|---|---|
| **Spectrum** | Economic Threshold $H_{init}/2$ (AFHRS) | | Inspection Intervals CG Life/2 (AFHRS) | | Total Life $t_{init}+t_{CG}$ (AFHRS) | Safe Life TL/3 (AFHRS) |
| | a = 0.05 | a = 0.12 | $a_{NDI}$ = 0.05 | $a_{NDI}$ = 0.12 | | |
| FSFT | 4,948 | 6,148 | 13,430 | 12,230 | 36,756 | 12,252 |
| RAAF AP-3C | 5,450 | 6,800 | 4,672 | 2,868 | 20,245 | 6,748 |
| RAAF P-3C | 4,050 | 4,650 | 3,992 | 2,967 | 16,084 | 5,361 |

### 4.2.2 FCA351-CDN-2

*Table 4: Summary of lives for FCA351-CDN-2*

| Factored AFHRS | | | | | | |
|---|---|---|---|---|---|---|
| **Spectrum** | Economic Threshold $H_{init}/2$ (AFHRS) | | Inspection Intervals CG Life/2 (AFHRS) | | Total Life $t_{init}+t_{CG}$ (AFHRS) | Safe Life TL/3 (AFHRS) |
| | a = 0.05 | a = 0.12 | $a_{NDI}$ = 0.05 | $a_{NDI}$ = 0.12 | | |
| FSFT | 9,678 | 10,968 | 3,395 | 2,291 | 26,147 | 8,716 |
| RAAF AP-3C | 14,500 | 16,000 | 5,722 | 3,593 | 40,443 | 13,481 |
| RAAF P-3C | 10,000 | 11,000 | 4,120 | 2,437 | 28,241 | 9,414 |

### 4.2.3 FCA352-PDN-1

*Table 5: Summary of lives for FCA352-PDN-1*

| Factored AFHRS | | | | | | |
|---|---|---|---|---|---|---|
| **Spectrum** | Economic Threshold $H_{init}/2$ (AFHRS) | | Inspection Intervals CG Life/2 (AFHRS) | | Total Life $t_{init}+t_{CG}$ (AFHRS) | Safe Life TL/3 (AFHRS) |
| | a = 0.05 | a = 0.12 | $a_{NDI}$ = 0.05 | $a_{NDI}$ = 0.12 | | |
| FSFT | 7,531 | 8,344 | 1,733 | 920 | 18,529 | 6,176 |
| RAAF AP-3C | 12,500 | 13,750 | 2,806 | 1,617 | 30,612 | 10,204 |
| RAAF P-3C | 9,000 | 9,500 | 1,978 | 1,042 | 21,956 | 7,319 |

### 4.2.4 FCA375-PSS-2

*Table 6: Summary of lives for FCA375-PSS-2*

| Factored AFHRS | | | | | | |
|---|---|---|---|---|---|---|
| **Spectrum** | Economic Threshold $H_{init}/2$ (AFHRS) | | Inspection Intervals CG Life/2 (AFHRS) | | Total Life $t_{init}+t_{CG}$ (AFHRS) | Safe Life TL/3 (AFHRS) |
| | a = 0.05 | a = 0.12 | $a_{NDI}$ = 0.05 | $a_{NDI}$ = 0.12 | | |
| FSFT | 7,241 | 11,612 | 25,780 | 21,409 | 66,042 | 22,014 |
| RAAF AP-3C | 9,800 | 14,900 | 7,708 | 5,107 | 35,016 | 11,672 |
| RAAF P-3C | 7,500 | 10,300 | 5,980 | 4,222 | 26,959 | 8,986 |

### 4.2.5 FCA811-1 and -2

The calculation of inspection intervals and thresholds for the empennage locations was not as straight forward as for the wing locations. DSTO needed to develop crack growth stress intensity factors with the help of detailed FEMs (Figure 13 is an example) and the translation between spectra was complicated by the various augmented loads sequences. See Figure 14 for the effect on crack growth and Figure 15 for the determination of test demonstrated $K_N$ for FCA811-2 as examples.

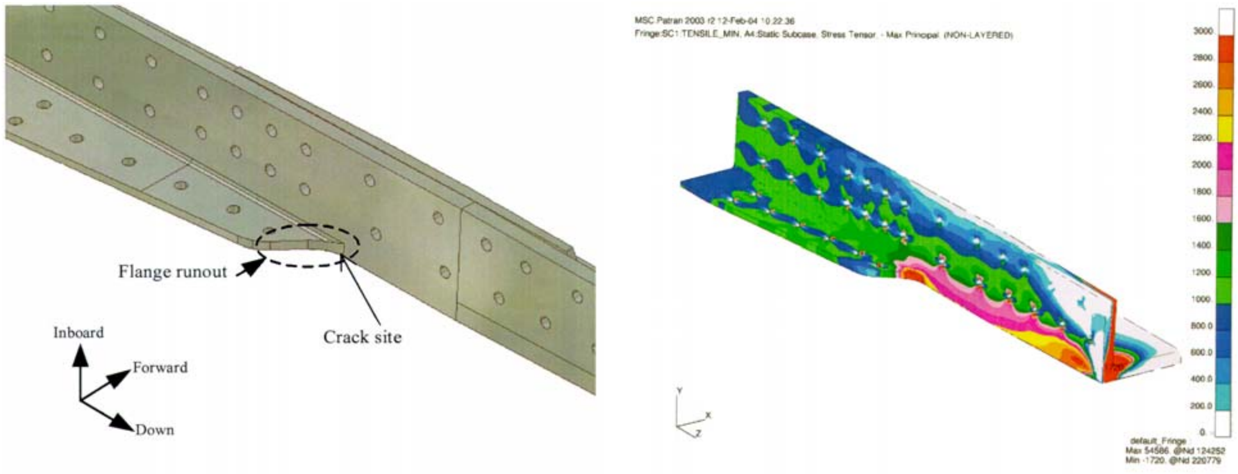


*Figure 13: Finite Element Model of FCA811-2 at Front Spar Cap Radius Runout*

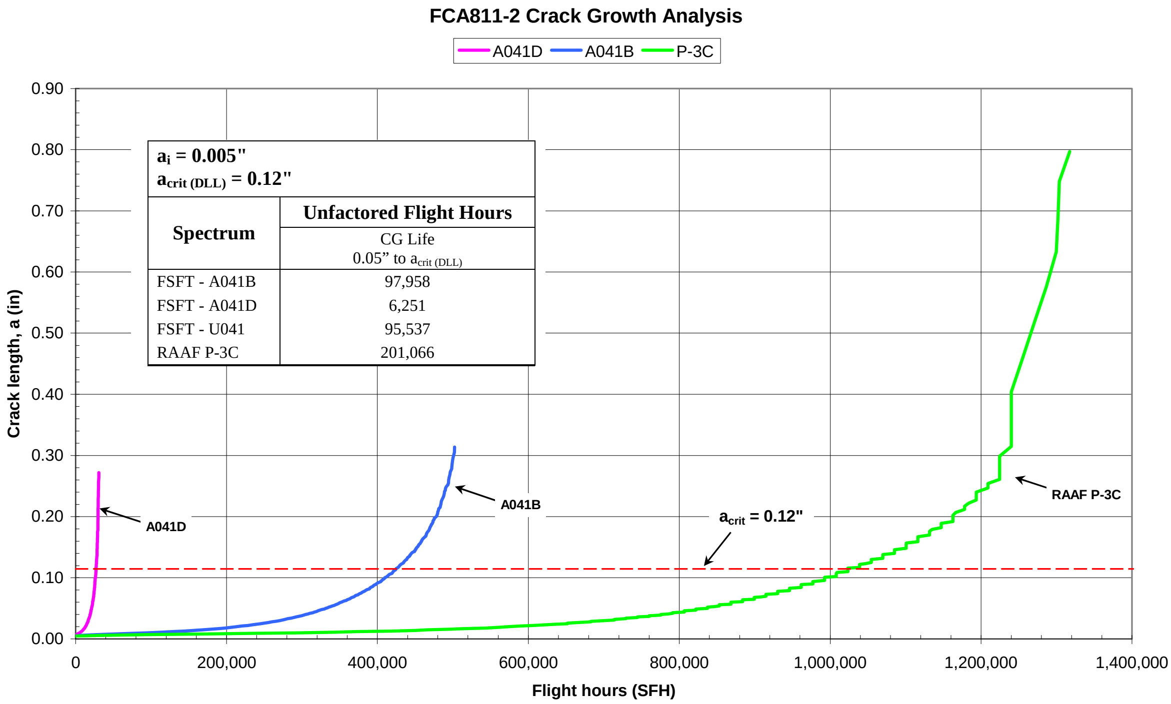


*Figure 14: Crack Growth Curves for DSTO Empennage Spectra*

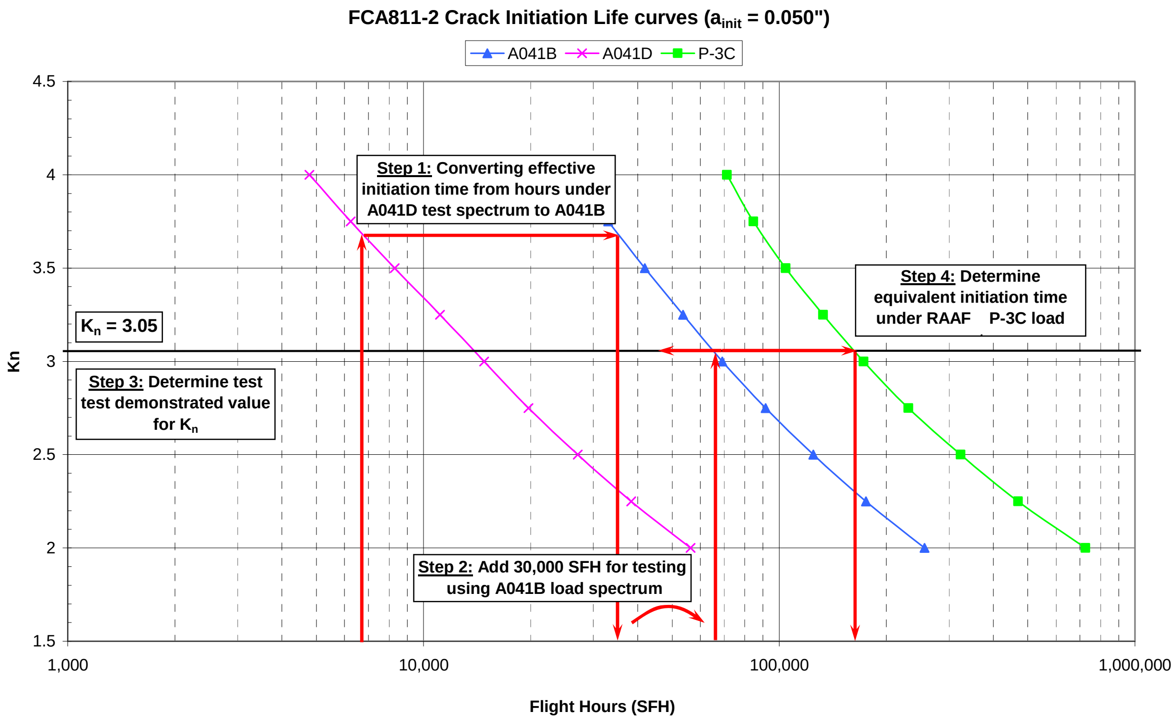


*Figure 15: Crack Initiation Plot for DSTO Empennage Spectra (FCA811-2 example)*

The results for FCA811-1 are in table 7. For FCA811-2, see table 8, the critical crack size under design limit load was 0.12″ and so inspection intervals for $a_{NDI}$=0.12″ are not calculated.

*Table 7: FCA811-1 Summary of TI analysis results in factored flight hours*

| Factored AFHRS | | | | | | |
|---|---|---|---|---|---|---|
| **Spectrum** | Economic Threshold $H_{init}/2$ (AFHRS) | | Inspection Intervals CG Life/2 (AFHRS) | | Total Life $t_{init}+t_{CG}$ (AFHRS) | Safe Life TL/3 (AFHRS) |
| | $a_{init}$ = 0.05 | $a_{init}$ = 0.12 | $a_{NDI}$ = 0.05 | $a_{NDI}$ = 0.12 | | |
| FSFT - A041B | 15,000 | 40,000 | 133,027 | 49,329 | 296,053 | 98,684 |
| FSFT - A041D | 2,800 | 8,600 | 8,096 | 2,824 | 21,792 | 7,264 |
| FSFT - U041 | 14,600 | 39,200 | 128,579 | 47,943 | 286,357 | 95,452 |
| RAAF P-3C | 39,250 | 100,000 | 332,785 | 123,823 | 744,070 | 248,023 |
| RAAF AP-3C | 46,250 | 119,000 | 317,074 | 116,010 | 726,647 | 242,216 |

*Table 8: FCA811-2 Summary of TI analysis results in factored flight hours*

| Factored AFHRS | | | | | | |
|---|---|---|---|---|---|---|
| **Spectrum** | Economic Threshold $H_{init}/2$ (AFHRS) | | Inspection Intervals CG Life/2 (AFHRS) | | Total Life $t_{init}+t_{CG}$ (AFHRS) | Safe Life TL/3 (AFHRS) |
| | $a_{init}$ = 0.05 | $a_{init}$ = 0.12 | $a_{NDI}$ = 0.05 | $a_{NDI}$ = 0.12 | | |
| FSFT - A041B | 32,500 | 45,818 | 48,979 | 0 | 162,958 | 54,319 |
| FSFT - A041D | 7,000 | 9,870 | 3,125 | 0 | 20,251 | 6,750 |
| FSFT - U041 | 32,000 | 44,850 | 47,769 | 0 | 159,537 | 53,179 |
| RAAF P-3C | 81,000 | 115,000 | 100,533 | 0 | 363,066 | 121,022 |
| RAAF AP-3C | 97,000 | 138,000 | 100,620 | 0 | 395,239 | 131,746 |

### 4.2.6 FCA886

The results for FCA 886, for the L-M and DSTO test configurations are given in tables 9 and 10 respectively.

*Table 9: FCA886 Summary of analysis results in factored flight hours, L-M test configuration*

| Factored AFHRS | | | | | | |
|---|---|---|---|---|---|---|
| **Spectrum** | Economic Threshold $H_{init}/2$ (AFHRS) | | Inspection Intervals CG Life/2 (AFHRS) | | Total Life $t_{init}+t_{CG}$ (AFHRS) | Safe Life TL/3 (AFHRS) |
| | $a_{init}$ = 0.05 | $a_{init}$ = 0.12 | $a_{NDI}$ = 0.05 | $a_{NDI}$ = 0.12 | | |
| FSFT - A041B | 12,000 | 16,500 | 12,755 | 9,675 | 49,510 | 16,503 |
| FSFT - A041D | 2,750 | 4,100 | 2,770 | 2,013 | 11,040 | 3,680 |
| FSFT - U041 | 5,500 | 6,865 | 5,461 | 4,096 | 21,921 | 7,307 |
| RAAF P-3C | 13,000 | 22,500 | 13,957 | 10,261 | 53,913 | 17,971 |
| RAAF AP-3C | 20,000 | 35,000 | 23,047 | 16,759 | 86,093 | 28,698 |

*Table 10: FCA886 Summary of analysis results in factored flight hours, DSTO test configuration*

| Factored AFHRS | | | | | | |
|---|---|---|---|---|---|---|
| **Spectrum** | Economic Threshold $H_{init}/2$ (AFHRS) | | Inspection Intervals CG Life/2 (AFHRS) | | Total Life $t_{init}+t_{CG}$ (AFHRS) | Safe Life TL/3 (AFHRS) |
| | $a_{init}$ = 0.05 | $a_{init}$ = 0.12 | $a_{NDI}$ = 0.05 | $a_{NDI}$ = 0.12 | | |
| FSFT - A041B | 103,000 | - | 12,755 | 9,675 | 231,510 | 77,170 |
| FSFT - A041D | 16,750 | - | 2,770 | 2,013 | 39,040 | 13,013 |
| FSFT - U041 | 57,500 | - | 5,461 | 4,096 | 125,921 | 41,974 |
| RAAF P-3C | 240,000 | - | 13,957 | 10,261 | 507,913 | 169,304 |
| RAAF AP-3C | 380,000 | - | 23,047 | 16,759 | 806,093 | 268,698 |

# 5. Life Calculations Using Def Stan 00-970

## 5.1 Fatigue Evaluation Requirements

Def Stan 00-970 [9] was developed primarily for, and draws experience from, single load path, compact, generally uninspectable structures that are typical of fighter type aircraft. The primary tenet of the standard for fatigue evaluation is that a safe life is firstly calculated for all features deemed susceptible to fatigue. For new aircraft the standard requires that the safe life normally at least equal the 'specified life' (i.e. planned in-service life). Materials selected shall have a good tolerance to damage, and damage tolerance evaluations need to be carried out if a component is vulnerable to damage during service. Inspectable components may remain in service beyond their safe life if; (a) the presence of cracks can be identified with confidence (i.e. the component is inspectable for the types of cracking that are of concern) and (b) inspection intervals are set to provide three chances of inspection prior to residual strength limits being breached. Residual strength limit is normally 1.2 DLL but can be reduced to 1.0 DLL for particular examples where DLL is an extreme case. Leaflet 35 of Volume 1 of [9] states that safe life scatter factors are a minimum of 3.33 on life. Other factors related to test spectrum representivity and loads monitoring are also described. For features with relatively high variability, tests must be underpinned by additional evidence such as analysis and inspections. Construction and use of safe S-N curves is central to the assessment of compliance.

### 5.1.1 Safe Life Calculation using Safe S-N

Def Stan 00-970 Leaflet 35 describes the safe S-N approach that may be used to calculate safe lives. The safe S-N method makes allowance for the increase in scatter that occurs with increasing life by factoring a mean S-N curve by life and stress factors and then combining the two resulting curves into a safe S-N curve which is then used as the 'working' curve for fatigue design and evaluation. The safe curve must take the same shape as the mean curve. It must begin at the safe static yield strength, retain the life factor as long as possible, and then transition to the stress factored curve by approximately $5\times10^6$ cycles. The leaflet describes a qualitative approach to producing the safe curve but numerical approaches may also be used. Further guidance on the safe S-N method including the selection of appropriate life and stress factors may be found in Leaflet 35. The mean S-N curves should be generated from representative element tests under constant amplitude loading to represent each of the features where failure may occur. The factors of 2.8 on (geometric) life and 1.49 on stress (mean fatigue limit) are commonly used in order to provide an equivalent to the fixed factor of 3.3 used for 1/1000 probability of failure. However, other factors may be used for different probabilities if desired, see for example Figure 16.

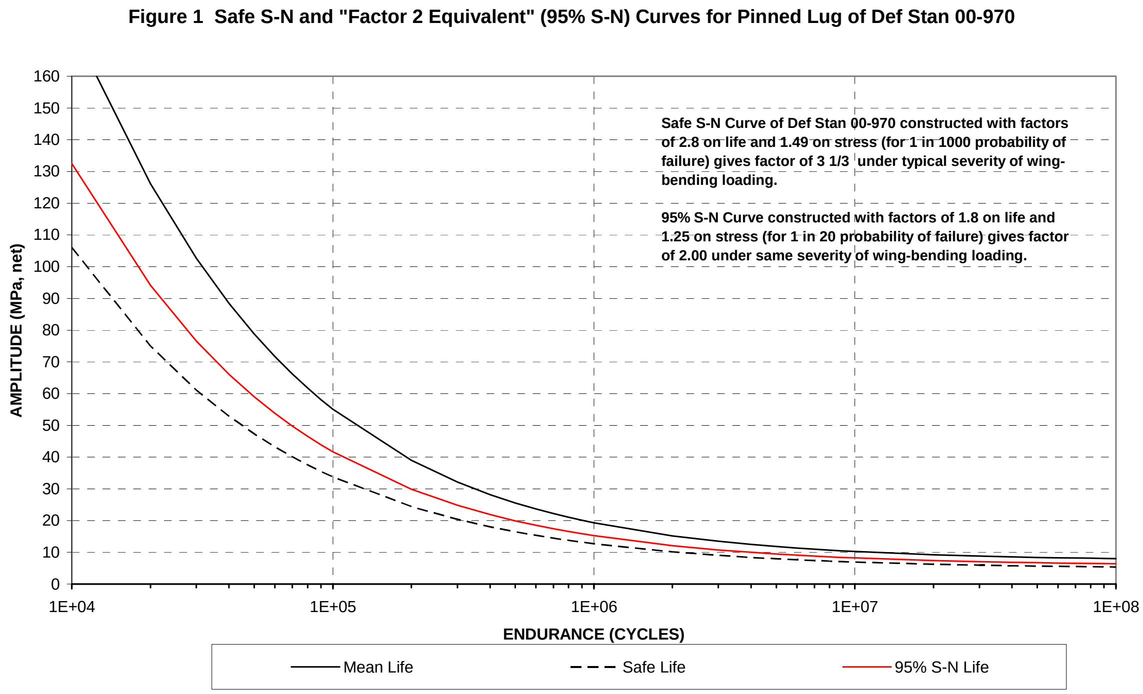


*Figure 16: Example Mean, Safe and 'Factor 2 Equivalent' Curves*

DSTO has developed a template with an underlying numerical procedure for the creation of safe S-N curves from mean S-N curves which will be described in [4] when published. This report also outlines the procedure for performing a safe S-N analysis which initially involves selecting an appropriate mean S-N curve that is representative of the critical location of interest. The relevant stress sequence is then scaled iteratively until its damage (using Miner's Rule with the mean S-N curve) is equivalent to a (for example) test demonstrated failure time. The safe S-N curve may then be used with the scaled sequence to determine the safe life. In the safe life results which follow, the FSFT total lives provided in Section 4.2 were used as the failure times to which the FSFT sequences were scaled. Once the scaling factors were determined, mean and safe lives were calculated for the FSFT and RAAF P-3C sequences at each FCA.

Mean and safe S-N curves have been generated for 7075-T6 aluminium sheet notched coupons with stress concentration factors of 2 and 4 (from [9]). Curves were also developed for a low-load transfer joint specimen made from 7010-T7651 aluminium. These mean and safe S-N curves are shown in Figure 17.

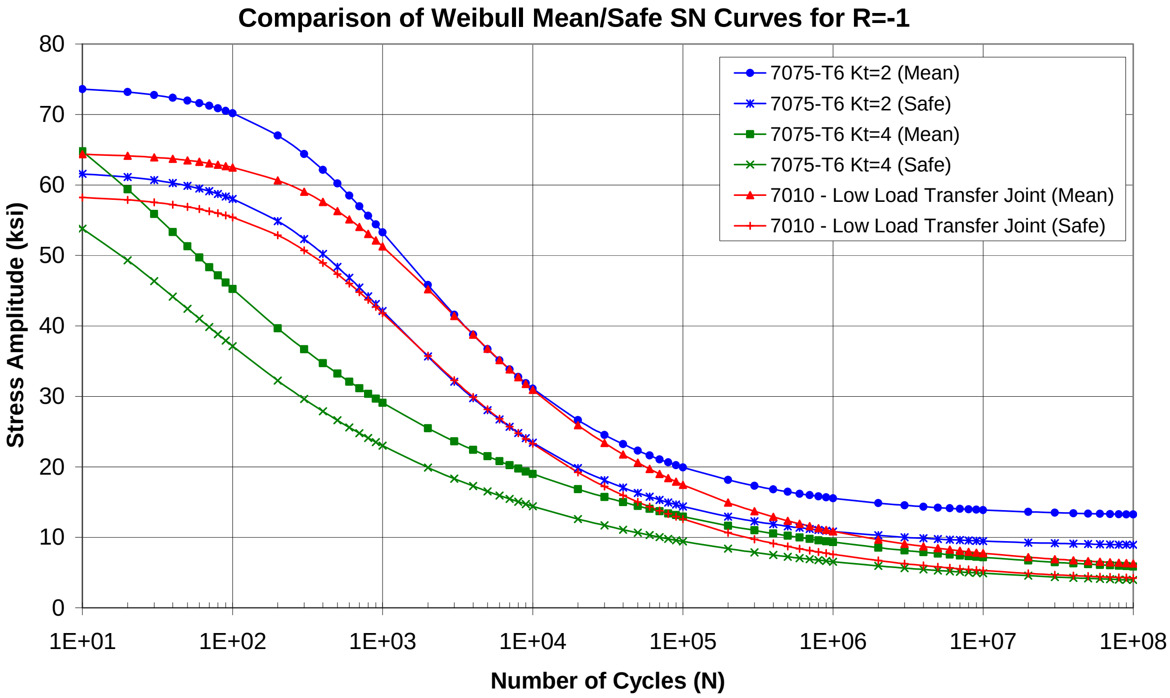


*Figure 17: Mean and Safe S-N Curves for Different $K_t$ Features*

### 5.1.2 Inspection Threshold

According to Leaflet 36 of [9], the time to first inspection or inspection threshold is normally equivalent to the safe life. Therefore, the calculation of Safe Life using the Safe S-N approach in this section will be used as the inspection threshold under the Def Stan 00-970 approach.

### 5.1.3 Inspection Interval

Again according to Leaflet 36, the inspectable life is the time of crack growth from a detectable crack size to a maximum acceptable size. The inspection interval is then the inspectable life divided by a factor of three (assuming monitored structure). Figure 18, taken from [9] shows this concept in graphical form. For this work in this report the detectable crack size is taken from the P-3 SLAP TI definition of 0.05" based on the performance of a bolt-hole eddy current inspection. The selection of maximum acceptable crack size under Def Stan 00-970 must take into account the considerations listed in Paragraph 5.3 of Leaflet 36, including onset of rapid crack growth, the maximum acceptable repair size or the loss of pressure or leakage. These considerations are satisfactorily covered by the 'obvious partial failure under limit load' criteria from AC 25.571-1C used in the P-3 SLAP TI work and so the maximum acceptable crack size used with the Def Stan 00-970 based methodology is equivalent to the critical crack size calculated in the P-3 SLAP TI reports. Note that the critical crack sizes were calculated at 1.0 x DLL but remain acceptable under Def Stan 00-970 in this case as DLL is an extreme event for the P-3. Therefore, based on these considerations, the inspection intervals may be calculated from the P-3 SLAP TI crack growth lives provided in Section 4.2, (ie the P-3 SLAP TI results obtained from using FASTRAN and the full scale test results) divided by three.

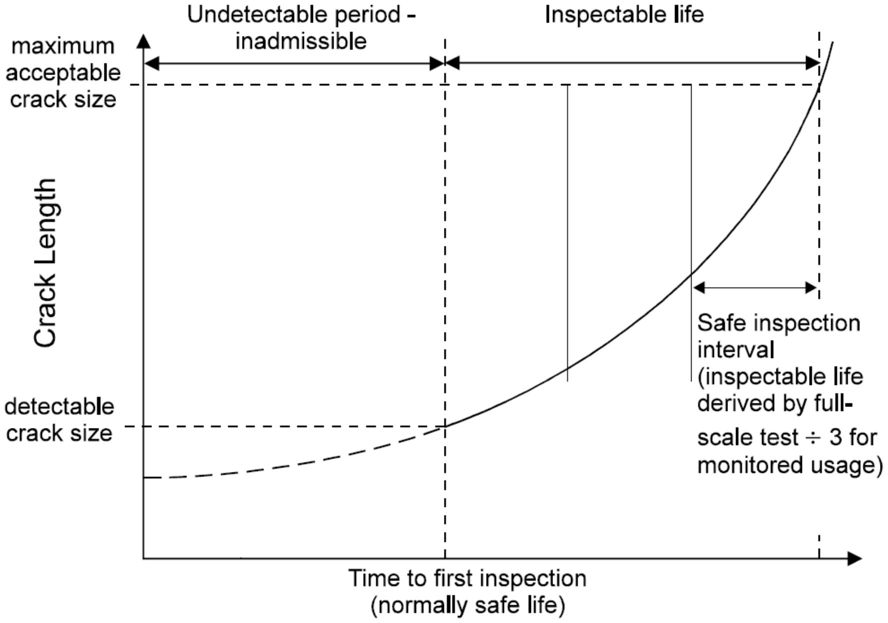


*Figure 18: Def Stan 00-970 Inspection Intervals (from [9])*

## 5.2 Results

For the wing and empennage FCAs Table 11 and Table 12 respectively provide the mean and safe lives for the FSFT and RAAF P-3C sequences based on the TI calculated total lives derived from the FSFT. The safe lives are also equivalent to the inspection thresholds for inspectable structure. For each FCA the calculations of safe life used two alternate safe curves in order to compare the results from two S-N curves that could be considered representative of the feature. The safe curve that requires the smallest scaling on stress would be considered the most applicable; however of interest is that the safe life results produced from the different stress-life curves produced quite similar lives, the biggest difference being 25% for FCA301.

Note that the empennage FCAs used the A041B FSFT sequence to determine the scaling factor. Also note that the FSFT mean hours shown in the tables below may not exactly equal the total lives of Section 4.2 because of a lack of precision in the scaling factor.

The inspectable lives and resulting inspection intervals are shown in Table 13 and Table 14 for each FCA and sequence.

*Table 11: Mean and Safe Lives based on Total Lives – Wing FCAs*

| FCA | Kt Config. | Scaling Factor | FSFT Lives (Hrs) | | RAAF P-3C Lives (Hrs) | |
|---|---|---|---|---|---|---|
| | | | Mean | Safe | Mean | Safe |
| 301-WEB-4 | 4.0 | 1.5238 | 36,756 | 5,638 | 78,300 | 12,026 |
| 301-WEB-4 | LLTJ | 1.9291 | 36,756 | 7,546 | 84,746 | 15,909 |
| 351-CDN-2 | 2.0 | 2.2605 | 26,147 | 6,379 | 90,629 | 19,412 |
| 351-CDN-2 | 4.0 | 1.4291 | 26,147 | 5,899 | 97,020 | 18,599 |
| 352-PDN-1 | 2.0 | 2.3743 | 18,530 | 4,065 | 72,720 | 15,327 |
| 352-PDN-1 | 4.0 | 1.5091 | 18,530 | 4,142 | 78,241 | 15,021 |
| 375-PSS-2 | 4.0 | 1.3701 | 66,041 | 12,724 | 294,302 | 47,201 |
| 375-PSS-2 | LLTJ | 1.8882 | 66,043 | 14,810 | 218,160 | 45,884 |

*Table 12: Mean and Safe Lives based on Total Lives – Empennage FCAs*

| FCA | Kt Config. | Scaling Factor | A041B Lives (Hrs) | | A041D Lives (Hrs) | | RAAF P-3C Lives (Hrs) | |
|---|---|---|---|---|---|---|---|---|
| | | | Mean | Safe | Mean | Safe | Mean | Safe |
| 811-1 | 4.0 | 1.2137 | 296,048 | 41,581 | 16,162 | 3,208 | 1,463,781 | 206,564 |
| 811-1 | LLTJ | 1.5578 | 296,167 | 45,634 | 24,662 | 6,195 | 1,510,287 | 212,724 |
| 811-2 | 2.0 | 2.1646 | 162,957 | 23,614 | 9,644 | 1,981 | 763,106 | 118,651 |
| 811-2 | 4.0 | 1.3263 | 162,955 | 24,568 | 9,461 | 2,012 | 813,933 | 121,990 |
| 886 – US | 4.0 | 4.0397 | 49,510 | 8,171 | 1,971 | 447 | 286,738 | 34,306 |
| 886 – Aus | 4.0 | 3.2694 | 231,512 | 30,476 | 8,381 | 1,693 | 1,692,703 | 142,475 |

*Table 13: Inspectable Lives and Inspection Intervals - Wing FCAs*

| FCA | FSFT (Hours) | | RAAF P-3C (Hours) | |
|---|---|---|---|---|
| | Insp. Life | Interval | Insp. Life | Interval |
| 301-WEB-4 | 26,860 | 8,953 | 7,984 | 2,661 |
| 351-CDN-2 | 6,790 | 2,263 | 8,240 | 2,747 |
| 352-PDN-1 | 3,466 | 1,155 | 3,956 | 1,319 |
| 375-PSS-2 | 51,560 | 17,187 | 11,960 | 3,987 |

*Table 14: Inspectable Lives and Inspection Intervals - Empennage FCAs*

| FCA | A041B (Hours) | | A041D (Hours) | | RAAF P-3C (Hours) | |
|---|---|---|---|---|---|---|
| | Insp. Life | Interval | Insp. Life | Interval | Insp. Life | Interval |
| 811-1 | 266,054 | 88,685 | 16,192 | 5,397 | 665,570 | 221,857 |
| 811-2 | 97,958 | 32,653 | 6,250 | 2,083 | 201,066 | 67,022 |
| 886 – US | 25,510 | 8,503 | 5,540 | 1,847 | 27,914 | 9,305 |
| 886 – Aus | 25,510 | 8,503 | 5,540 | 1,847 | 27,914 | 9,305 |

# 6. Life Calculations Using JSSG 2006

## 6.1 JSSG Durability and Damage Tolerance Overview

The United States DoD Joint Service Specification Guide JSSG 2006 [10] covers all aspects of military aircraft structures including structural strength and durability. This specification guide replaces the USAF Guide Specification AFGS-87221A and the USN MIL-S-8000 series of requirements for fatigue design and evaluation. The result is that both the USAF-originated damage tolerance approach and the USN safe life approach are included in the Guide. The flexibility in JSSG 2006 seems to be such that it allows USAF and US Navy to continue to take their preferred but different approaches.

Airframe lifing under JSSG 2006 follows a durability and damage tolerance approach. The guide specification provides a mixture of both design requirements and in-service management (inspection thresholds and intervals) requirements. Ideally all primary and secondary structure should possess sufficient durability to meet the design service life of the aircraft. Durable structure does not preclude cracking, but it must resist fatigue cracking throughout its service life to prevent adverse safety, economic, operational and maintenance costs. A durability limit may be determined through fatigue life analysis with a scatter factor, or via fracture mechanics where a typical initial flaw (i.e. 0.01″), should not grow to a crack length which would result in functional impairment in two lifetimes. A complete airframe durability test should be performed to demonstrate the structure meets the required service life. Durability testing should occur for two lifetimes under a severe spectrum followed by inspections of critical structure. If structural anomalies occur within two lifetimes of testing, then the deficient structure should either be modified or managed under a safety by inspection program.

The durability limit is not utilised to set the in-service inspection requirements. A damage tolerance analysis (DTA) should be undertaken for all safety of flight structure as 'USAF experience has shown that designing a durable structure is not sufficient to ensure safety of flight' [10]. The damage tolerance capability of the airframe should be sufficient for the life of the aircraft and the structure should also possess adequate residual strength in the presence of flaws for specified periods of service usage. All safety of flight structure should be classified as either slow crack growth or fail-safe. Single load path structure without crack arrest features is classed as slow growth structure. Structure with multiple load paths and crack arrest features may be classed as either slow crack growth or fail-safe. Inspection intervals are normally half the minimum period of safe unrepaired service usage depending on the inspectability of the structure. The calculation of inspection intervals for slow growth structure is different to fail-safe structure for which the additional growth in the adjacent element may also be included. One lifetime of damage tolerance testing using a baseline spectrum should be performed to verify crack growth rate predictions and a structural teardown and inspection should occur at the end of such testing.

## 6.2 USAF Approach

The USAF typically derive their in-service management actions from the crack growth-only approach set out under JSSG 2006 Section A3.12 Damage Tolerance.

### 6.2.1 Inspection Thresholds and Intervals

The P-3 critical areas examined in this report are categorised as multiple load path with crack arrest features and so could be designated as slow crack growth structure or fail-safe structure. Fail safe structure allows the calculation of crack growth time from initial flaw to the crack growth limit to include a period of crack growth in an adjacent member after failure of the primary member. Just how much time is allowed for growth in the secondary member depends upon whether the structure is classified under JSSG rules as multiple load path dependent structure, multiple load path independent structure or crack arrest structure and is a result of different flaw size requirements and allowable degrees of inspectability. Figure 19 provides a diagram showing the calculation of crack growth for fail-safe multiple load path dependent structure.

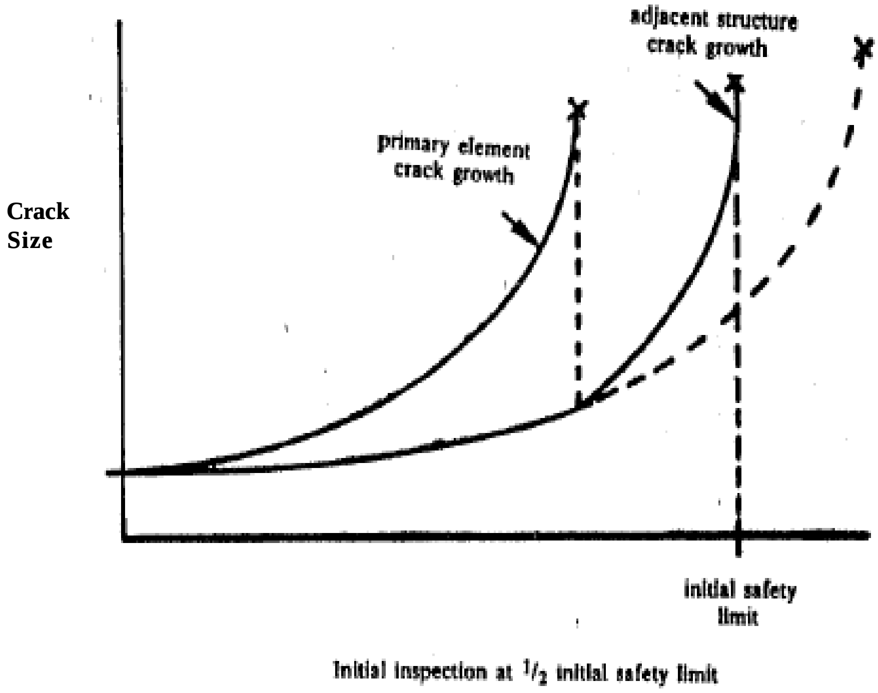


*Figure 19: Inspection Threshold and Crack Growth for Fail-Safe Multiple Load Path Dependent Structure, from JSSG 2006 [10].*

For the P-3 wing, the evidence from the P-3 SLAP TI supporting work was that any growth time post the failure of the primary element was insignificant compared to the total crack growth time. So for the same reasons used in the TI, i.e. avoiding unnecessary complication, and avoiding the possibility of large multi-element cracks, the damage growth limits in this analysis are again restricted to the failure of the primary element. Consequently, under JSSG 2006 the inspection intervals were calculated using a slow crack growth approach. The initial flaws sizes are taken from Table XXX 'Initial Flaw Assumptions' of JSSG 2006 to be a 0.05″ corner flaw from a hole for all FCAs except FCA811-2 and FCA886, where a semicircular surface flaw with a depth of 0.12″ was assumed (an approximation as JSSG actually calls for a 0.125″ deep flaw). The crack growth intervals (again taken from Section 4.2 and originating from the DSTO P-3 SLAP TI and using FASTRAN) from $a_{init}$ to $a_{crit}$ were divided by 2 and the results are presented in Table 15 for each FCA.

In the standard USAF approach, the inspection interval for slow growth structure is also the time of the first inspection; see A3.12.2.c and A.3.12.2.1 of [10]. For FCA811-2 there are no inspection intervals in Table 15 as $a_{crit}$ = 0.12", ie the starting crack size in Figure 14 is the same size as the critical crack size. If a DTA had been conducted as part of the aircraft design it could have been expected to lead to a re-design of the part. For in-service structural integrity, this location therefore cannot be managed via a standard USAF DTA approach unless an $a_{ndi}$ less than 0.12" could be justified. In this example, the location is in fact difficult to inspect but might be amenable to eddy current inspection with a smaller $a_{ndi}$.

### 6.2.2 Results

The resulting inspection thresholds and recurring intervals using the USAF approach in JSSG 2006 are given in Table 15.

*Table 15: JSSG 2006 (USAF Approach) Inspection Thresholds and Intervals*

| FCA | Sequence | Crack Growth $a_{init}$ to $a_{crit}$ (AFHRS) | Inspection Threshold (AFHRS) | Inspection Interval (AFHRS) |
|---|---|---|---|---|
| 301-WEB-4 | FSFT | 26,860 | 13,430 | 13,430 |
| | RAAF AP-3C | 9,344 | 4,672 | 4,672 |
| | RAAF P-3C | 7,984 | 3,992 | 3,992 |
| 351-CDN-2 | FSFT | 6,790 | 3,395 | 3,395 |
| | RAAF AP-3C | 11,444 | 5,722 | 5,722 |
| | RAAF P-3C | 8,240 | 4,120 | 4,120 |
| 352-PDN-1 | FSFT | 3,466 | 1,733 | 1,733 |
| | RAAF AP-3C | 5,612 | 2,806 | 2,806 |
| | RAAF P-3C | 3,956 | 1,978 | 1,978 |
| 375-PSS-2 | FSFT | 51,560 | 25,780 | 25,780 |
| | RAAF AP-3C | 15,416 | 7,708 | 7,708 |
| | RAAF P-3C | 11,960 | 5,980 | 5,980 |
| 811-1 | FSFT A041B | 266,054 | 133,027 | 133,027 |
| | FSFT A041D | 16,192 | 8,096 | 8,096 |
| | RAAF AP-3C | 634,148 | 317,074 | 317,074 |
| | RAAF P-3C | 665,570 | 332,785 | 332,785 |
| 811-2 | FSFT A041B | 0 | 0 | 0 |
| | FSFT A041D | 0 | 0 | 0 |
| | RAAF AP-3C | 0 | 0 | 0 |
| | RAAF P-3C | 0 | 0 | 0 |
| 886 – USN | FSFT A041B | 19,350 | 9,675 | 9,675 |
| | FSFT A041D | 4,026 | 2,013 | 2,013 |
| | RAAF AP-3C | 33,518 | 16,759 | 16,759 |
| | RAAF P-3C | 20,522 | 10,261 | 10,261 |
| 886 – Aus | FSFT A041B | 19,350 | 9,675 | 9,675 |
| | FSFT A041D | 4,026 | 2,013 | 2,013 |
| | RAAF AP-3C | 33,518 | 16,759 | 16,759 |
| | RAAF P-3C | 20,522 | 10,261 | 10,261 |

## 6.3 USN Approach

The USN approach traditionally determines life based on the time to initiate a 0.010″ crack. This crack initiation time is then factored by two to derive the safe life. This approach was used by L-M for their test interpretation work for the USN. The safe life is then given a value of 1 or 100% of a Fatigue Life Index in an Individual Aircraft Tracking (IAT) system. For the P-3 SLAP the USN subsequently departed from their traditional IAT approach by adopting a TLI or Total Life Index approach using FASTRAN as the life calculation tool.

In this section, safe lives are calculated for the P-3 wing FCAs only. The determination of the crack initiation life at 0.010″ follows the same process as employed in the wing/fuselage TI report [1] to calculate the 0.05″ crack initiation life. Table 16 summarises the 0.010″ crack initiation lives and associated $K_N$ values at each FCA for the FSFT spectrum. Note that the FSFT defect information in Table 16 are from Appendix A, the FASTRAN lives were obtained from crack growth curves provided in [1], while the $K_N$ values were determined from FAMS fatigue life curves also provided in [1]. The RAAF crack initiation lives (determined from the FAMS fatigue life curves of [1] at the appropriate $K_N$ value) and resulting safe lives are provided in Table 17. The inspection intervals determined under the USN approach are consistent with the method used by the USAF, see Table 15 and therefore will not be separately listed.

*Table 16: Determination of the Test Demonstrated $K_N$ ($K_{N-TD}$) for 0.010"*

| FCA | FSFT | | FASTRAN | | | FSFT | $K_{N-TD}$ |
|---|---|---|---|---|---|---|---|
| | SFHRS Defect Found ($t_{test}$) | Crack Size when found | $t_{a=test}$ | $t_{a=0.010}$ | $\Delta t_{FASTRAN}=\Delta t_{test}$ ($t_{a=test}-t_{a=0.010}$) | $t_{a=0.010}$ ($t_{test}-\Delta t_{test}$) | |
| 301-WEB-4 | 38,000 | 0.941 | 41,127 | 9,813 | 31,314 | 6,686 | 6.56 |
| 351-CDN-2 | 22,613 | 0.15 | 22,245 | 15,217 | 7,028 | 15,585 | 4.68 |
| 352-PDN-2 | 16,785 | 0.13 | 5,656 | 1,227 | 4,429 | 12,356 | 4.92 |
| 375-PSS-2 | 48,988 | 0.478 | 49,157 | 6,101 | 43,056 | 5,932 | 6.43 |

*Table 17: JSSG 2006 (USN Approach) Inspection Thresholds (Safe Life)*

| FCA | Sequence | Life at 0.01″ (AFHRS) | Safe Life (AFHRS) |
|---|---|---|---|
| 301-WEB-4 | FSFT | 6,686 | 3,343 |
| | RAAF AP-3C | 7,850 | 3,925 |
| | RAAF P-3C | 5,900 | 2,950 |
| 351-CDN-2 | FSFT | 15,585 | 7,793 |
| | RAAF AP-3C | 23,700 | 11,850 |
| | RAAF P-3C | 16,600 | 8,300 |
| 352-PDN-1 | FSFT | 12,356 | 6,178 |
| | RAAF AP-3C | 20,500 | 10,250 |
| | RAAF P-3C | 15,300 | 7,650 |
| 375-PSS-2 | FSFT | 5,932 | 2,966 |
| | RAAF AP-3C | 9,450 | 4,725 |
| | RAAF P-3C | 7,850 | 3,925 |

# 7. Life Calculations Using Probability Analysis

## 7.1 Probability Analysis Overview

Many of the initial inspection thresholds calculated in the DSTO P-3 wing/fuselage TI report [1] were considered overly conservative. This assessment was based on known conservatism built into the TI process (i.e. the use of the most severe failure on either the left hand or right hand wing as a peg for the subsequent average life analysis) and the smaller number of cracks than expected that were subsequently found in fleet aircraft which had over-flown the calculated thresholds. An opportunity was therefore identified to extend the inspection thresholds in the P-3 SMP [3] and give relief to the RAAF P-3 fleet. Given the considerable amount of P-3 fleet inspection data available, a probabilistic approach described in [14] was deemed a suitable method for threshold extension.

The probabilistic approach was simplistic in its methodology as it assumed the fleet inspection findings (in terms of AFHRS) are log-normally distributed, and that the aircraft inspected are a representative sample of the fleet. From this information it was then possible to determine the probability of cracking in the fleet. Furthermore, if the relative severity between two fleets, fleet A and fleet B, is known, then it is possible to calculate the probability of cracking versus AFHRS for fleet B from the data from fleet A.

Care must be taken in this method to ensure that aircraft whose usage is significantly different to the fleet average are not allowed to skew the analysis. Isolated aircraft that have flown an overly severe mission mix (i.e. test flight aircraft) or benign mission mix (i.e. solely VIP flying) should be (and were) excluded from the analysis.

From the fleet inspection data the percentage of aircraft with cracks and the average AFHRS of the aircraft with cracks may be calculated for a given FCA. With this data point and the application of an appropriate standard deviation, a plot of cumulative probability versus log AFHRS may be created. This plot will then allow the determination of the AFHRS associated with a given probability such as 1/1000. Alternatively, the probability of cracking may be determined for a selected number of AFHRS. Application of a relative severity factor between two fleets allows the calculation of probabilities versus AFHRS for the second fleet. In the case of the analysis conducted in [3], the USN fleet results had to be converted to results under RAAF severity.

### 7.1.1 Fatigue Life Variability

Scatter in fatigue is represented by the value of standard deviation of the assumed normal population. Sufficient data was available from a number of FCA locations that had been inspected in the USN fleet to determine their individual standard deviations. Each individual aircraft could be plotted and the slope of the line on the probability graph could be determined. This was done in Reference 26 of the SMP [3], with the majority of the resulting standard deviation values falling between 0.15 and 0.18. A couple of FCA locations outside this range produced higher and lower values of standard deviation however this was judged to be the result of limited amounts of data. For the majority of the FCA locations examined in [3] the conservative end of the range was used in the subsequent probabilistic based

calculations of safe life. For locations where a large amount of data was available, and the dome nut holes of FCA352 were an example, the standard deviation value obtained for that particular FCA was used (0.15 in the case of FCA352). Note that these values of standard deviation represent scatter in cracking in a fleet of aircraft. This scatter is made up of two elements, the underlying scatter in material performance, and the scatter in usage severity of the individual aircraft about the fleet mean.

### 7.1.2 Variations in Simplicity and the Addition of Crack Growth

The most simplified version of the method assumes all cracks are of the same size. This limitation could be overcome with the provision of a suitable crack growth curve. Cracks could then be regressed back to a selected baseline crack length and the associated AFHRS determined. If it is not possible to regress the cracks back to a baseline length, it is conservative to assume that all cracks are equal to the largest crack. From this approach graphs showing Probability of Cracking versus Flight Hours can be produced.

The probability of component failure can also be determined. This is done by the addition of the crack growth time from a baseline crack length to the $a_{crit}$ value (calculated using the FASTRAN crack growth curves for the FCA). This then allows Probability of Failure versus AFHRS to be plotted.

The probabilistic method and its assumptions are explained in more detail in [6]. Guidance for using the template developed for this analysis may also be found in this reference.

The results taken from [3] for the probability analyses for the four lower wing locations (FCA301-WEB-4, FCA351-CDN-2, FCA352-PDN-1 and FCA375-PSS-2) are included below. Analysis was not possible for the empennage locations as fleet inspections programs have not been performed for these locations at this time. Probability analysis was only performed for the RAAF P-3C sequence. As the fleet failure data came from the USN, a value of relative severity between the USN average usage sequence and the RAAF P-3C sequence was generated for each FCA. These calculations were done using FAMS, as the cracks found in the fleet were generally small.

## 7.2 Results

The results for the four wing locations taken from [1] are given in this Section, including probability of cracking (equivalent to the size found in the USN fleet which was generally small) and the probability of failure which included the period of calculated permissible crack growth to $a_{crit}$. Although the AFHRS to different values of probability of cracking can be derived from the plots (two are shown), only the AFHRS to probability of failure of 1/1000 have been carried forward to the comparison table in Section 10.1.

### 7.2.1 FCA301-WEB-4

| | |
|---|---|
| Aircraft Inspected | 62 * |
| Inspected Aircraft Log Average AFHRS | 15,823 |
| Aircraft with cracks | 11 * |
| Largest detected crack | 1.5″ (regressed to 0.13″) |

*USN BuNo. 160290 was also inspected and found to be cracked in this location. However this is a test aircraft and the flight spectrum is not representative of fleet flying, and therefore was not considered in the analysis.

| | |
|---|---|
| AFHRS where 1/40 probability of cracking occurs | 13,602 |
| AFHRS where 1/1000 probability of failure occurs | 14,215 |

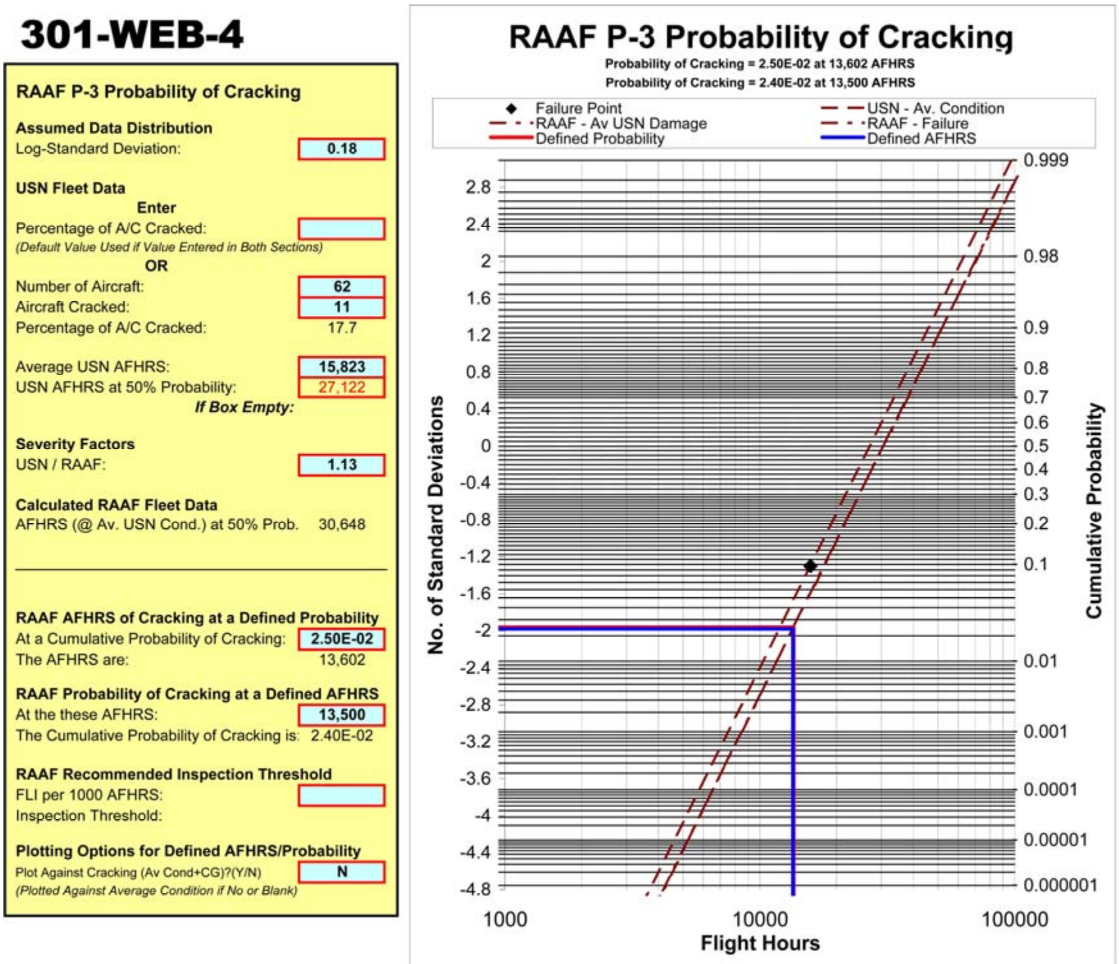


*Figure 20: FCA301-WEB-4 Probability of Cracking Plot*

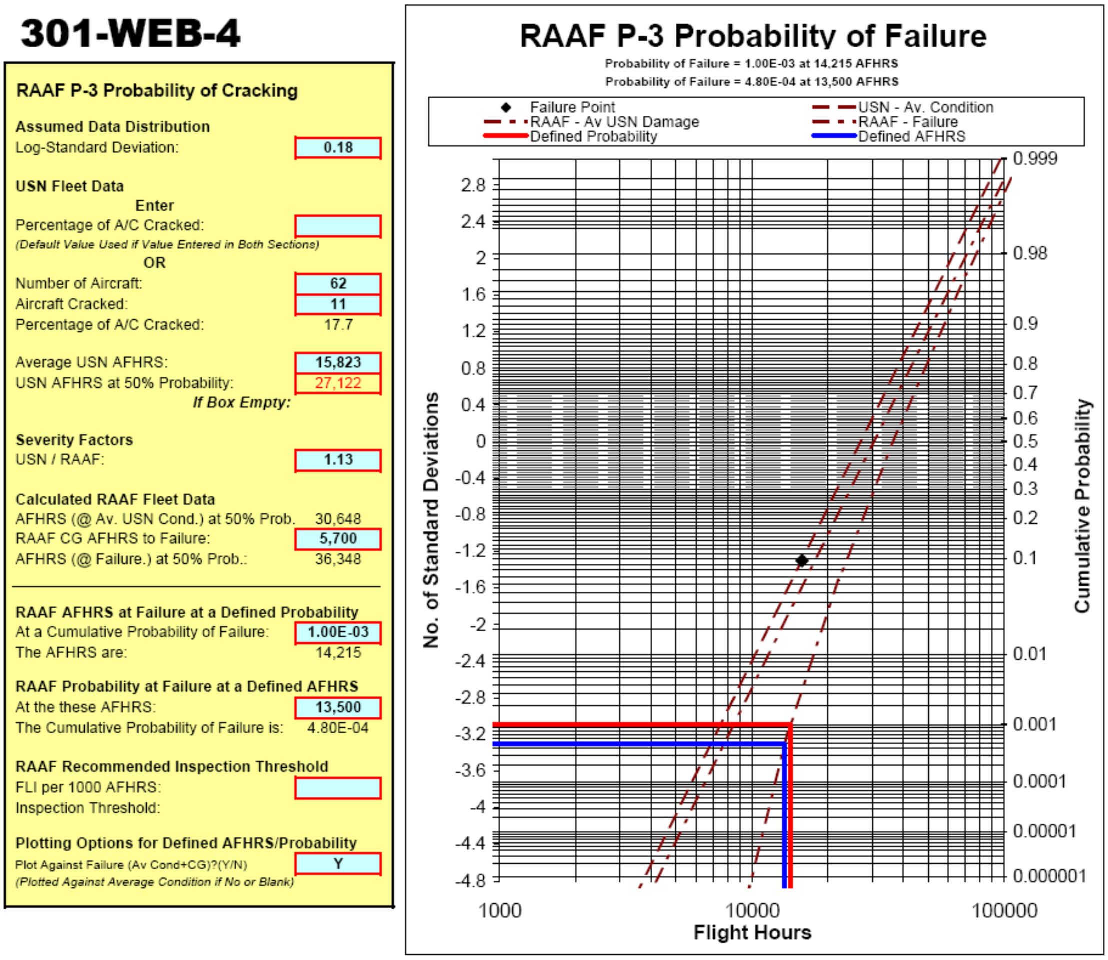


*Figure 21: FCA301-WEB-4 Probability of Failure Plot*

### 7.2.2 FCA351-CDN-2

| | |
|---|---|
| Aircraft Inspected | 68 |
| Inspected Aircraft Log Average AFHRS | 19216 |
| Aircraft with cracks | 6 |
| Largest detected crack | 0.169″ |
| | |
| AFHRS where 1/40 probability of cracking occurs | 19,615 |
| AFHRS where 1/1000 probability of failure occurs | 15,979 |

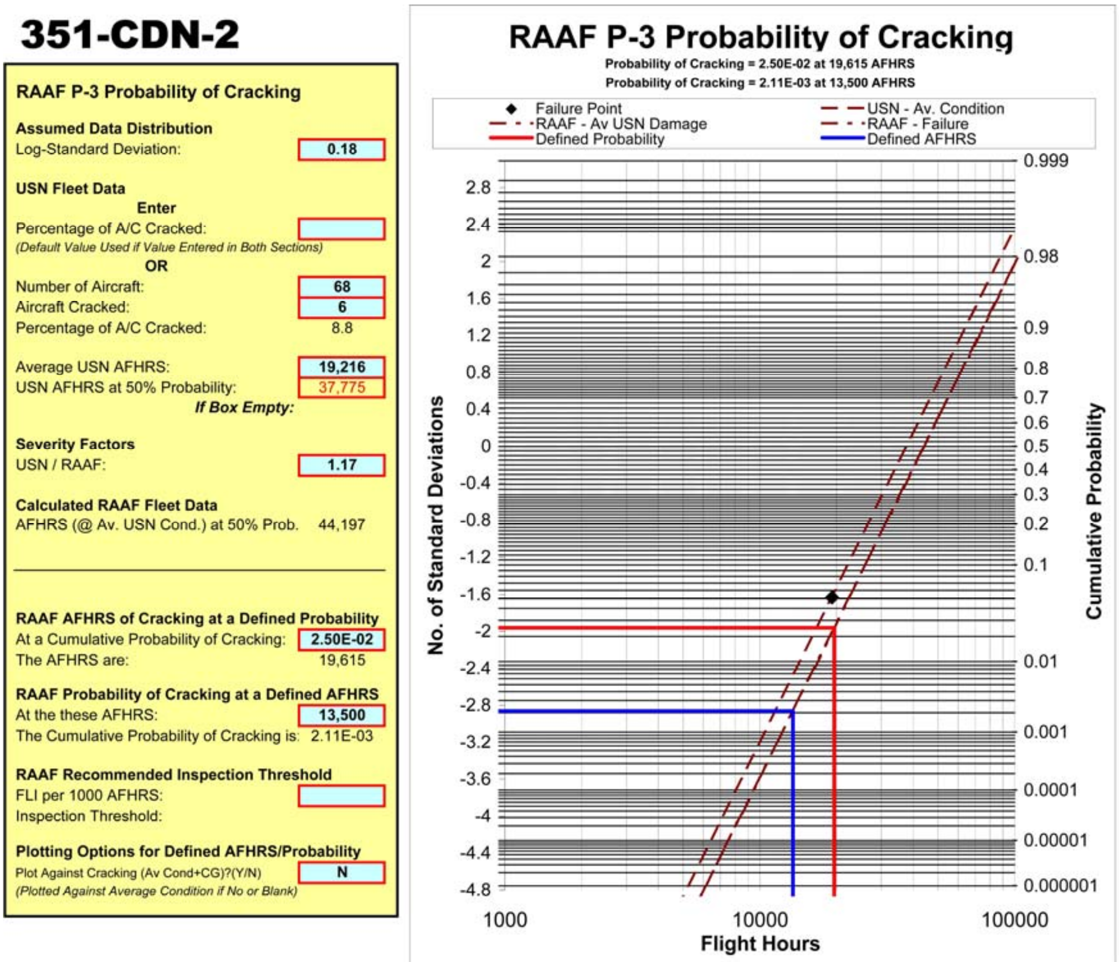


*Figure 22: FCA351-CDN-2 Probability of Cracking Plot*

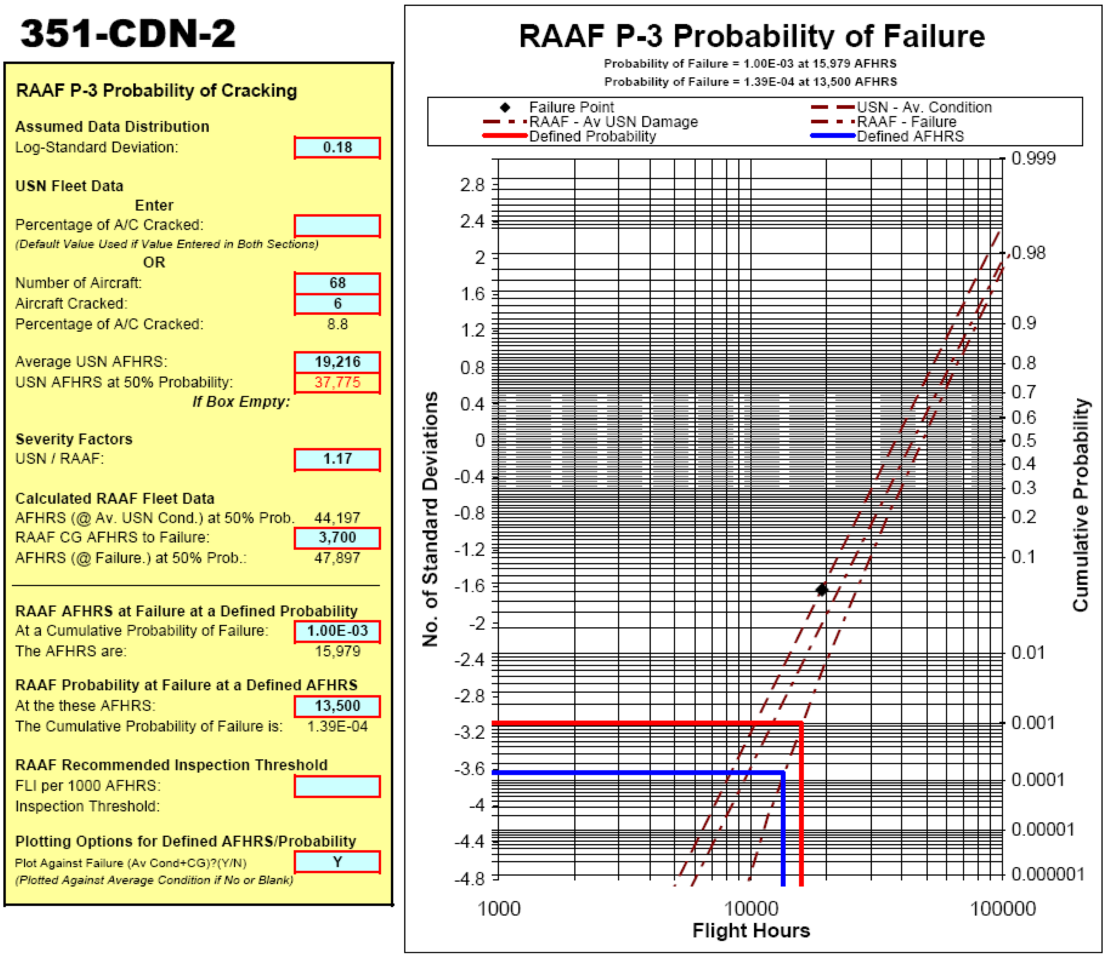


*Figure 23: FCA351-CDN-2 Probability of Failure Plot*

### 7.2.3 FCA352-PDN-1

| | |
|---|---|
| Aircraft Inspected | 101 * |
| Inspected Aircraft Log Average AFHRS | 17,241 |
| Aircraft with cracks | 45 * |
| Largest detected crack | 0.25″ (regressed to 0.13″) |

*USN BuNo 160290 was also inspected and found to be cracked in this location. However this is a test aircraft and the flight spectrum is not representative of fleet flying, and therefore was not considered in the analysis.

| | |
|---|---|
| AFHRS where 1/40 probability of cracking occurs | 13,265 |
| AFHRS where 1/1000 probability of failure occurs | 12,078 |

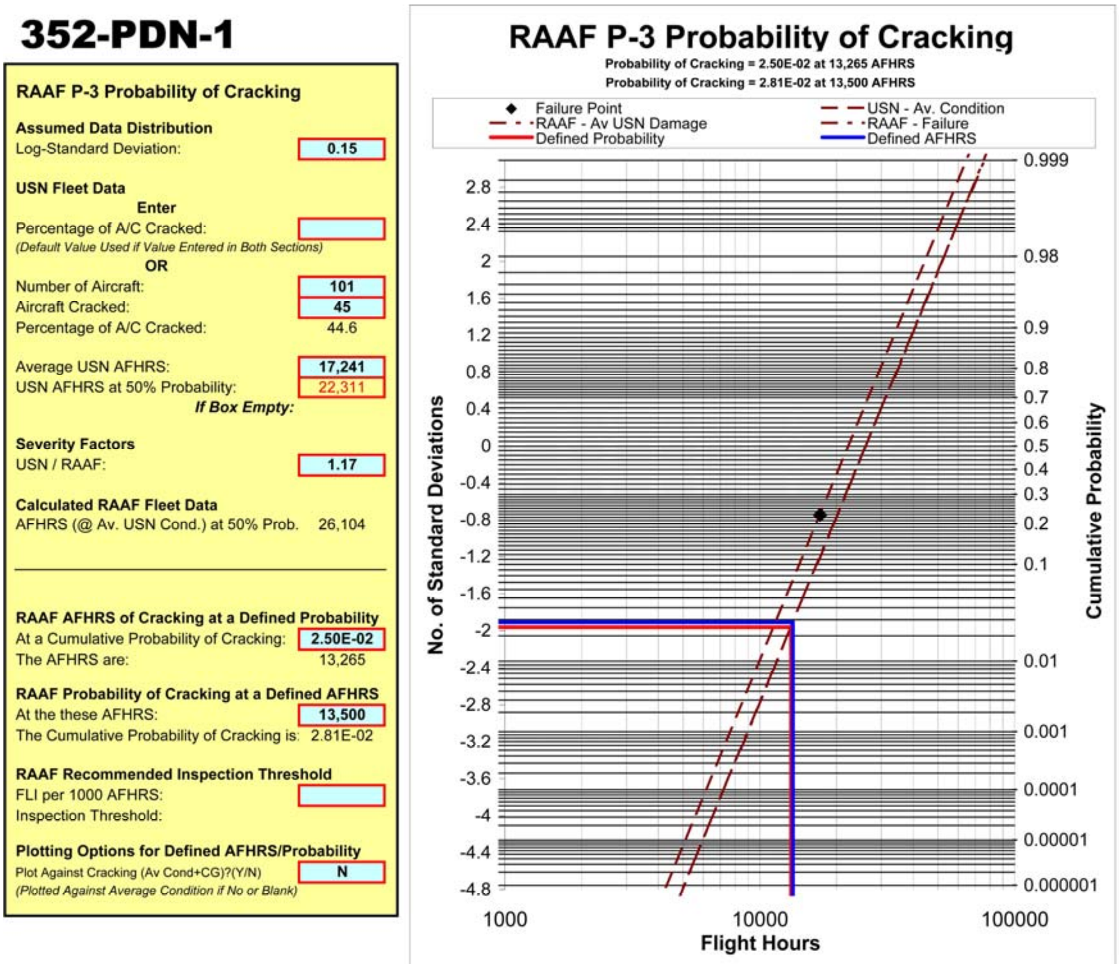


Figure 24: FCA352-PDN-1 Probability of Cracking Plot

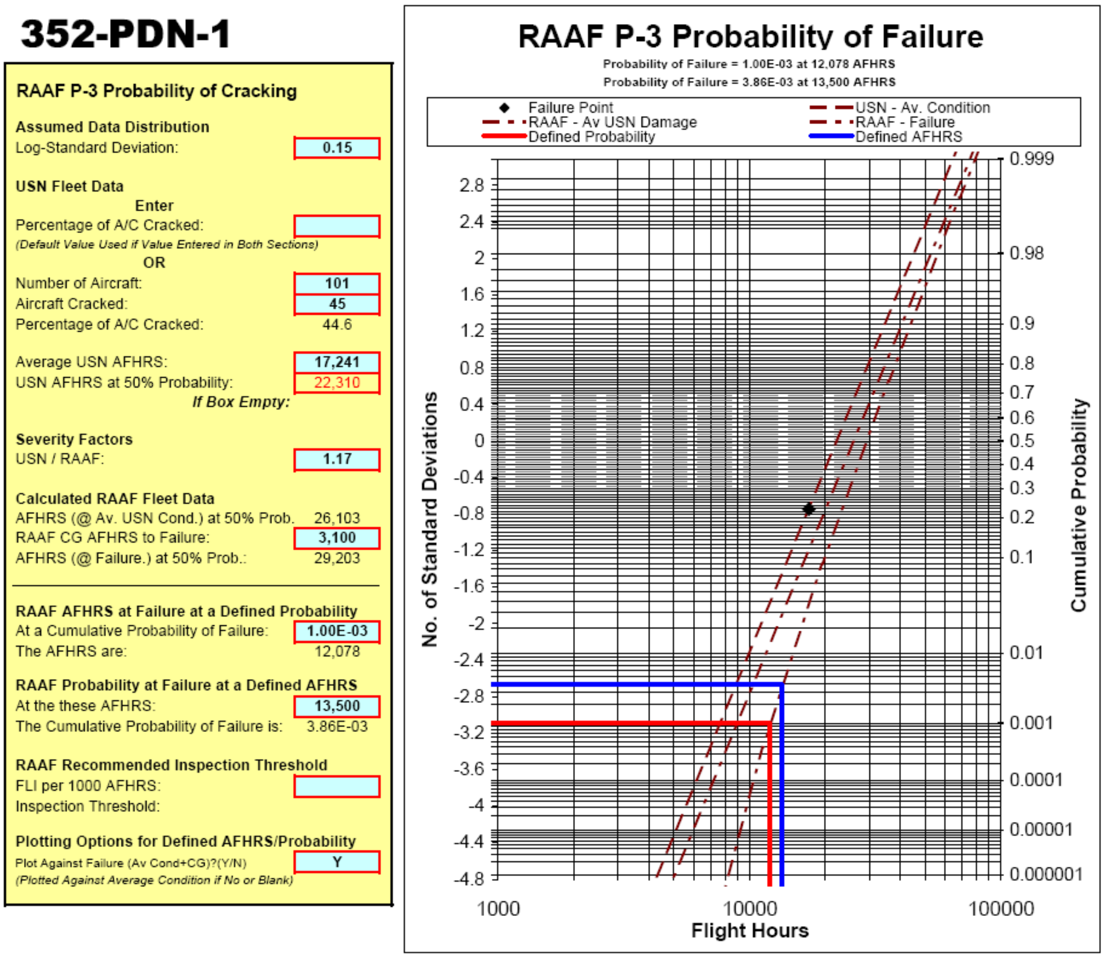


*Figure 25: FCA352-PDN-1 Probability of Failure Plot*

### 7.2.4 FCA375-PSS-2

| | |
|---|---|
| Aircraft Inspected | 12 |
| Inspected Aircraft Log Average AFHRS | 18,199 |
| Aircraft with cracks | 4 |
| Largest detected crack | 0.03″ |
| | |
| AFHRS where 1/40 probability of cracking occurs | 12,780 |
| AFHRS where 1/1000 probability of failure occurs | 22,300 |

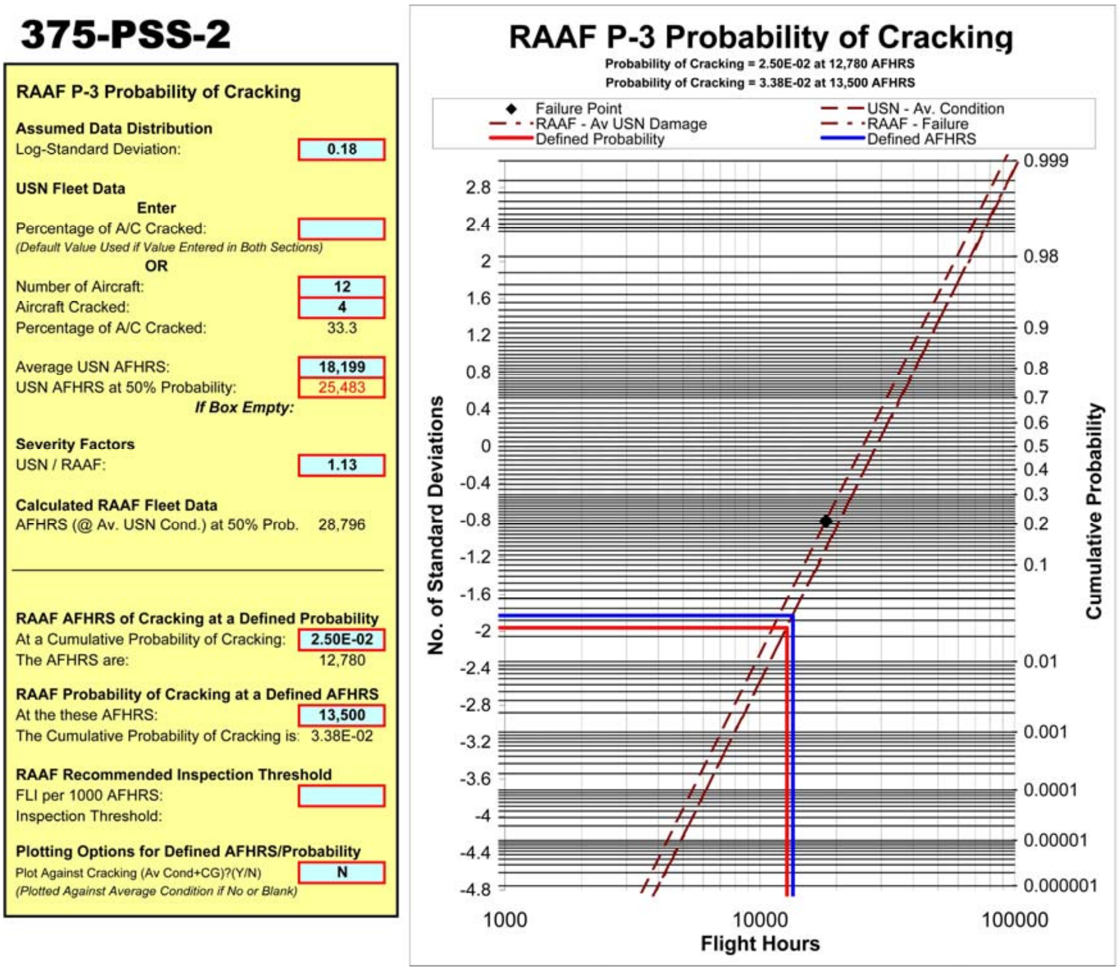


*Figure 26: FCA375-PSS-2 Probability of Cracking Plot*

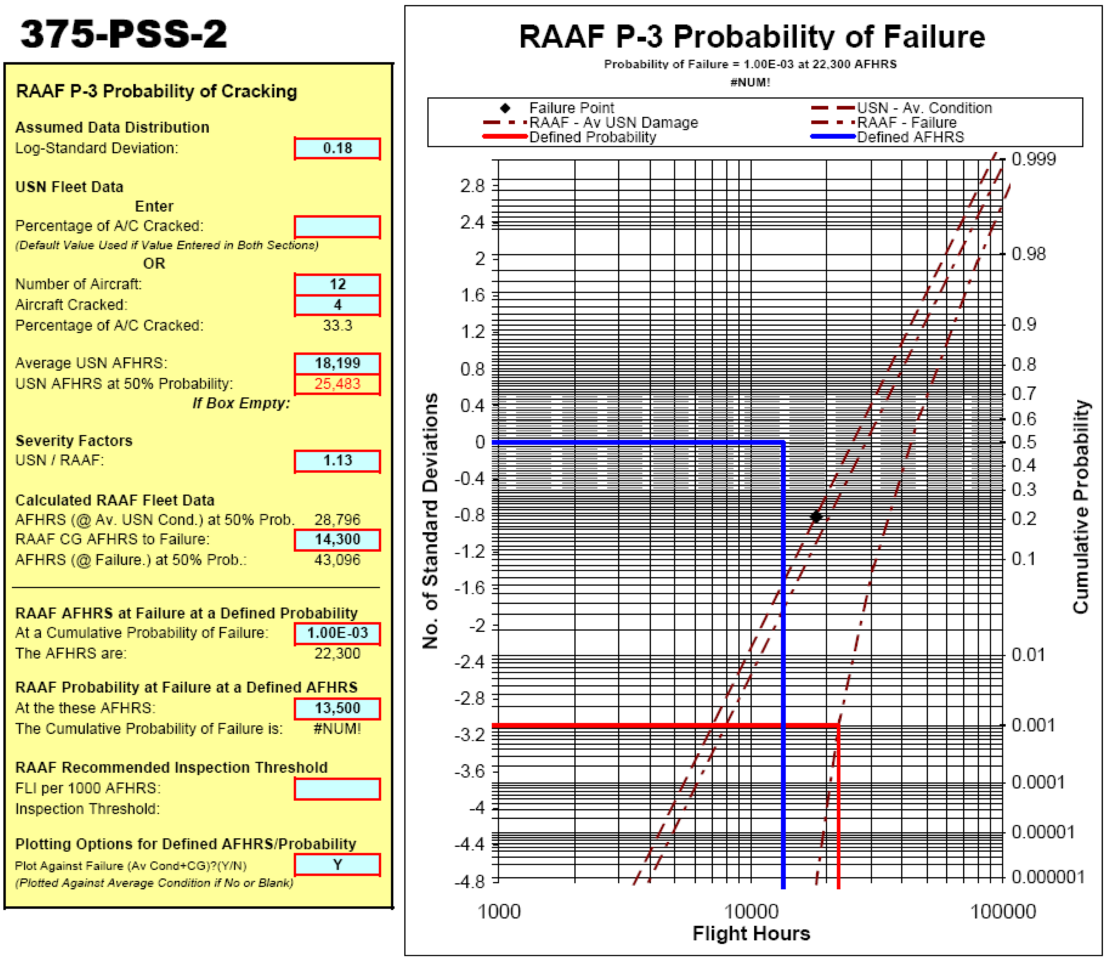


*Figure 27: FCA375-PSS-2 Probability of Failure Plot (Note: the probability of failure at the defined AFHRS of 13,500 is not calculated)*

# 8. Life Calculations Using the Effective Block Approach

## 8.1 Overview of EBA

The so-called effective block approach (EBA) has been proposed recently within DSTO to address the experimentally observed growth rates of fatigue cracks at critical locations on F/A-18 airframes, [15] and [16]. It was claimed that the growth of these cracks in structures made of 7050 aluminium alloy could not be adequately predicted using classical models such as Paris law or the plasticity-induced crack closure models based on constant amplitude (CA) crack growth rates (CGR). The EBA approach treats each program block of spectrum load as a single cycle of equivalent crack growth. In essence, this approach replaces the complexity of calculating cycle-by-cycle load sequence effects with a single cycle that incorporates the combined result. The assumption is that the sequence effect will be consistent from block-to-block as the crack grows. The CGR is expressed in a similar equation to that of the Paris law, with two model parameters; the crack growth coefficient (*C*) and the Paris-like exponent (*m*) determined by fitting the crack growth rate data obtained from spectrum loading experiments. However, since each individual spectra is equivalent to a unique cycle, these model parameters are expected to be dependent on the particular spectrum and the stress level as well as the geometry and the material through which the crack passes. A procedure was then devised to allow the use of the EBA model parameters obtained under one load spectrum (the tested spectrum) to predict the crack growth under a different load spectrum (the untested spectrum). This procedure relies on the relative severity of these two spectra being determined using an independent third-party model or tool such as FASTRAN. An initial crack size $a_0$ either needs to be assumed initially, or derived by back projection from the tested spectrum and assumed to be the same for the untested spectrum. The EBA has been shown to produce crack growth curves that correlate well with the experimental results for the F/A-18 cases studied [16]. A full explanation of the EBA may be found in [11].

EBA based predictions using P-3 coupon test data and for a natural crack that developed on the P-3 SLAP wing/fuselage test article are provided in the following sections.

## 8.2 EBA Life Predictions from P-3 Coupon Test Data

NLR conducted a coupon test program [17] to assist with the interpretation of the P-3 SLAP wing/fuselage FSFT for the SLAP customers with average fleet usage different to the USN 85th percentile 'severe' spectra used on the full scale tests (this included Australia). This same coupon data, see Figure 28, was also able to be used to evaluate the effectiveness of the EBA in predicting the total and crack growth lives of the RAAF P-3C FCA361 sequence. FCA361 is very similar in terms of spectra and structural configuration to FCA351, essentially representing the chordwise row of dome nut holes just outboard of the inboard nacelle that mirror the row inboard of the inboard nacelle covered by FCA351 and FCA352. The determination of RAAF EBA lives may be found in [11]. These calculations are repeated in this report, and the predictions are shown graphically in Figure 29 and in Table 18 and Table 19 which contain the total lives and crack growth lives respectively. RAAF P-3C FCA361 lives are provided for averaged coupon data, and for the EBA using three different methods to determine the Paris-like exponent *m*. The initial crack size of 1.52E-5 m (0.0006") was obtained using exponential extrapolation of the data obtained under the FSFT spectrum, see Figure 28.

The final crack length, $a_f$ = 10 mm (0.394”), was chosen based on the typical final crack length observed from the coupons.

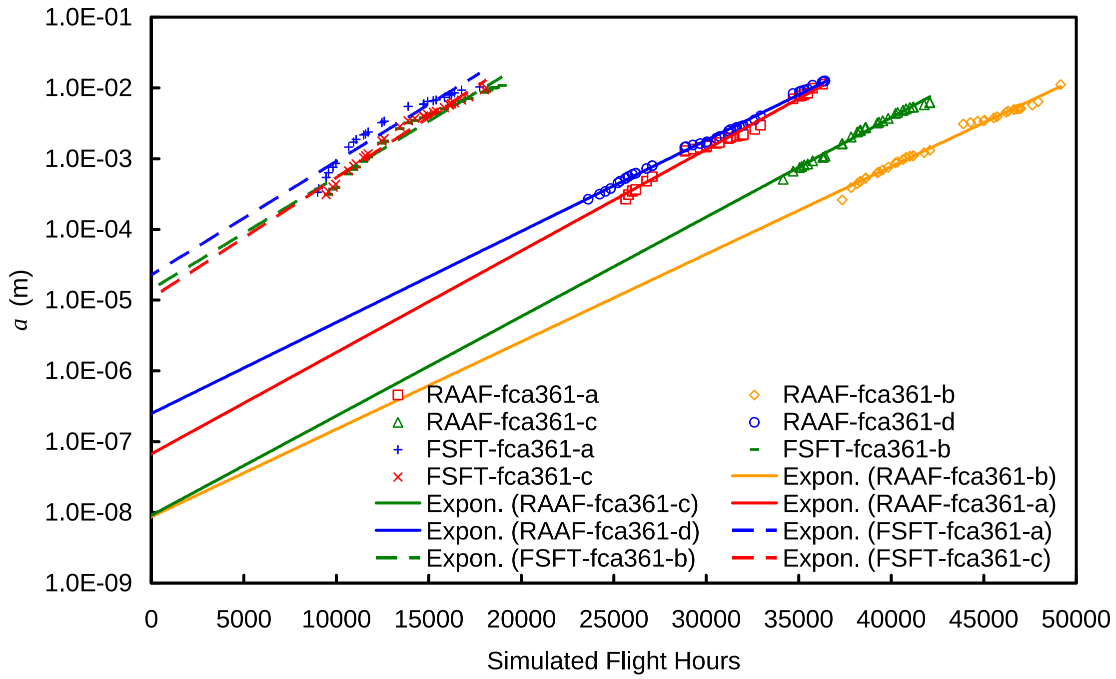


*Figure 28: Exponential Extrapolation to Evaluate $a_0$*

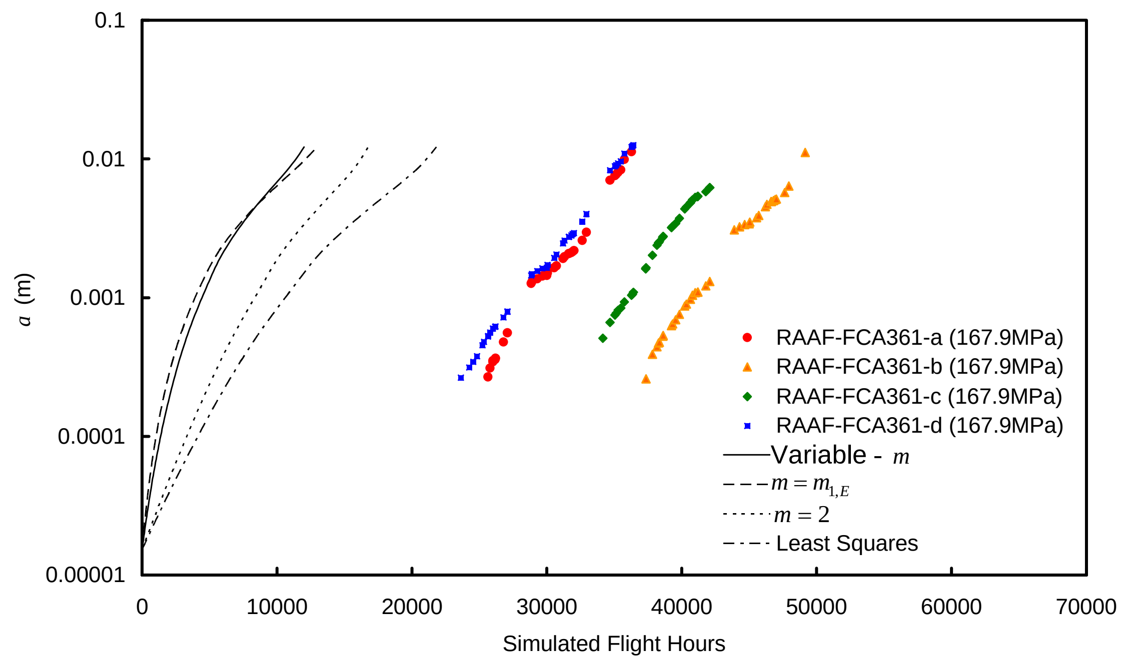


*Figure 29: EBA Predictions for RAAF P-3C FCA361 Spectrum using NLR Coupon Data*

*Table 18: Comparison of RAAF P-3C FCA361 Total Lives*

| | Total life ( $a_f$ = 10 mm(0.394")) (SFH) | Difference between the prediction and the RAAF coupon average (%) |
|---|---|---|
| RAAF Coupon average | 40986 | |
| EBA - Method 1: $m = 2$ | 16312 | 60.2% |
| EBA - Method 2: $m = m_{1,E}$ | 12262 | 70.1% |
| EBA - Method 3: Variable - $m$ | 11503 | 71.9% |

For the inspection interval calculations, an $a_{NDI}$ value of 1.27 mm (0.05") is consistent with the value used in the P-3 TI report and represents an effective NDI value for a bolt hole eddy current inspection.

*Table 19: Comparison of RAAF P-3C FCA361 Crack Growth Lives (Inspection Intervals)*

| | Life (1.27 mm – 10 mm (0.05" - 0.394")) (SFH) | Difference between the prediction and the RAAF coupon average (%) |
|---|---|---|
| RAAF Coupon average | 7444 | |
| EBA - Method 1: $m = 2$ | 7401 | 0.6% |
| EBA - Method 2: $m = m_{1,E}$ | 7890 | -6.0% |
| EBA - Method 3: Variable - $m$ | 6647 | 10.7% |

## 8.3 EBA Life Prediction from a P-3 FSFT Wing Test Crack

The EBA method was also trialled using a natural crack result from an aircraft structure. On the P-3 SLAP wing/fuselage FSFT article, a crack was found in the outer wing lower panel/cap splice location at WS 220 after 16,785 hours of cycling. This location is designated FCA361-PSS-4. An EBA analysis of this FSFT crack is described in detail in [11] including how the 15,000 hour P-3 FSFT load sequence was split into a number of smaller sub-blocks. A summary of the resulting predictions is shown graphically in Figure 30 and in Table 20 and Table 21 which contain the total lives and crack growth lives (i.e. inspection intervals) respectively. FSFT FCA361-PSS-4 lives are provided for the FSFT, FASTRAN and for the EBA using three different methods of calculating the Paris-life exponent *m*. Note that the FASTRAN prediction is pegged to the test life and is thus used only as a comparison in the calculation of inspection intervals.

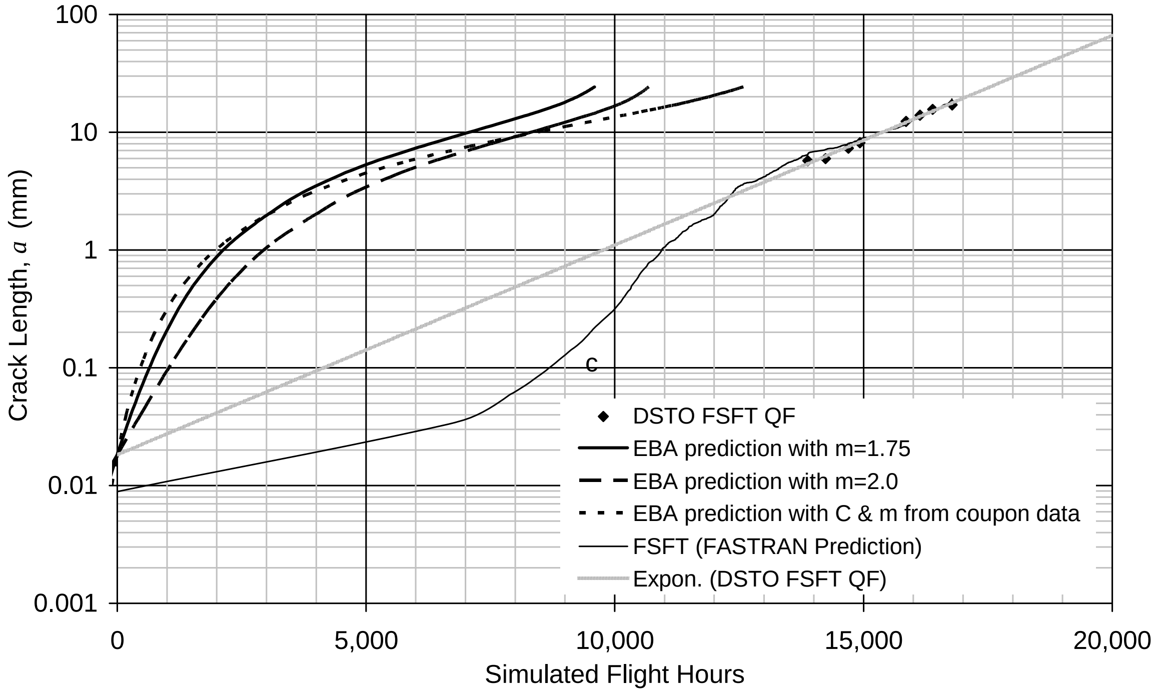


*Figure 30: EBA Predictions of a Crack discovered at FCA361-PSS-4 on the P-3 FSFT Article*

*Table 20: P-3 FSFT FCA361-PSS-4 EBA based total life predictions against fractographic data.*

| | *Total life (SFH $a_f$ = 17 mm)* | *Difference between the FSFT article and EBA predictions (%)* |
|---|---|---|
| FSFT article | 16785 | |
| EBA prediction with $m$ = 1.75 | 8826 | 47.4% |
| EBA prediction with $m$ = 2.00 | 10026 | 40.3% |
| EBA prediction with $C$ and $m$ evaluated from the coupon test data | 11144 | 33.6% |
| FASTRAN | | Pegged to final life |

*Table 21: P-3 FSFT FCA361-PSS-4 crack growth predictions against fractographic data*

| | *Life (5.7mm – 17mm) (SFH)* | *Difference between the FSFT article and EBA predictions (%)* |
|---|---|---|
| FSFT article | 2905 | |
| EBA prediction with $m$ = 1.75 | 3606 | -24.2% |
| EBA prediction with $m$ = 2.00 | 3642 | -25.4% |
| EBA prediction with $C$ and $m$ evaluated from the coupon test data | 5279 | -81.7% |
| FASTRAN | 3030 | -4.3% |

# 9. P-3 Coupon Test Results and Life Comparison

## 9.1 Coupon Test Program

### 9.1.1 Test Purpose

A coupon test program was performed subsequent to the DSTO TI work to provide experimental data against which the analytical results determined in the P-3 TI could be compared. Coupon and analytical results were compared for crack initiation (CI), crack growth and total lives. The coupon testing used the same spectra as the TI. The final versions of the various spectra had not previously undergone coupon testing. The aim of the comparison was to evaluate the accuracy of the TI tools FAMS and FASTRAN and the calibration process performed as part of the TI using early versions of the FSFT and RAAF spectra.

### 9.1.2 Coupon Test Description

Notched coupons with a $K_{t\,gross}$ of 5.0 were used in the test program as illustrated in Appendix D. These 'double ear' coupons were made from 7075-T6 aluminium bare sheet. Note that, whilst the coupon drawing specifies a coupon thickness of 3.175 mm (0.125"), due to availability of material the coupons were manufactured from sheet with thickness of 3.048 mm (0.12"). The coupons were manufactured by Boeing Australia.

Coupon testing utilised FSFT and RAAF P-3C and AP-3C sequences representative of stresses at FCA301 and FCA361. These two FCAs are located on the wing front spar lower cap of the P-3, with FCA301 at the root and FCA361 at the outer side of the inboard engine nacelle (see Figure 31). The typical critical features were pin-loaded fastener holes in the spar cap and adjacent spar web or lower panel skin.

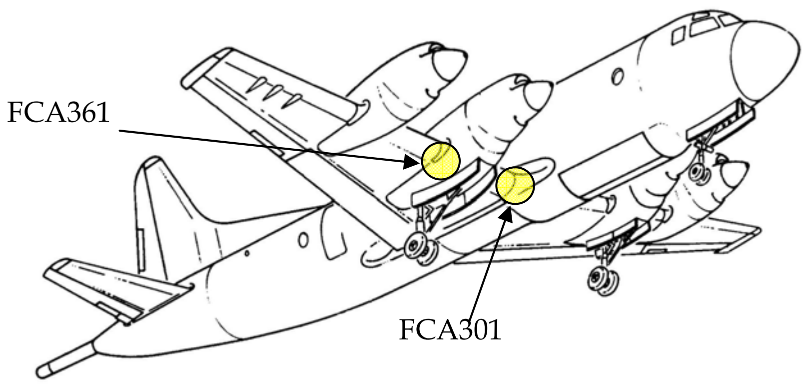


*Figure 31: Location of FCA301 and FCA361*

A test matrix of the coupons is provided in Table 22. The gross stress levels applied to each of the coupons are also included. The Direct Current Potential Drop (DCPD) system [12] was used to monitor crack growth during testing.

*Table 22: Coupon Test Matrix*

| FCA Location | Spectrum | Spectrum Cycles | Max Gross Area Stress ksi | Max Gross Area Stress MPa | Test Freq Hz | No. of Coupons |
|---|---|---|---|---|---|---|
| 301 | FSFT | 439,405 | 31.16 | 214.8 | 15 | 3 |
| | RAAF P-3C | 1,102,622 | 23.93 | 164.1 | 15 | 3 |
| | RAAF AP-3C | 935,296 | 25.14 | 173.4 | 15 | 3 |
| 361 | FSFT | 422,624 | 24.11 | 166.2 | 15 | 3 |
| | RAAF P-3C | 1,299,597 | 19.10 | 131.7 | 15 | 3 |
| | RAAF AP-3C | 1,096,385 | 19.17 | 132.2 | 15 | 3 |

### 9.1.3 Test Results

Figure 32 and Figure 34 provide the DCPD measured crack growth data for each of the coupons tested under the FCA301 and FCA361 spectra respectively. These DCPD results were also plotted on a log-linear scale in Figure 33 and Figure 35. The DCPD 'noise' arising from the electrical system has been omitted from the log-linear crack growth plots in order to show only that part of the data that was monotonically increasing. The DCPD system applies a current through the coupon and measures changes in voltage that can be related to the loss of cross-sectional area as the crack grows under cyclic loading. A new multi-part polynomial which converts DCPD voltages to crack lengths was determined as part of the test program and this is described in Appendix B. Note that the crack lengths provided in Figure 32 to Figure 35 represent growth from one side of the notch edge for a double edge crack. Symmetric crack growth was typically observed.

A summary of the CI, total and crack growth lives are presented in

Table 23 and Table 24 for FCA301 and FCA361 respectively. The coupon test analysis was conducted using the metric system, however to provide consistency with the first part of this report the crack length units have been converted to imperial dimensions. The initiation lives were calculated at crack lengths of 0.05″ and 0.12″ which are compatible with the $a_{NDI}$ limits used in the TI process. CI lives were not calculated at a crack length of 0.01″ as the DCPD system was unable to reliably measure cracks this small. The total lives represent the time to coupon failure or the time to a given crack length. For the FCA301 coupons, total lives were determined for a crack length of 0.12″ (3.048 mm) while for FCA361 a crack length of 0.197″ (5 mm) was used. These crack limits were selected so that a common critical crack length could be used for comparison with analytical calculations in the next section which use a constant $a_{crit}$. The FCA301 crack length is smaller than the FCA361 length because the FCA301 AP-3C coupons contain limited DCPD crack growth data. Crack growth lives are also presented for growth from an initial crack of 0.05″ or 0.12″ to coupon failure or a given crack size (i.e. 0.12″ or 0.197″). Once again, the crack lengths in

Table 23 and Table 24 represent growth from one side of the notch edge for a double edge crack.

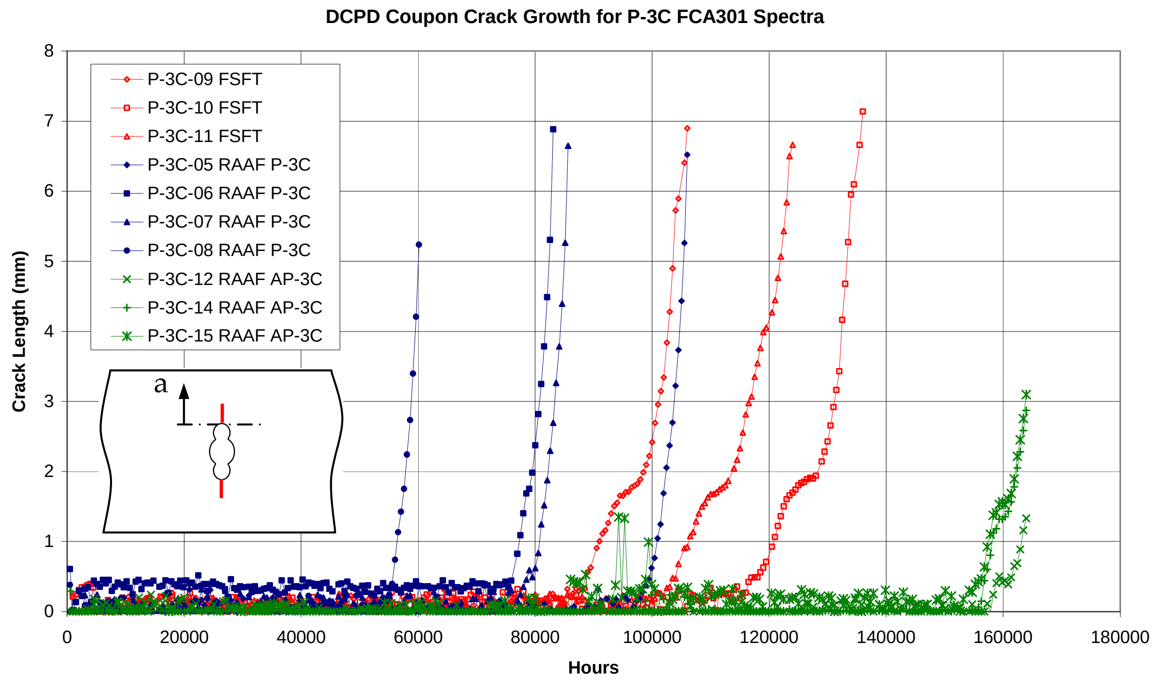


*Figure 32: DCPD Based Recorded Coupon Crack Growth for FCA301*

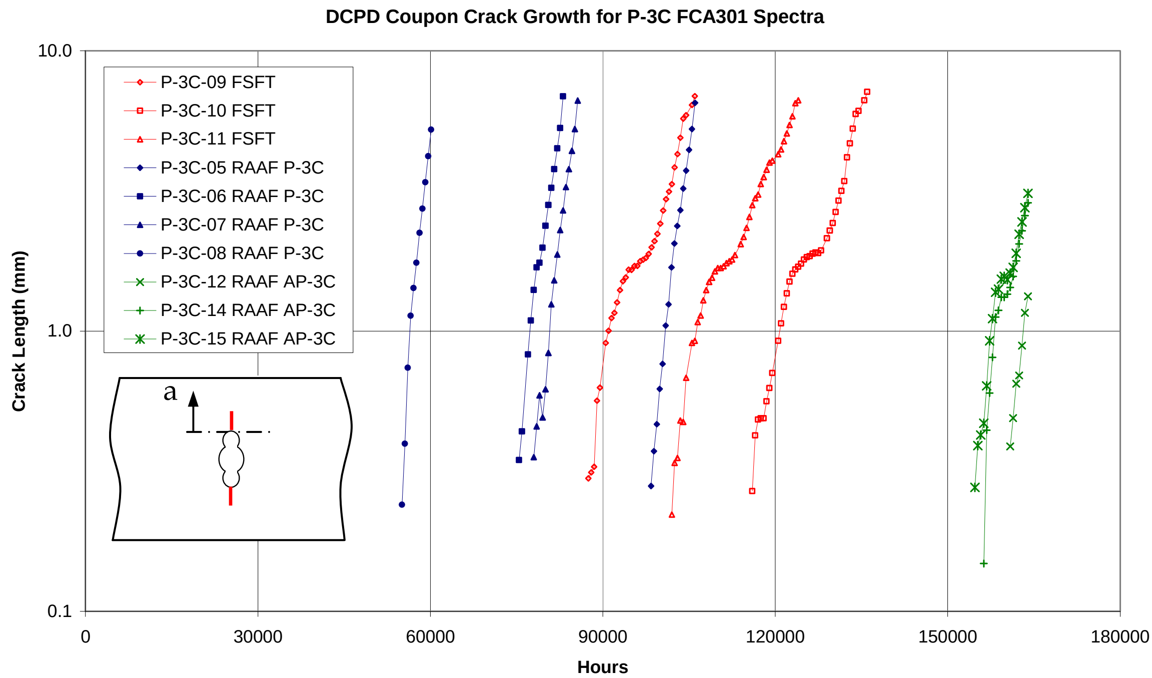


*Figure 33: DCPD Coupon Crack Growth for FCA301 (Log-Linear axes and with 'noise' removed)*

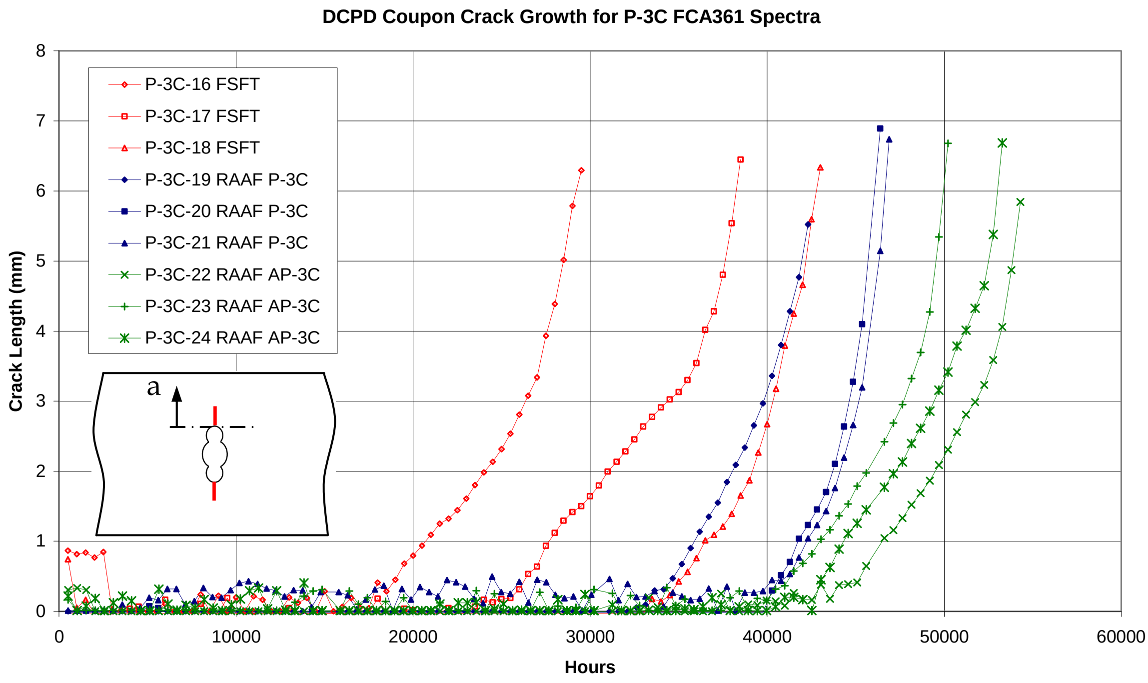


*Figure 34: DCPD Based Recorded Coupon Crack Growth for FCA361*

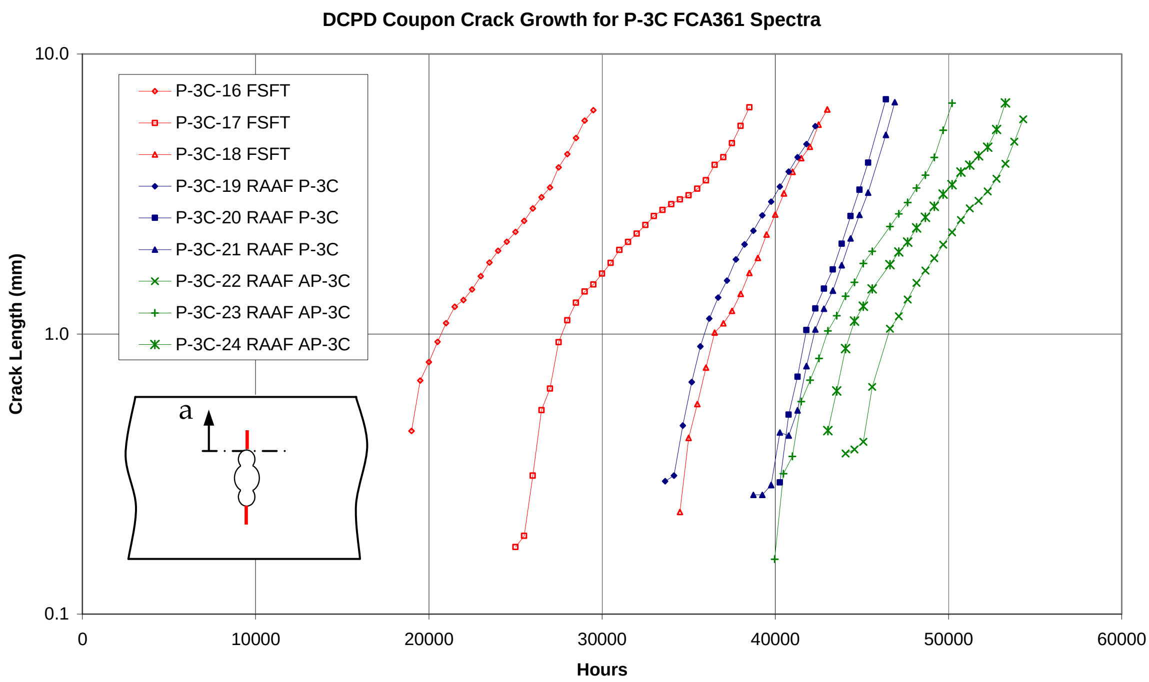


*Figure 35: DCPD Coupon Crack Growth for FCA361 (Log-Linear axes with 'noise' removed)*

*Table 23: Coupon Crack Initiation, Total and Crack Growth Lives for FCA301 Sequences*

| FCA301 Spectrum | Coupon Id | CI Lives (Hours) | | "Total" Lives (Hours) | | Crack Growth Lives (Hours) | | |
|---|---|---|---|---|---|---|---|---|
| | | 0.05″ | 0.12″ | 0.12″ | Failure | 0.05″ to 0.12″ | 0.05″ to Failure | 0.12″ to Failure |
| FSFT | P-3C-09 | 92,521 | 101,243 | 101,243 | 106,547 | 8,722 | 14,027 | 5,304 |
| | P-3C-10 | 121,674 | 131,264 | 131,264 | 136,547 | 9,590 | 14,873 | 5,284 |
| | P-3C-11 | 107,442 | 116,884 | 116,884 | 124,142 | 9,442 | 16,699 | 7,258 |
| | Log Ave | 106,546 | 115,812 | 115,812 | 121,781 | 9,243 | 15,160 | 5,881 |
| RAAF P-3C | P-3C-05 | 101,466 | 103,815 | 103,815 | 106,242 | 2,350 | 4,777 | 2,427 |
| | P-3C-06 | 77,773 | 80,811 | 80,811 | 83,183 | 3,038 | 5,410 | 2,372 |
| | P-3C-07 | 81,094 | 83,401 | 83,401 | 85,823 | 2,307 | 4,729 | 2,421 |
| | P-3C-08 | 56,819 | 58,860 | 58,860 | 60,586 | 2,042 | 3,767 | 1,726 |
| | Log Ave | 77,653 | 80,109 | 80,109 | 82,333 | 2,408 | 4,632 | 2,215 |
| RAAF AP-3C | P-3C-12 | 163,763 | - | - | 169,167 | 3,567* | 5,404 | - |
| | P-3C-14 | 159,142 | - | - | 167,539 | 5,542* | 8,397 | - |
| | P-3C-15 | 158,109 | 163,873 | 163,873 | 166,786 | 5,764 | 8,677 | 2,913 |
| | Log Ave | 160,319 | 163,873 | 163,873 | 167,828 | 4,957 | 7,329 | 2,913 |

* Generated as equivalent % of P-3C-15 results due to DCPD failure

*Table 24: Coupon Crack Initiation, Total and Crack Growth Lives for FCA361 Sequences*

| FCA361 Spectrum | Coupon Id | CI Lives (Hours) | | "Total" Lives (Hours) | | Crack Growth Lives (Hours) | | | |
|---|---|---|---|---|---|---|---|---|---|
| | | 0.05″ | 0.12″ | 0.197″ | Failure | 0.05″ to 0.197″ | 0.05″ to Failure | 0.12″ to 0.197″ | 0.12″ to Failure |
| FSFT | P-3C-16 | 21,628 | 26,443 | 28,487 | 30,841 | 6,858 | 9,213 | 2,043 | 4,398 |
| | P-3C-17 | 28,435 | 34,609 | 37,633 | 39,820 | 9,199 | 11,385 | 3,025 | 5,211 |
| | P-3C-18 | 37,664 | 40,372 | 42,180 | 44,700 | 4,516 | 7,035 | 1,818 | 4,327 |
| | Log Ave | 28,506 | 33,306 | 35,626 | 38,005 | 6,580 | 9,037 | 2,235 | 4,629 |
| RAAF P-3C | P-3C-19 | 36,510 | 39,863 | 41,954 | 42,848 | 5,444 | 6,338 | 2,091 | 2,985 |
| | P-3C-20 | 42,395 | 44,674 | 45,693 | 47,019 | 3,299 | 4,625 | 1,019 | 2,345 |
| | P-3C-21 | 42,918 | 45,224 | 46,309 | 47,576 | 3,391 | 4,658 | 1,085 | 2,352 |
| | Log Ave | 40,500 | 43,185 | 44,610 | 47,765 | 3,934 | 5,150 | 1,322 | 2,544 |
| RAAF AP-3C | P-3C-22 | 47,468 | 51,873 | 53,863 | 55,309 | 6,396 | 7,841 | 1,991 | 3,436 |
| | P-3C-23 | 43,818 | 47,781 | 49,532 | 50,689 | 5,714 | 6,871 | 1,750 | 2,908 |
| | P-3C-24 | 45,119 | 49,510 | 52,504 | 53,719 | 7,385 | 8,600 | 2,994 | 4,209 |
| | Log Ave | 45,443 | 49,693 | 51,935 | 53,204 | 6,462 | 7,738 | 2,185 | 3,477 |

## 9.2 Comparison of P-3 SLAP TI Predictions to Coupon Results

The following sub-sections firstly apply the P-3 wing/fuselage TI process using the P-3 coupons results just described. The crack initiation (CI) and total lives from this analysis will then be compared to those from the coupons to evaluate the effectiveness and robustness of the FAMS and FASTRAN tools used in the original TI process. Analyses will be performed at FCA301 and FCA361.

CI lives were calculated in the TI process using the FAMS software and DSTO-developed strain-life data for 7075-T651. DSTO developed two versions of the 7075-T651 strain-life data (dated 6-Jan-05 and 19-Jan-05). Whilst both versions were used in the original TI this inconsistency has been corrected for the current study and the later version of the 7075-T651 strain-life data has been used for all spectra. The possible difference to 7075-T6 is acknowledged but judged insignificant for relative life comparisons.

### 9.2.1 FCA361

FASTRAN analyses of the FCA361 FSFT and RAAF spectra are provided in Figure 36 which also includes the DCPD coupon crack growth data. Note that the DCPD crack growth data has again been clipped at a threshold where the DCPD system was deemed to be affected by 'noise' and no longer be measuring crack lengths accurately. The coupon stress intensity solution used in the FASTRAN run is provided in Appendix C. An initial crack length of 0.028 mm (0.0011″) was determined by pegging the FASTRAN predicted crack growth curve to the average coupon life for the FSFT spectra, while the crack limit (i.e. $a_{crit}$) was set to 5 mm (0.197″). The same initial crack size was then used for all FCA 361 spectra.

Table 25 summarises the unfactored crack growth times from the FASTRAN analysis. Table 26 and Table 27 in conjunction with Figure 37 provide the $K_{N\text{-}TD}$ as well as the time to crack initiation for a 0.05″ and 0.12″ flaw respectively. Table 28 and Table 29 provide the unfactored and factored inspection thresholds and intervals for FCA361 respectively.

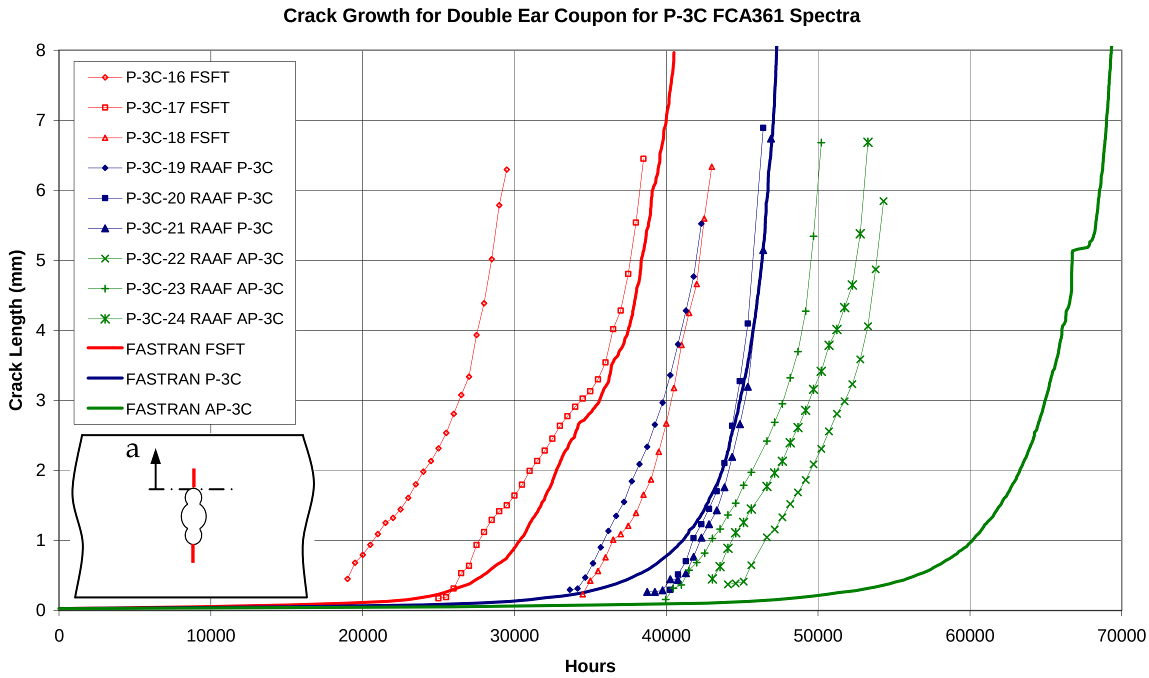


*Figure 36: FASTRAN only analysis v coupon results at FCA361, $a_i$ = 0.028 mm (0.0011")*

*Table 25: Crack Growth Results for FCA361*

| **$a_i$ = 0.0011"**<br>**$a_{crit}$ = 0.197"**<br>**Stress Factor = 1.0** | | | | | |
|---|---|---|---|---|---|
| **Spectrum** | **Unfactored Flight Hours** | | | | |
| | $a_i$ to 0.05" | $a_i$ to 0.12" | $a_i$ to $a_{crit}$ | CG Life 0.05" to $a_{crit}$ | CG Life 0.12" to $a_{crit}$ |
| FSFT | 31,093 | 35,690 | 38,356 | 7,263 | 2,666 |
| RAAF AP-3C | 61,186 | 65,025 | 66,745 | 5,559 | 1,720 |
| RAAF P-3C | 42,019 | 44,900 | 46,311 | 4,292 | 1,411 |

*Table 26: Determination of the Test-Demonstrated $K_N$ ($K_{N-TD}$) for 0.05"*

| **FSFT** | | **FASTRAN** | | | **FSFT** | **$K_{N-TD}$** |
|---|---|---|---|---|---|---|
| SFHRS Defect Found ($t_{test}$) | Crack Size when found | $t_{a=test}$ | $t_{a=0.050}$ | $\Delta t_{FASTRAN}=\Delta t_{test}$ ($t_{a=test}-t_{a=0.050}$) | $t_{a=0.050}$ ($t_{test}-\Delta t_{test}$) | 3.96 |
| 28,506 | 0.05 | 31,093 | 31,093 | 0 | 28,506 | |

*Table 27: Determination of the Test-Demonstrated $K_N$ ($K_{N-TD}$) for 0.12"*

| **FSFT** | | **FASTRAN** | | | **FSFT** | **$K_{N-TD}$** |
|---|---|---|---|---|---|---|
| SFHRS Defect Found ($t_{test}$) | Crack Size when found | $t_{a=test}$ | $t_{a=0.120}$ | $\Delta t_{FASTRAN}=\Delta t_{test}$ ($t_{a=test}-t_{a=0.120}$) | $t_{a=0.120}$ ($t_{test}-\Delta t_{test}$) | 3.73 |
| 28,506 | 0.05 | 31,093 | 35,690 | -4,597 | 33,103 | |

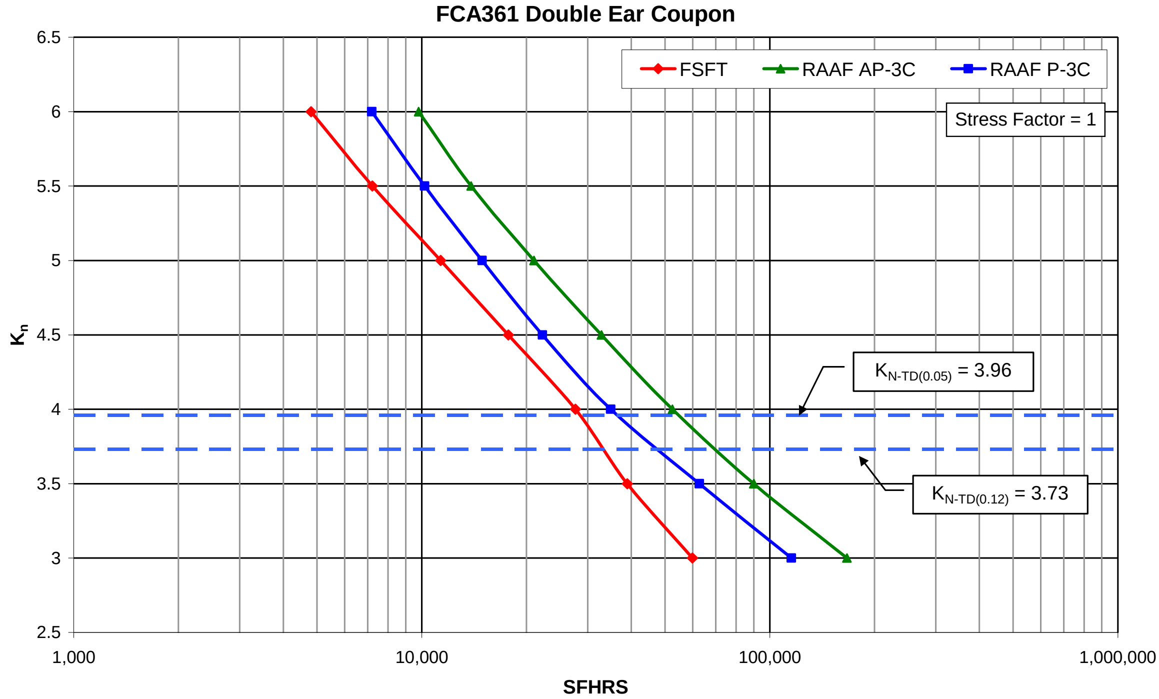


*Figure 37: FAMS Fatigue Life Curves for FCA361*

*Table 28: Summary of the Unfactored Results for FCA361*

| Unfactored Flight Hours | | | | | | |
|---|---|---|---|---|---|---|
| **Spectrum** | Δa 0.005 to 0.05 | Δa 0.005 to 0.12 | CG Life Δa = 0.05 to $a_{crit}$ | CG Life Δa = 0.12 to $a_{crit}$ | 0.05" Crack Initiation ($H_{init-0.05}$) | 0.12" Crack Initiation ($H_{init-0.12}$) |
| FSFT | 9,487 | 14,084 | 7,263 | 2,666 | 28,506 | 33,103 |
| RAAF AP-3C | 15,769 | 19,608 | 5,559 | 1,720 | 54,500 | 69,200 |
| RAAF P-3C | 12,311 | 15,192 | 4,292 | 1,411 | 36,500 | 47,100 |

*Table 29: Summary of Economic and Safety Thresholds for FCA361*

| Factored AFHRS | | | | | | |
|---|---|---|---|---|---|---|
| **Spectrum** | Economic Threshold $H_{init}/2$ (AFHRS) | | Inspection Intervals CG Life/2 (AFHRS) | | Total Life $t_{init}+t_{CG}$ (AFHRS) | Safe Life TL/3 (AFHRS) |
| | a = 0.05 | a = 0.12 | $a_{NDI}$ = 0.05 | $a_{NDI}$ = 0.12 | | |
| FSFT | 14,253 | 16,552 | 3,632 | 1,333 | 35,769 | 11,923 |
| RAAF AP-3C | 27,250 | 34,600 | 2,780 | 860 | 60,059 | 20,020 |
| RAAF P-3C | 18,250 | 23,550 | 2,146 | 706 | 40,792 | 13,597 |

In Figure 38 the crack initiation results from the coupon tests are compared to the FAMS predictions for the FCA361 spectra. Coupon results are provided for a 0.05" crack determined via DCPD measurements. The coupon data is plotted at the $K_N$ determined from Figure 37 for a crack of 0.050".

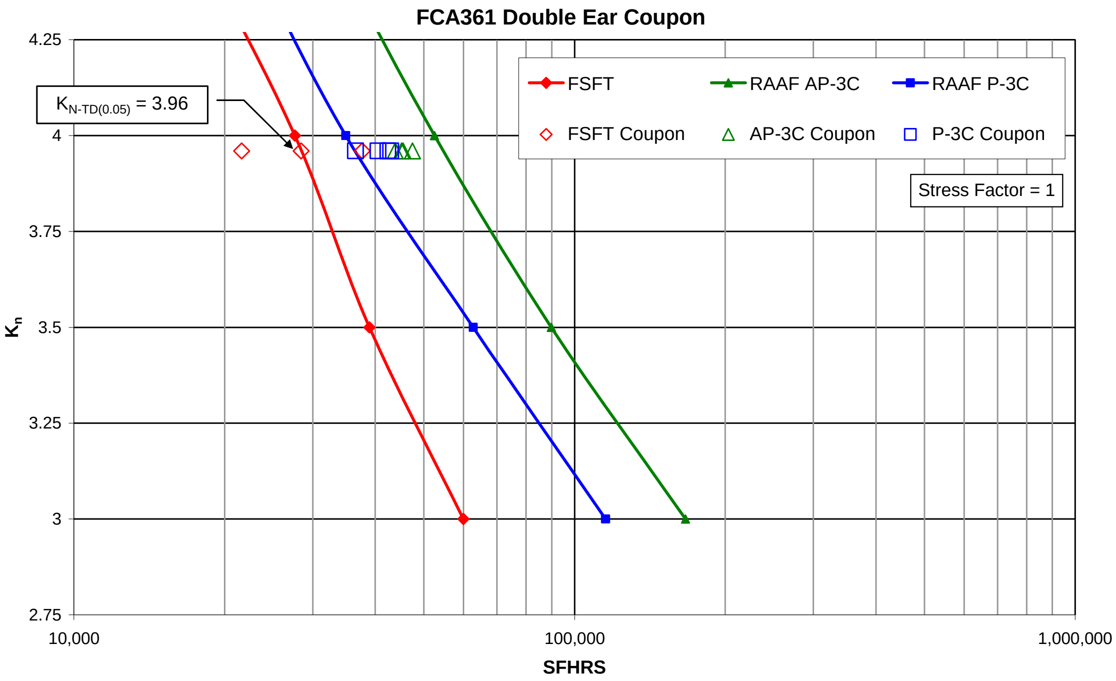


*Figure 38: Comparison Plot of Coupon Data and FAMS Results for FCA361*

Figure 39 and Figure 40 compare the crack growth from the coupon data and FASTRAN for FCA361 for the RAAF P-3C and AP-3C spectra respectively, facilitating a comparison of coupon crack growth versus FASTRAN prediction. In each case the FASTRAN curve has been shifted on the x axis to align with the coupon failure time to allow better comparison of the shape of the FASTRAN curve with the coupon data. The comparison shows a good match between experiment and prediction down to about 1 mm (0.040")

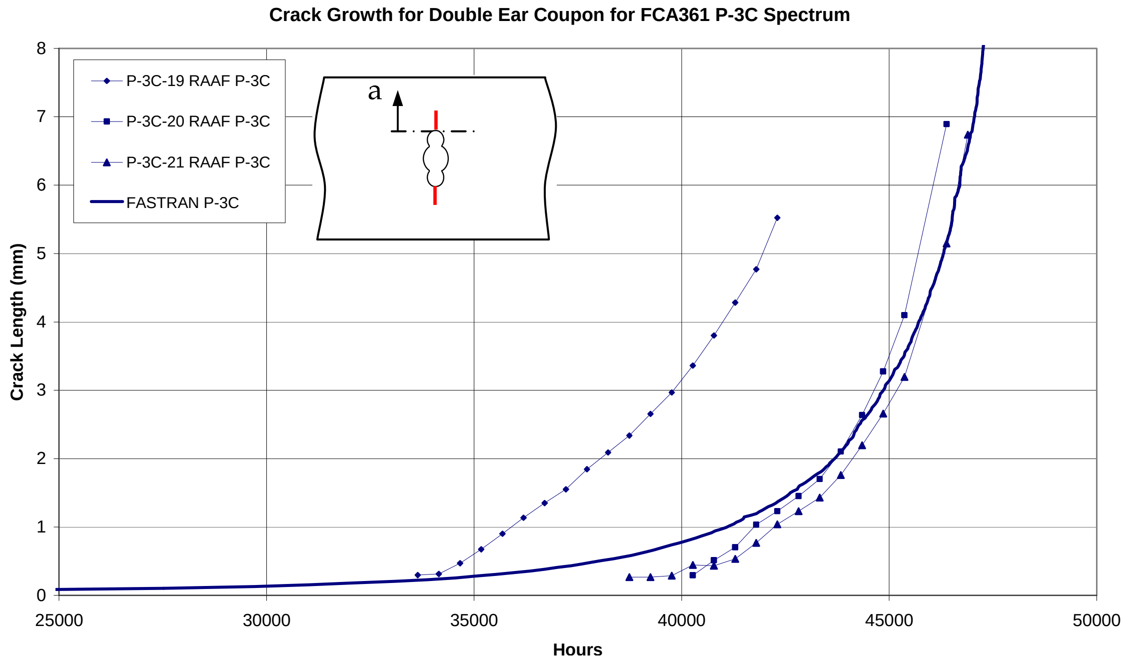


*Figure 39: Comparison Plot of Coupon Data and FASTRAN Results for RAAF P-3C at FCA361*

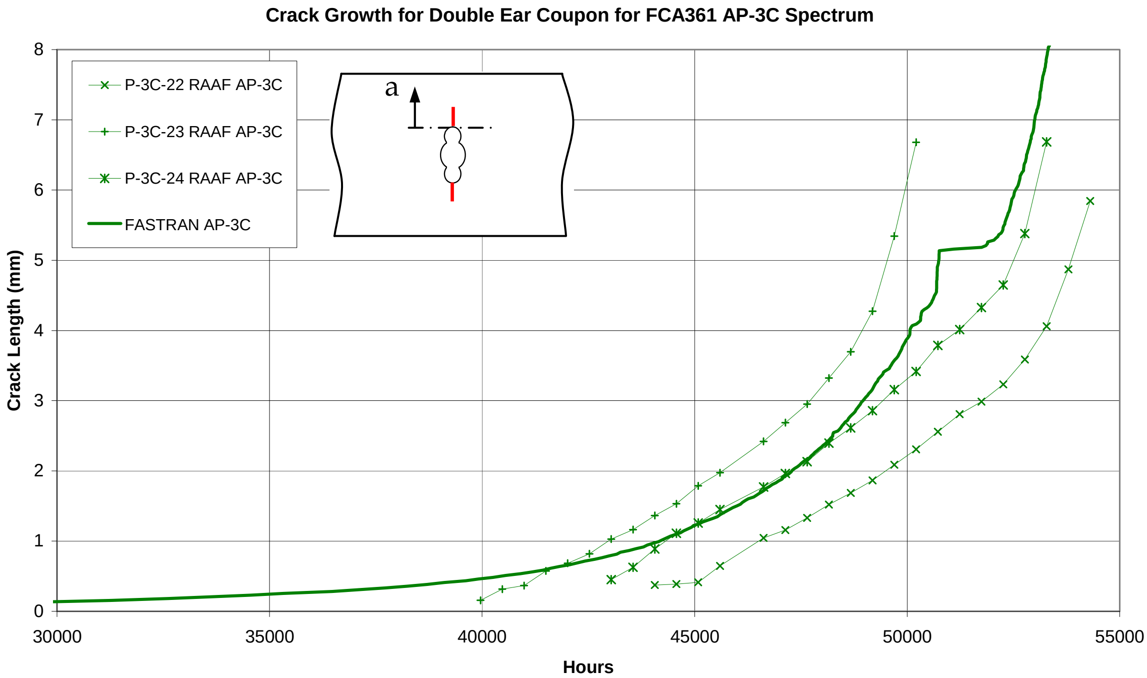


*Figure 40: Comparison Plot of Coupon Data and FASTRAN Results for RAAF AP-3C at FCA361*

Figure 41 compares the crack growth results from the FCA 361 coupon tests with the total life prediction from the combined FAMS and FASTRAN tools thus replicating the P-3 SLAP TI methodology. FASTRAN crack growth is plotted from 0.05″ to failure commencing at the FAMS initiation lives for a 0.05″ crack provided in Table 28.

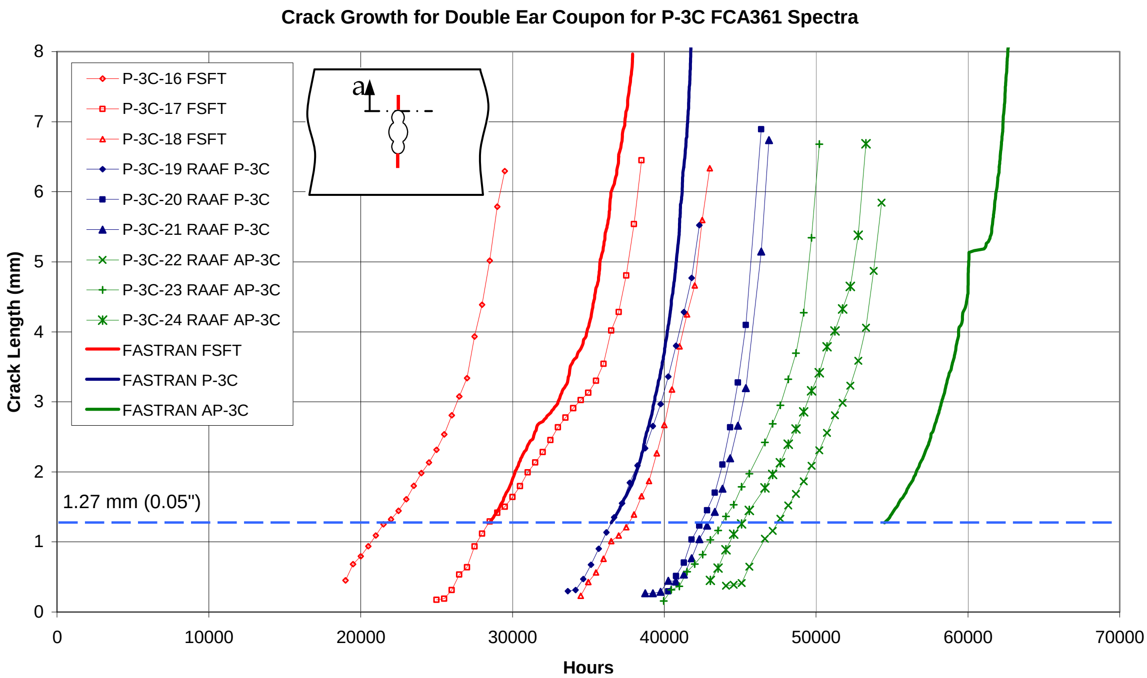


*Figure 41: Comparison of combined FAMS & FASTRAN total life predictions to the coupon crack growth for FCA361*

### 9.2.2 FCA301

FASTRAN analysis of the FCA301 FSFT and RAAF spectra is provided in Figure 42 which also includes the DCPD coupon crack growth data. Note that the DCPD crack growth data has again been clipped at a threshold where the DCPD system was deemed to no longer be measuring crack lengths accurately. The coupon stress intensity solution used in the FASTRAN run is provided in Appendix C. An initial crack length of 0.00035″ (0.0089 mm) was determined by pegging the FASTRAN prediction to the results for the FSFT spectra and then using the same $a_i$ for each of the other spectra. The crack limit (i.e. $a_{crit}$) was set at 0.12″ (3.048 mm).

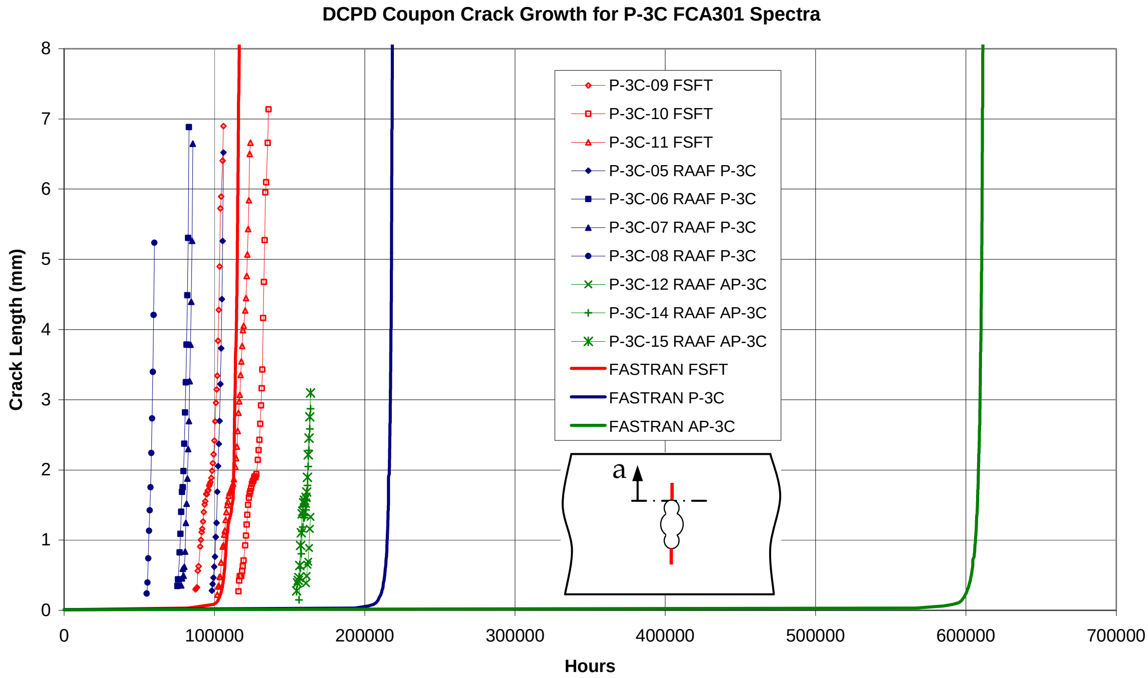


*Figure 42: Coupon FASTRAN Analysis at FCA301*

Table 30 summarises the unfactored crack growth times from the FASTRAN analysis. Table 31 in conjunction with Figure 43 provides the $K_{N\text{-}TD}$ as well as the time to crack initiation for a 0.05″ flaw. Table 32 and Table 33 provide the unfactored and factored inspection thresholds and intervals for FCA301 respectively.

*Table 30: Crack Growth Results for FCA301*

| **$a_i$ = 0.00035”**<br>**$a_{crit}$ = 0.12”**<br>**Stress Factor = 1.0** | | | | | |
|---|---|---|---|---|---|
| **Spectrum** | **Unfactored Flight Hours** | | | | |
| | $a_i$ to 0.05″ | $a_i$ to 0.12″ | $a_i$ to $a_{crit}$ | CG Life 0.05″ to $a_{crit}$ | CG Life 0.12″ to $a_{crit}$ |
| FSFT | 109,817 | - | 115,238 | 5,421 | - |
| RAAF AP-3C | 607,094 | - | 610,489 | 3,395 | - |
| RAAF P-3C | 215,473 | - | 217,828 | 2,355 | - |

*Table 31: Determination of the Test-Demonstrated $K_N$ ($K_{N\text{-}TD}$) for 0.05"*

| FSFT | | FASTRAN | | | FSFT | $K_{N\text{-}TD}$ |
|---|---|---|---|---|---|---|
| SFHRS Defect Found ($t_{test}$) | Crack Size when found | $t_{a=test}$ | $t_{a=0.050}$ | $\Delta t_{FASTRAN}=\Delta t_{test}$ ($t_{a=test}-t_{a=0.050}$) | $t_{a=0.050}$ ($t_{test}-\Delta t_{test}$) | 2.31 |
| 106,546 | 0.05 | 109,817 | 109,817 | 0 | 106,546 | |

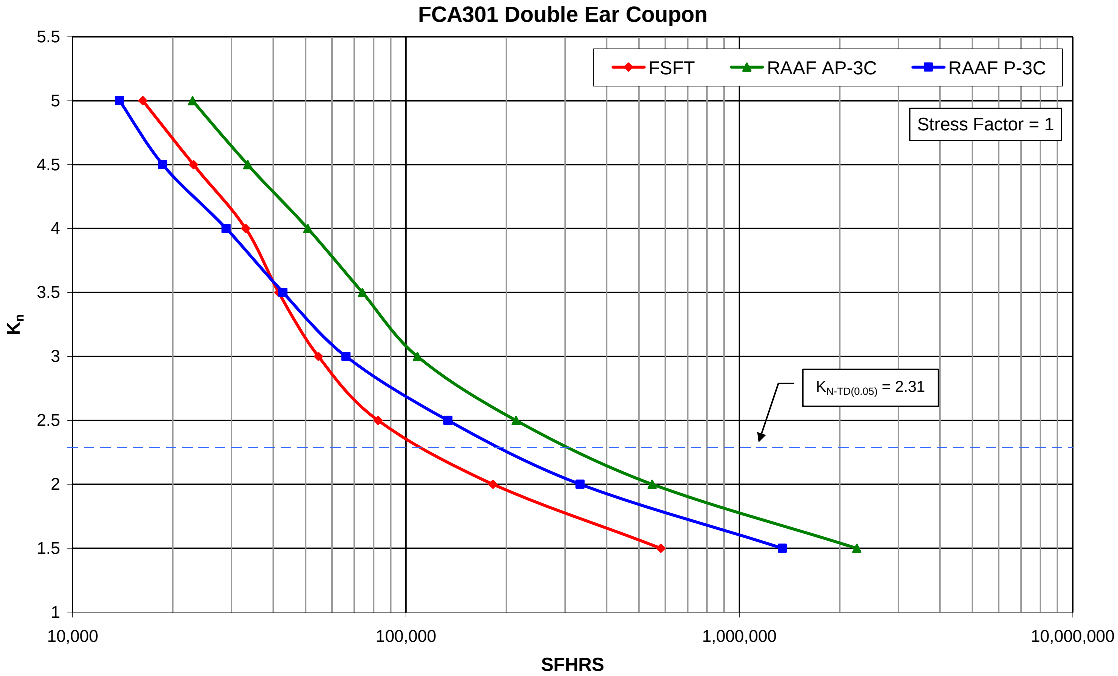


*Figure 43: FAMS Fatigue Life Curves for FCA301*

*Table 32: Summary of the Unfactored Results for FCA301*

| Unfactored Flight Hours | | | | | | |
|---|---|---|---|---|---|---|
| **Spectrum** | $\Delta a$ 0.005 to 0.05 | $\Delta a$ 0.005 to 0.12 | CG Life $\Delta a$ = 0.05 to $a_{crit}$ | CG Life $\Delta a$ = 0.12 to $a_{crit}$ | 0.05" Crack Initiation ($H_{init\text{-}0.05}$) | 0.12" Crack Initiation ($H_{init\text{-}0.12}$) |
| FSFT | 7,537 | 12,958 | 5,421 | - | 106,546 | - |
| RAAF AP-3C | 10,229 | 13,624 | 3,395 | - | 294,000 | - |
| RAAF P-3C | 6,884 | 9,239 | 2,355 | - | 183,000 | - |

*Table 33: Summary of Economic and Safety Thresholds for FCA301*

| Factored AFHRS | | | | | | |
|---|---|---|---|---|---|---|
| **Spectrum** | Economic Threshold $H_{init}/2$ (AFHRS) | | Inspection Intervals CG Life/2 (AFHRS) | | Total Life $t_{init}+t_{CG}$ (AFHRS) | Safe Life TL/3 (AFHRS) |
| | a = 0.05 | a = 0.12 | $a_{NDI}$ = 0.05 | $a_{NDI}$ = 0.12 | | |
| FSFT | 53,273 | - | 2,711 | - | 111,967 | 37,322 |
| RAAF AP-3C | 147,000 | - | 1,698 | - | 297,395 | 99,132 |
| RAAF P-3C | 91,500 | - | 1,178 | - | 185,355 | 61,785 |

Figure 44 compares the crack initiation results from the coupon tests and the FAMS predictions for FCA301. Coupon results are provided for a 0.05″ crack. In each plot the coupon data $K_N$ is determined by pegging the log average FSFT coupon result (for a 0.05″ crack) to the FAMS FSFT curve.

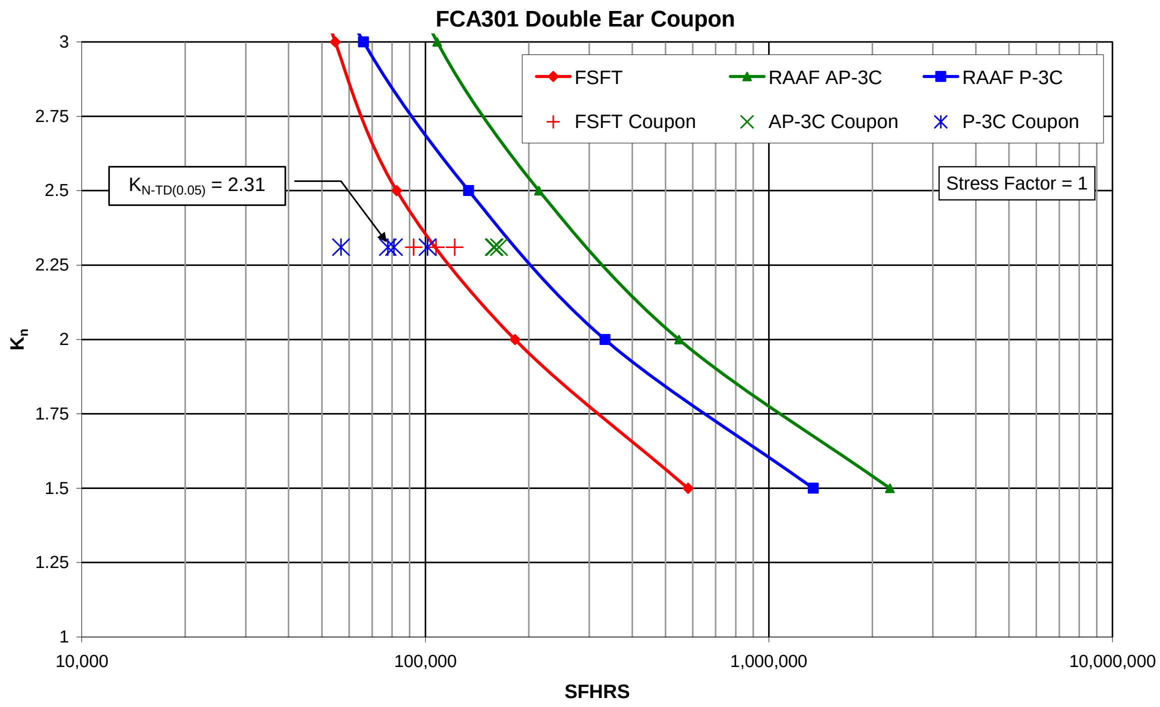


*Figure 44: Comparison Plot of Coupon Data and FAMS Results for FCA301*

Figure 45 compares the crack growth results from the FCA 301 coupon tests with the total life prediction from the combined FAMS and FASTRAN predictions as conducted by the P-3 SLAP TI methodology. FASTRAN crack growth is plotted from 0.05″ to failure commencing at the FAMS initiation lives for a 0.05″ crack provided in Table 32.

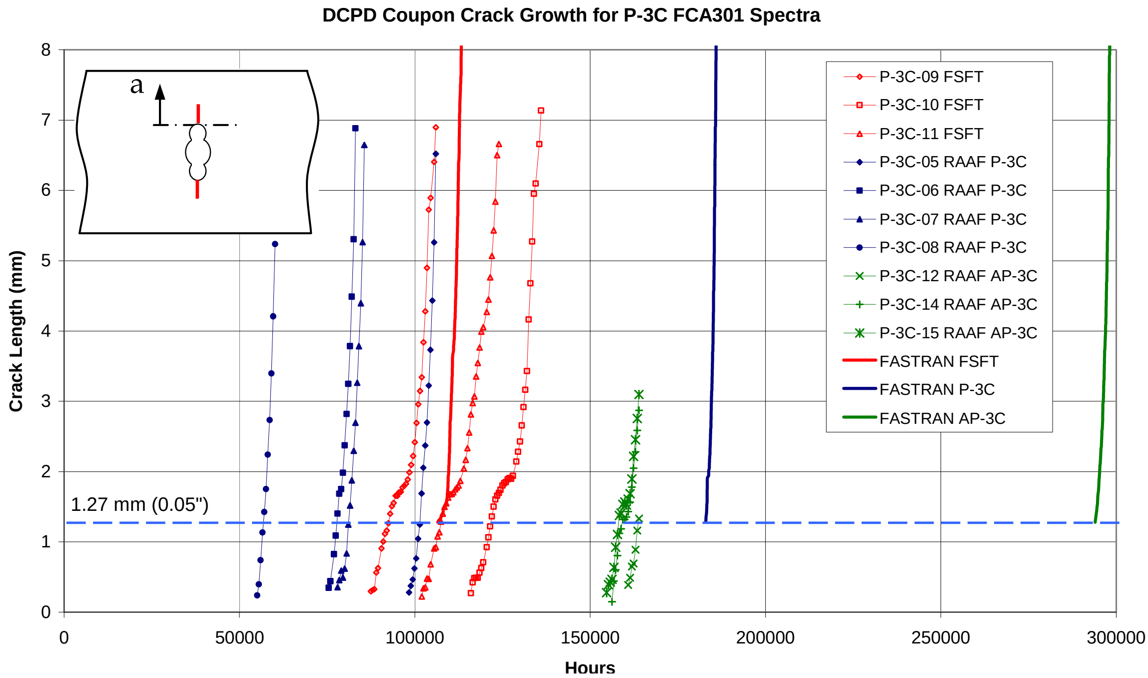


*Figure 45: Comparison of combined FAMS & FASTRAN total life predictions to the coupon crack growth for FCA301*

## 9.3 Evaluation of Coupon and Analytical Results

The FAMS, FASTRAN and combined FAMS and FASTRAN approaches to the prediction of the experiments under the FCA 361 spectra appear to be satisfactory. The same can be said for the FASTRAN predictions of the established crack growth for the FCA 301 spectra; however there appears to be a significant discrepancy between the FAMS prediction for the FSFT spectra at FCA 301 and the coupon experiment. Whilst the relative lives between the P-3C spectra and the AP-3C spectra appear consistent, there is a significant inconsistency between these results and the results for the FSFT spectra. Essentially the relative severity or order of failure between the FSFT spectra and the other two spectra is not correct. As a consequence the results from the FASTRAN-only life predictions and the combined FAMS and FASTRAN total life predictions are significantly different to the experiments.

So what went wrong with the FAMS prediction for FCA301? This issue needs further study. Initial exploration regarding alternate equivalent strain equations and strain-life material curves has not provided a 'magic bullet' solution and so more in-depth investigations are necessary. It is noted that the difference between the first RAAF spectra used early on in the TI process to verify the FAMS calibration and the later versions used to generate the final results was greater for FCA301 than FCA361. It is also noted that the difference between the FSFT spectra and the RAAF spectra is more marked for FCA 301 than for FCA 361, particularly in mean stress. To assist with the future investigations further coupon tests were run at a higher stress level. The stress augmentation chosen was a factor of 1.3, equivalent to the level used in the original P-3 SLAP coupon tests for FCA 301. Figure 46 shows this data and in this figure the coupon results are now pegged to the FSFT FAMS predictions at the higher stress level, with the coupon test results for the lower stress level placed a factor of 1.3 lower on the $K_n$

scale. The coupon tests confirm that the FAMS prediction of a cross-over in severity between the FSFT spectra and the RAAF P-3C spectra does not occur at the stress levels tested. Recent coupon results from the current P-3 Group could fill in more of the picture but so far only the FSFT spectra has been tested.

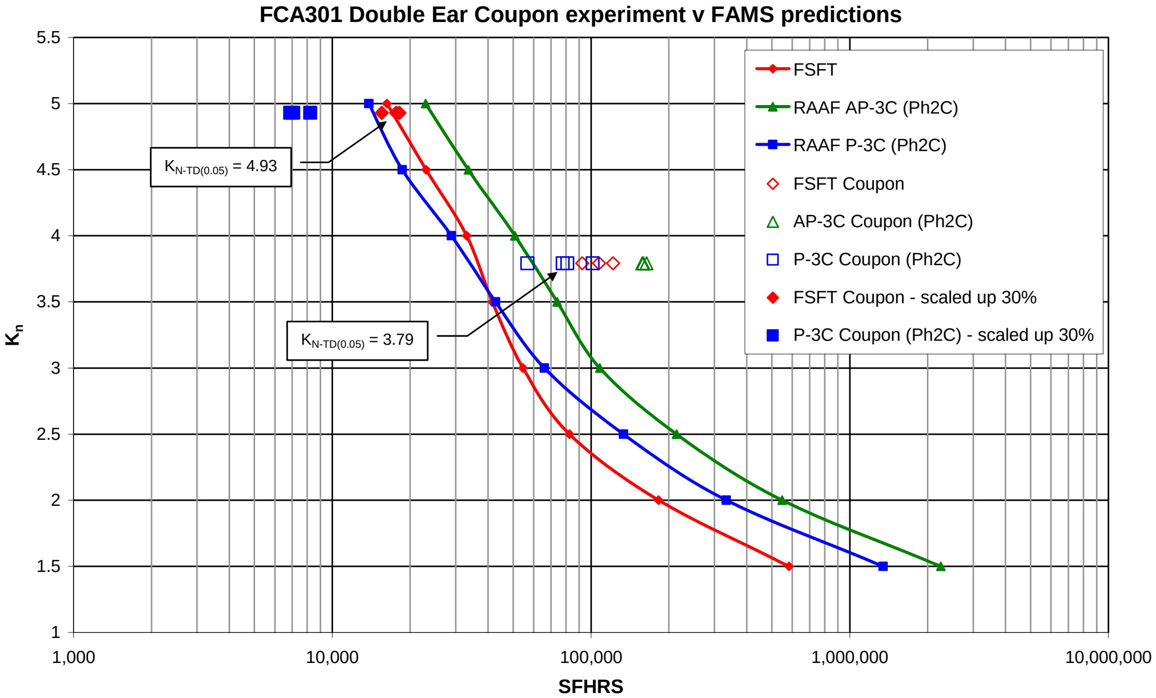


*Figure 46: Coupon tests at two stress levels with data 'pegged' to FSFT predictions at upper stress level*

### 9.3.1 Comparison against Test Interpretation Results for FCA301

The change in RAAF spectra between the early loads system used at the time of the FAMS and FASTRAN tool calibration work and the loads system used to generate the final TI sequences reflected L-M efforts to correct and adjust the ground loads in particular to better match flight test data. At FCA301 the changes were significant enough to suggest that many of the in-service spectra were now more severe than the spectra that had been applied to the FSFT in the centre wing area. This is obvious if one compares the relative severity (relative crack initiation lives) between the FSFT and early RAAF P-3 spectra for FCA301 from [20] (relative severity = 1:1.5) with the FSFT and later RAF spectra from the TI for FCA301-CSS-1 (relative severity = 1:0.71) As well as pointing to the fact that the FSFT article was probably being under-tested relative to fleet damage accrual, this significant change in severity of the RAAF sequences from that used for FAMS verification to that used in the final TI results reaffirmed the need to check that FAMS could in fact predict that change.

If one considers the lower batch of coupon results plotted in Figure 46, these coupons were run at the same stress levels and spectra used in the TI analysis. Plotting the coupon results at a $K_n$ value of 3.79 is in fact broadly consistent with $K_n$ values used in the various critical features in the centre wing area and consistent with the $K_{n\text{-}TD}$ value derived from the FCA361

coupons of 3.96. Additionally, the theoretical value of $K_n$ for the coupon design is between 3.84 and 3.57 depending upon the formula used, see [22]. Comparing the relative spectra severity (as represented by CI life) for a typical TI analysis feature at FCA301 against the recent coupon results, we can see that in fact the relative lives are in very good agreement, see Table 34.

*Table 34: Relative lives for TI FAMS predictions and coupons under FCA301 spectra*

| **Spectrum** | 0.050″ Crack Initiation for FCA301-CSS-1 Kn = 3.75 | | Coupon test results | |
|---|---|---|---|---|
| | FAMS prediction | Relative life | Crack initiation | Relative life |
| FSFT | 48987 | 1 | 106,546 | 1 |
| RAAF P-3C | 35000 | 0.71 | 77,653 | 0.73 |
| RAAF AP-3C | 60,600 | 1.24 | 160,319 | 1.5 |

These results therefore suggest that the FAMS predictions made in the TI regarding the relative crack initiation lives are now supported by experiment. What remains, therefore, is the confusion that can occur during the 'life pegging' process when the coupon lives cause the resulting $K_{n\text{-}TD}$ value to depart significantly from the anticipated theoretical value. This can been seen for the coupon results for FCA301 were the coupon lives were between 2–2.5 times longer than the lives being experienced on the FSFT for the same spectra and stress level. Whilst this difference in life can be explained by different manufacturing processes on an equivalent configuration hole, the resulting shift of $K_n$ from an anticipated value of about 3.75 to a value of 2.31, compounded by the cross-over of FAMS predicted spectrum severity has played havoc with the pegged total life process.

# 10. Discussion

## 10.1 Comparison of Standards: Safe Life and Inspection Thresholds

Table 35 presents the safe lives or inspection thresholds for the RAAF P-3C spectrum derived from the different airworthiness standards and their associated life prediction methodologies examined in this report.

*Table 35: RAAF P-3C Inspection Thresholds/Safe Lives*

| FCA | FAR 25 | DSTO 'Economic' | Def Stan 00-970[$] | JSSG 2006 USAF | JSSG 2006 USN | Probability Analysis |
|---|---|---|---|---|---|---|
| | Total life/3 as per SLAP TI | Fatigue life to 0.050"/2 | Life using Safe S-N process | Crack growth from 0.050" / 2 | Fatigue life to 0.010" / 2 | 1/1000 probability from Fleet failure data |
| 301-WEB-4 | 5,361 | 4,050 | 12,026 | 3,992 | 2,950 | 14,215 |
| 351-CDN2 | 9,414 | 10,000 | 18,599 | 4,120 | 8,300 | 15,979 |
| 352-PDN-1 | 7,319 | 9,000 | 15,021 | 1,978 | 7,650 | 12,078 |
| 375-PSS-2 | 8,986 | 7,500 | 47,201 | 5,980 | 3,925 | 22,300 |
| 811-1 | 248,023 | 39,250 | 206,564 | 332,785 | - | - |
| 811-2 | 121,022 | 81,000 | 121,990 | - | - | - |
| 886 – USN | 17,971 | 13,000 | 34,306 | 10,261 | - | - |
| 886 – Aus | 169,304 | 240,000 | 142,475 | 10,261 | - | - |

[$] Safe lives provided for material configuration which produced lowest stress scaling factor

For the wing FCAs, the first thing to notice is that the FAR 25 based thresholds are not very different to the DSTO 'economic' threshold, implying a ratio of crack initiation (0.050") to total life of about two thirds. The Def Stan 00-970 based safe lives are on the whole higher, with the calculation for FCA375 considerably higher. The USN calculations of safe life, based on crack initiation to 0.010", are comparable to the FAR based values in two out of the four FCAs but considerably shorter for the other two FCAs. The USAF preferred method of calculating inspection thresholds via crack growth from 0.050" produced significantly shorter values than those from the FAR approach used in the DSTO P-3 SLAP TI.

For the empennage locations, the Def Stan 00-970 and FAR based calculations are comparable for the RAAF spectra. The JSSG 2006 crack growth-based calculations are significantly different.

### 10.1.1 Scatter Factors

In its Section 7, FAR 25.571-1C lays out a methodology for determining the appropriate scatter factor for a safe life evaluation. With all normal issues accounted for, the minimum scatter factor would be expected to be 3. This value was used in the P-3 SLAP TI.

From the Def Stan 00-970 analysis in this report we can see in Table 11 and Table 12 that the safe S-N analysis produced ratios of safe life to mean life of about 5 and 6 for the wing locations and between 6.5 and 12 for the empennage locations. To generate scatter factors of these magnitudes from the standard Def Stan 00-970 approach and using the same probability of 1 in 1000 requires the following values of "implied" standard deviation, σ, backed out from the Bullen equation;

$$\text{Log SF} = -t.\sigma\,(1+ 1/n)^{0.5}$$

using n=2 for one test result, t=3.2905 (probability of 1/2000 equating to 1/1000 for two components per aircraft) and SF = 6, then the standard deviation σ= 0.193.

This value can be compared to the values of standard deviation of between 0.15 and 0.18 obtained from the in-service fleet inspection data used in the probability approach of Section 8. Given that the values of standard deviation from the probabilistic data include a component of individual aircraft variability about the fleet mean, this suggests that the implied standard deviation resulting from the application of the safe S-N method to the wing FCAs is appropriately conservative but possibly overly high.

### 10.1.2 Comparison against Fleet Demonstration

Being based on measured fleet cracking data, the probability analysis reflects the true loading and spectrum environment of the P-3 fleet as well as the effects of aircraft build quality, maintenance and material performance. All approaches to the determination of safe lives using the DSTO TI process and the results of the FSFT are approximations of that environment. These processes included one or more of the approximations (sometimes deliberately conservative) outlined below;

(a) Deliberate conservatism in some elements of the FSFT load spectrum such as flight gust criteria, and aircraft landing response.

(b) The use of the earliest crack from either left or right wing rather than perhaps the log mean of the results from two wings.

(c) The uncertainties in the predictive abilities of tools such as FAMS and FASTRAN.

(d) The conservative performance of FASTRAN under RAAF spectra estimated to be between 0% and 25% based on DSTO P-3 SLAP coupon test results.

Whilst the probabilistic analysis itself carries some conservatism in the calculation of safe lives as a result of generally defaulting to the conservative end of the range of standard deviations derived from the fleet data (a value of 0.18 was typically used), the above conservative elements of the TI process still result in fleet data-based values of safe life that are higher than all the prediction approaches. In normal circumstances, fleet-sourced data of cracking beyond a designated safe life point is not usually available, particularly of course for single load path uninspectable structure that exists on fighter type aircraft where such data only arrives from

the dangerous situation of a complete overestimation of the true safe life[1]. Ordinarily, therefore, the amount of conservatism included in the fatigue life estimation for a particular aircraft type is simply not known. In the case of the P-3 SLAP the existence of fleet inspection data is thus a bonus, and in the first case gives comfort that the whole P-3 SLAP testing and analysis process had not led to unconservative life estimation.

In the P-3 SLAP TI and SMP processes, the conservatism in the original calculations of inspection threshold in the TI were seen by the operator and regulator as materially and unnecessarily increasing the cost of the maintenance burden. The fleet data was thus used to allow the thresholds to be extended, with the analysis and justification contained in the subsequent DSTO developed structural maintenance plan. An increase in the threshold of about 30% was seen as worthwhile pursuing from a fleet cost of ownership basis.

The probabilistics-based extension of calculated inspection thresholds used in the P-3 SLAP SMP would be similarly valid for predictions based on the Def STAN 00-970, JSSG (USN) approaches. An inspection extension for the USAF crack growth based approach would not be consistent with its damage tolerance philosophy as that approach links the initial inspection to crack growth from a set 0.050". Of interest, the Def Stan 00-970 values are at first glance the closest to the probability analysis results from the fleet failure data, despite the generous scatter factors imbedded in the analysis. A prediction of twice the fleet based safe life value for FCA375 could not be regarded as a safe prediction however.

## 10.2 Comparison of Standards: Inspection Intervals

The following table provides the inspection intervals under the RAAF P-3C spectrum.

*Table 36: RAAF P-3C Inspection Intervals from 0.05"except for * where $a_{NDI}$ = 0.12*

| FCA | FAR 25 | Def Stan 00-970 | JSSG 2006 USAF | JSSG 2006 USN |
|---|---|---|---|---|
| 301-WEB-4 | 3,992 | 2,661 | 3,992 | 3,992 |
| 351-CDN2 | 4,120 | 2,747 | 4,120 | 4,120 |
| 352-PDN-1 | 1,978 | 1,319 | 1,978 | 1,978 |
| 375-PSS-2 | 5,980 | 3,987 | 5,980 | 5,980 |
| 811-1 | 332,785 | 221,857 | 332,785 | 332,785 |
| 811-2 | 100,533 | 67,022 | - | - |
| 886 – USN | 13,957 | 9,305 | 10,261* | 10,261* |
| 886 – Aus | 13,957 | 9,305 | 10,261* | 10,261* |

The major point of difference is the use of a factor of three in the Def Stan 00-970 process versus the factor of two used within all the other processes. For FCA 811-2, the JSSG 2006 based approach is affected by the $a_{crit} = a_{NDI}$ issue identified in Section 6.2.1 For FCA 866, the different intervals are the result of using different $a_{NDI}$ values. An $a_{NDI}$ of 0.12 is mandated in JSSG 2006 for the FCA 886 surface feature.

[1] Another possibility is the removal and continued cycling under test of retired components.

## 10.3 Comparison of Methods: Total Life

A number of different methods were examined in this report for the prediction of total life; EBA, crack growth from an initial flaw via FASTRAN, and the total life method used in the DSTO P-3 SLAP TI which combined FAMS and FASTRAN predictions. The method of calculating total life followed the TI process, i.e. calibration of tools, pegging to coupon or FSFT results under USN 85th percentile spectra and then prediction of life under RAAF spectra. The predictions for each method can be compared using the recent coupon results and in one case, a crack from the wing/fuselage FSFT. The comparisons are shown in Table 37.

*Table 37: Comparison of Experimental and Predicted Lives from various methods for FCA361*

| Experiment | Spectra | Prediction Method | Report Section | Experiment Life | Analytical Life | % diff of anal to Exp. |
|---|---|---|---|---|---|---|
| NLR $K_t$=5 Coupons | FCA361 RAAF | EBA (m=2) | 8.2 | 40968 | 16312 | -60% |
| FSFT wing spar cap | USN 85% | EBA (m=2) | 8.3 | 16785 | 10026 | -40% |
| | | | | | | |
| DSTO $K_t$=5 Coupons | FCA361 P-3C | FAMS + FASTRAN | 9.1 and 9.2 | 44610 | 40792 | -8.5% |
| | | FASTRAN Only | | | 46311 | 3.8% |
| | FCA361 AP-3C | FAMS + FASTRAN | | 51935 | 60059 | 16% |
| | | FASTRAN only | | | 65025 | 25% |

The comparison of total life to model predictions at FCA361 shows that the EBA performed poorly both for the coupon trial and for the FSFT crack. Difficulties in using the EBA for the P-3C spectra have been noted and reported before in [11] and is a result of the stress level and spectral content of the P-3 load spectra which often results in a period of 'initiation' or slower initial crack growth that is not proportional to the subsequent rate of established crack growth. The simplified crack growth rate equation used by EBA of;

$$\frac{\mathrm{d}a}{\mathrm{d}B} = C_B K_{\mathrm{eff}}^{m_B} \quad \text{where } C_B \text{ and } m_B \text{ are } \textit{spectrum-specific} \text{ material constants}$$

in which the block-by-block crack growth life prediction is dependent on a single constant and a single exponent to represent the full genesis and growth history of the crack cannot thus model all types of crack growth seen on the P-3. The necessity of dividing the P-3 15,000 hour spectra into sub-blocks does not prevent an EBA type analysis but does add to the uncertainty associated with the derived rate parameters. One can also conclude from the coupon results shown in Figure 28 that the model derived value of initial crack size is not independent of spectra, a situation contrary to the necessary assumption in the EBA process that initial crack size is spectra and stress level independent. Figure 30 also demonstrates a potentially difficult issue with fractography of cracks in transport aircraft; the significant time period between zero hours and the first reliable fractographic readings. The crack examined here was in fact an early failure under the severe FSFT spectrum. Even so, its analysis necessitated a back

projection significantly longer than was needed, for example, in the original F/A-18 EBA work, giving rise to questions about the robustness of the $a_0$ values that are derived as a result. The above observations are valid for one wing location and for FSFT and coupon results for no more than two spectra. Different material and transport aircraft spectra may or may give better fractographic results, but equally, other P-3 wing spectra such as FCA301 also show delayed initiation.

The FAMS and FASTRAN predictions in the TI for the final sequences for FCA361 and FCA301 are true blind predictions of the DSTO coupon results that were obtained three years later. The results for FCA361 give confidence in the DSTO TI methodology of a combined FAMS and FASTRAN life prediction for these previously un-tested spectra used in the TI. The FASTRAN-only predictions also show promise, with perhaps the prediction for AP-3C a little outside a desirable 10- 20% maximum error band. As the derivation of initial crack size is crucial to the FASTRAN prediction, confidence in the robustness of the FASTRAN-only total life predictions will rest on building confidence in the selection of an appropriate $a_0$ and the consistent performance of FASTRAN at the very lowest crack growth rates.

The results for FCA301 are not included in Table 37 due to the unresolved issues related to the FAMS predictions as discussed in Section 9.3. Whilst that analysis concludes that the latest coupon results verify that the FAMS-derived relative spectrum severities used in the TI are reasonable, the results also expose a significant issue with $K_{n\text{-}TD}$ 'pegging' and so further work needs to be done to explore the issue.

## 10.4 Comparison of Methods: Crack Growth Life

A comparison of experimental and predicted crack growth lives is provided in Table 38. For the prediction of a crack growth interval, the EBA method performed well for the coupons but less well for the FSFT crack. The method would need to be further examined to see if the result could be improved for this particular situation. The FASTRAN predictions for the P-3C spectra were also good, but for the AP-3C spectra the results suggest an undesirable conservatism consistent with the original concerns regarding the DSTO TI results. The results suggest effort to reduce the conservatism would provide pay-off to the RAAF P-3 fleet.

*Table 38: Comparison of Experimental and Predicted Crack Growth Lives from various methods*

| Experiment | Spectra | Prediction Method | Report Section | Experiment CG Life | Analytical CG Life | % diff of anal to Exp. |
|---|---|---|---|---|---|---|
| NLR $K_t$=5 Coupons | FCA361 RAAF | EBA (var. methods) | 8.2 | 7444 | 6647 - 7890 | -11 – 6% |
| FSFT | USN 85% | EBA (var. methods) | 8.3 | 2905 | 3606 - 5279 | 24 - 82% |
| | | | | | | |
| DSTO $K_t$=5 Coupons | FCA361 P-3C | FASTRAN | 9.1 and 9.2 | 3934 | 4292 | 9% |
| | FCA361 AP-3C | FASTRAN | | 6462 | 5559 | -14% |
| | FCA301 P-3C | FASTRAN | 9.1 and 9.2 | 2408 | 2355 | -2% |
| | FCA301 AP-3C | FASTRAN | | 4957 | 3395 | -32% |

# 11. Conclusion & Applicability

## 11.1 Conclusion

The experimental and analytical results available from the P-3 SLAP provided an opportunity to examine the effects of applying different airworthiness standards and their associated different lifing methodologies on in-service structural management actions.

The comparison of safe life and inspection threshold calculations showed, perhaps unsurprisingly, considerable variation between approaches. For the wing locations no approach could be regarded as unsafe when compared against fleet data, although the Def Stan 00-970 result for FCA375 needs further examination and perhaps refinement. The USAF damage tolerance approach based on crack growth from 0.050″ generally provided the shortest inspection thresholds, being less than a third of the FAR 25 values in one case. Given the historical performance of the P-3 and other similar aircraft such as C130, where the structural design is typically multi-load path and the materials used are conventional, early failure from large flaws has not been exposed as an issue for these aircraft and it is hard to see justification for adopting this conservative (and therefore expensive) approach. This is not at odds with the emerging consensus in the structural integrity community that the adoption of damage tolerance has been most successful in controlling aspects of the design of new aircraft such as stress levels and inspectability, but its usefulness as a means of managing legacy conventional multi-load path structures is more limited.

For the empennage locations, the application of the augmented load sequence to the test article was successful in that it generated the test failures that were necessary to fully evaluate the life of structure and allow the application of the Def Stan 00-970 advocated safe S-N approach without the need for "supplementary evidence" to clear the structure. From the analysis of the empennage failures, the Def Stan 00-970 and FAR 25 based approaches produced comparable values of Safe Life/inspection threshold and it is likely that if the test was not extended to reveal these failures the resulting inspection burden would have been more extensive in order to cover the otherwise uncertainty in failure location.

The major point of difference between the various airworthiness standards with regard to the calculation of inspection intervals is the use by Def Stan 00-970 of a factor of 3 verses a factor of 2 for the other approaches. The underlying justification for the larger factor in Def Stan 00-970 could be pursued further with the UK MoD. Certainly the coupon results in the P-3 program suggest that established crack growth has lower scatter than the period of crack 'initiation'.

The comparison of the latest coupon results to the earlier predictions of total life for FCA361 confirms that the FAMS and FASTRAN results can be used with confidence in the P-3 SLAP TI for this location. FASTRAN can also be used with confidence for the inspection interval calculations; however the predictions for the AP-3C sequence showed the same 15-30% conservatism that was also seen in some of the original coupon verification work as part of the TI. Improvements to the FASTRAN model and the associated material data would be of help in any program seeking to remove unnecessary in-service maintenance costs.

The FAMS predictions in the TI for FCA 301 were consistent with experimental results in terms of relative crack initiation life. This is an important result given the significant change in RAAF spectrum severity between the spectra used for initial tool verification and the final spectra used in the TI. However, the $K_{n\text{-}TD}$ pegging process required significant adjustment in the $K_n$ from the anticipated theoretical value in order to accommodate the longer coupon lives and this shift was confounded by the cross-over of the FAMS life prediction curves for the FSFT and RAAF P-3C spectra. Inaccurate total life predictions for the coupons were produced as a result. Initial exploration of the problems has not identified a solution and further investigations are now warranted.

The use of FASTRAN as a total life predictor also showed promise but these results need to be balanced against other results provided in [21] which were less consistent. Nevertheless, with improvements to the performance of the model and in the underlying material data at very small crack sizes, it might be possible for FASTRAN to produce reliable total life predictions. The EBA results for total life prediction show that this more simple method is not likely to be suited to the types of stress levels and spectra associated with transport aircraft, although calculations of inspection intervals are more likely to be reliable.

## 11.2 Statement of Applicability

This report provides results of analyses of outputs from the application of a number of lifing standards that have used data relating to P-3 aircraft with a combination of spectra, critical features and stress levels typical for a transport type aircraft.

This report demonstrates that alternative approaches (both standards and methods), when applied, have the potential to yield a range of outcomes. Unsurprisingly, these alternative approaches will likely be more conservative, or less conservative, than the baseline result obtained by the original design standard. The level of safety attained by application of any particular combination of standard and method is notional at best; however real cost of ownership and availability benefits or penalties can result from the choice of standard. Selective use of particular features from different standards is not recommended however; as standards have generally been developed, applied, and proven over time as complete "packages". Changing or mixing methods from different standards should always be undertaken with the utmost care.

While the end result of this comparison is demonstrated differences in hours for Safe or Total Life, Inspection Threshold and Inspection Frequency, there is no attempt to normalise or specifically select input variables to achieve a particular outcome. The demonstrated variation in outputs, when using each standard and method described in this Report, results from an "as is" interpretation of a standard. Specifically, there is no attempt to achieve a common probability of failure – despite DEF STAN 00-970 and the Probabilistic fleet analysis targeting a notional 1/1000 probability of failure. Nor have the assumptions or judgements permitted by some of the standards, that result in setting of safety factors (etc.), been aligned between the standards (even if this were possible). Consequently, this comparison, at best, demonstrates that there is a potential for differences when using different standards. The results, which are manifested as differences in flight hours to inspection threshold, total life, etc. are by no means absolute; whether they could be considered as indicating differing levels

of safety relative to each other requires further exploitation of the methods within each standard to assess inherent conservatisms (or non-conservatisms) and their limitations in application.

This report does not advocate the use of one airworthiness standard over another for the in-service fatigue life management of military transport aircraft. Equally none of the current tools can be considered "best" for all situations. Additionally, it should not be presumed that any tool will automatically be satisfactory for any new situation. Assessment in accordance with the methodology of this current work may provide a limited, but useful, comparison with the results from the original design standard and lifing methodology. As more data are collected on platforms it may indeed prove possible to use the methodology of this work more regularly to assess lifing across a number of standards - whence a degree of consistency may provide greater confidence in lifing predictions.

Generally, the use of a standard and methodologies compatible with that invoked during design and then adopted as the Certification Structural Design Standard (i.e. in subsequent ADF certification) will be the most appropriate

# 12. References


1. P-3C Service Life Assessment Program – Australian Test Interpretation Report for the USN Wing/Fuselage/Landing Gear Test Articles, B. Teunisse, M. Phillips, D. Mongru, P. Jackson, E. Matricciani and D. Hartley, DSTO-TR-1929, October 2006

2. P-3C Service Life Assessment Program – Australian Test Interpretation Report for the Empennage Test Articles, D. Hartley, P. Jackson, E. Matricciani, B. Teunisse and M. Phillips, DSTO-TR-1856, August 2005

3. Australian P-3 Structural Management Plan, D. Mongru, K. Maxfield, B. Murtagh, E. Matricciani, L. Meadows and P. Jackson, DSTO-TR-1947, December 2006

4. User Guide to the Safe S-N Analysis Chart Template, K. Maxfield and B. Murtagh, DSTO-TR-XXXX, To be published

5. P-3C Service Life Assessment Program User's Guide to using FAMS and FASTRAN, M. Phillips, DSTO-DP-1062, 2003

6. User Guide to the Aircraft Cumulative Probability Chart Template, B. Murtagh and K. Maxfield, DSTO-TR-2332, 2009

7. Federal Aviation Regulations Part 25 - Airworthiness Standards: Transport Category Airplanes, October 1994, Federal Aviation Administration

8. Advisory Circular – Damage Tolerance and Fatigue Evaluation of Structure, AC No. 25.571-1C, 29 April 1998, Federal Aviation Administration

9. Defence Standard 00-970, Design and Airworthiness Requirements for Service Aircraft, Issue 5, 31 January 2007, UK Ministry of Defence

10. Joint Service Specification Guide – Aircraft Structures, JSSG-2006, 30 October 1998, US Department of Defense

11. An Evaluation of the Effective Block Approach Using P-3C and F-111 Crack Growth Data, C. Wallbrink, R. Amaratunga, W. Hu, P. Jackson and D. Mongru, DSTO-TR-2195, September 2008.

12. Direct Current Potential Drop System Evaluation for 7075-T6 Notched and Centre Crack Growth Coupons, D. Mongru, DSTO-DP-1110, January 2009

13. Metallic Materials Properties Development and Standardization (MMPDS), R. Rice, J. Jackson, J. Bakuckas and S. Thompson, DOT/FAA/AR-MMPDS-01, US Department of Transportation – Federal Aviation Administration, January 2003

14. Forecasting the Risk of Fleetwide Fatigue Cracking in Aircraft Structure, E.K. Walker, Workshop Notes for RAAF and AMRL, May 1996

15. Fatigue Assessment of the F/A-18 Horizontal Stabilator Spindle, M. McDonald and L. Molent, DSTO-TR-1620, 2004

16. Assessment of Fatigue Crack Growth Prediction Models for F/A-18 Representative Spectra and Material, M. McDonald, L. Molent and A.J. Green, DSTO-RR-0312, 2006

17. Results of the FMS Spectra Coupon Test Program Performed within the framework of the P-3C Service Life Assessment Program, R.P.G. Veul and L.C. Ubels, NLR-CR-2003-488, December 2003

18. P-3C SLAP Load DataBase and Spectra Sequencing Tool (DBI/SST) DSTO Validation, E. Matricciani and P. Jackson, DSTO-TR-1720, June 2005

19. Development of the RAAF P-3C Fatigue Sequences for the P-3 Service Life Assessment Program (SLAP) Test Interpretation – Part 1 and 2, E. Matricciani and P. Jackson, DSTO-TR-1704, May 2005

20. Computer Programs and Methodology used for DSTO P-3C SLAP Test Interpretation, B. Teunisse, M. Phillips, P. Jackson, E. Matricciani, W. Hu, R. Amaratunga, D. Hartley and D. Mongru, DSTO-TR-1834, March 2006

21. DSTO Coupon Testing Documentation in Support of the P-3 SLAP, M Phillips, D. Hartley, R. Amaratunga, DSTO-TR-1765, July 2005

22. Lockheed-Martin Corporation, Fatigue Analysis of Metallic Structure (FAMS) Stress Ratio Effects LG05ER0145, N00019-05-D-005 CDRL A007, P-3 T/M/S FLMP, 2006

# Appendix A: P-3 Case Studies Critical Locations

## A.1. FCA301-WEB-4

FCA301-WEB-4 is located on the lower outer wing spar web, and is related to cracking in fastener holes common to the front spar cap, just outboard of the centre wing/outer wing splice. This location is shown in Figure A- 1.

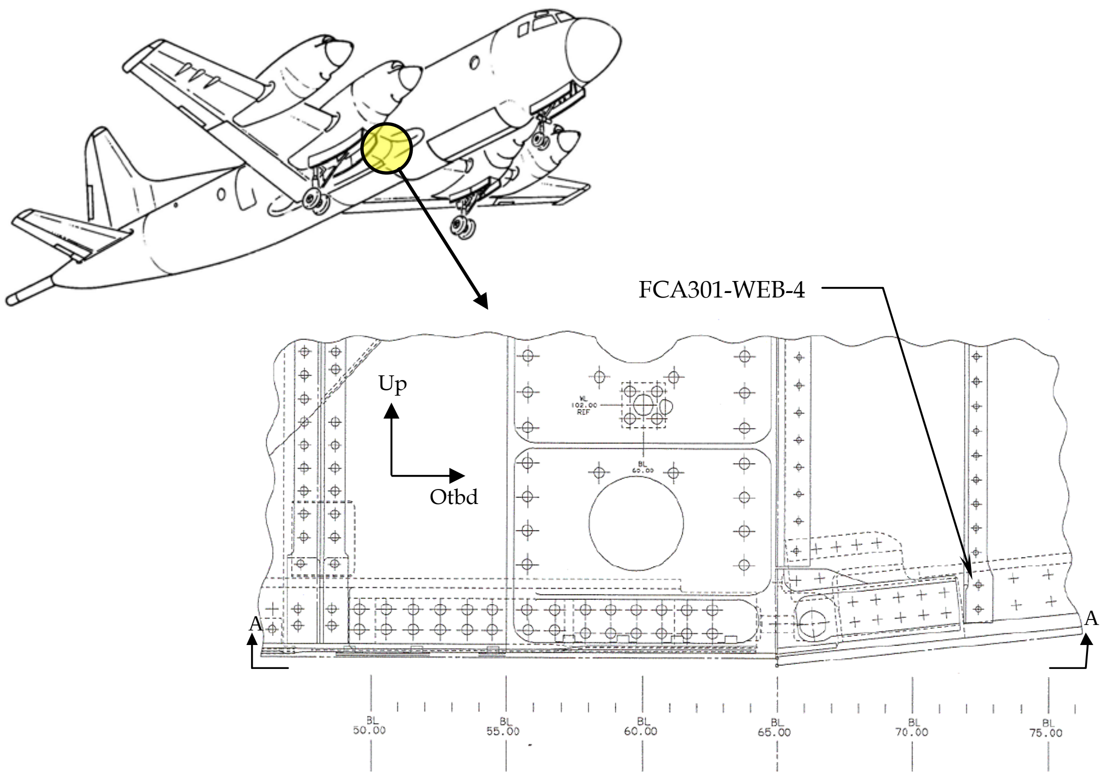


*Figure A- 1: Location of FCA301-WEB-4*

This location was found cracked on both the LH and RH wings of the FSFT article at wing station (WS) 72. Cracking was detected at the same time (33,298 test hours), however, the RH wing had been subjected to an additional 10,988 AFHRS of pre-test usage. Cracking on the LH wing was more significant with a 0.941" single edge crack. A summary of the FSFT cracks found at this FCA is provided in Table A-1.

*Table A-1: FCA301-WEB-4 FSFT Results*

| Finding No. | FS | WS | Hole Dia. (inch) | Crack Length (inch) | Hours |
|---|---|---|---|---|---|
| 1552 | 571 | 72.5 L | 0.25 | 0.941 | 38,000 |
| 1540 | 571 | 72.5 R | 0.25 | 0.75 | 48,988 |

Fleet inspections have been undertaken by the USN on 63 aircraft in this region. A very significant crack, measuring 1.5″ was found in the lower hole of the web at WS 72. A summary of the fleet cracks found at this FCA (from WS 65 to WS 83) is provided in Table A-2.

*Table A-2: FCA301-WEB-4 Fleet Inspection Results*

| **Fleet Findings (Nov 2005) within FCA301-WEB-4** | | | | | | |
|---|---|---|---|---|---|---|
| **Source** | **Aircraft Inspect.** | **Aircraft with Cracks** | **Length (inch)** | **Number of Cracks** | **Station** | **Time (AFHRS)** |
| **USN (20)** | 63 | 12 | ≤0.03 | 2 | WS 83 | 4,435 |
| | | | ≤0.03 | 14 | WS 70 – 83 | 14,300 – 19,744 |
| | | | 0.05 – 0.13 | 3 | WS 67 – 79 | 13,409 – 17,380 |
| | | | 1.5 | 1 | WS 72 | 17,839 |

## A.2. FCA351-CDN-2

FCA351-CDN-2 is concerned with cracking of the front lower spar cap at the inboard nacelle fillet fairing Dome Nut Hole (DNH) common to the fillet fairing, lower wing panel 1 and the lower spar cap at WS 156. A diagram of this location, illustrating the cracking, is included as Figure A- 2.

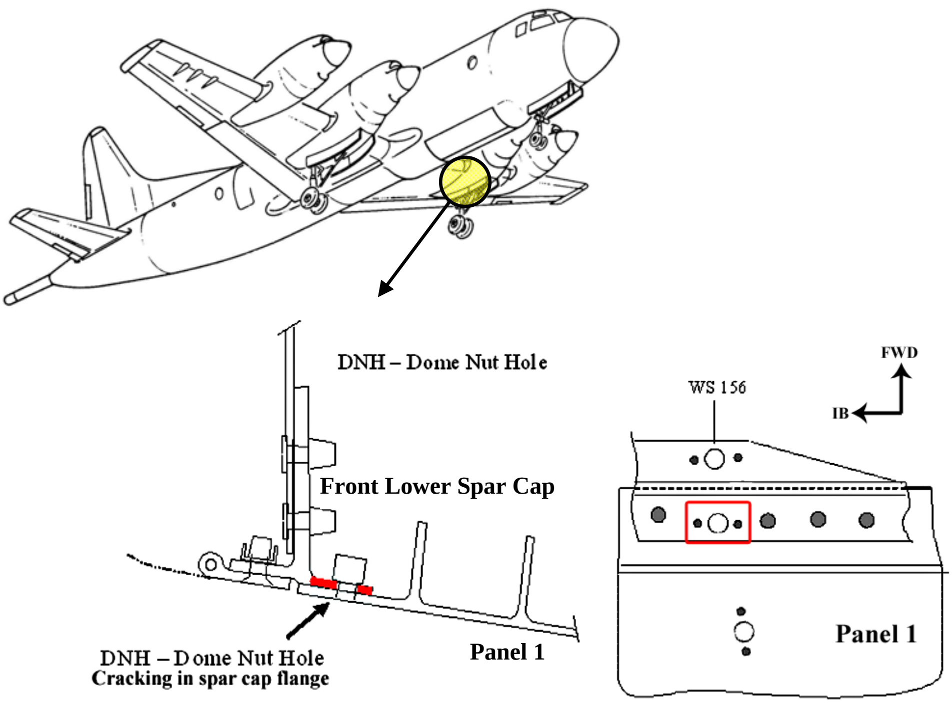


*Figure A- 2: Location of FCA351-CDN-2*

There was only one crack discovered on the FSFT in this location. This crack was detected during inspections on the RH wing after 22,601 SFHRS (includes 10,988 hours of in-service usage). The test continued without modification, and the crack was monitored and allowed to

grow. The crack progressed from a 0.15″ single edge crack to a 0.72″ double edge crack by 27,773 SFHRS when the lower front spar between WS 134 and WS 249 was cut from the structure and a replacement splice was inserted. No cracking was detected on this replacement structure, or the LH wing (38,000 SFHRS). A summary of the crack findings is included in Table A-3.

*Table A-3: FCA351-CDN-2 FSFT Results*

| Finding No. | FS | WS | Hole Dia. (inch) | Crack Length (inch) | Hours |
|---|---|---|---|---|---|
| 1337 | 571 | 156 R | 0.25 | 0.15[1] | 22,601 |

[1] Single edge crack continued to grow to a 0.72″ double edge crack by the time the RH outer wing front spar lower cap between WS 134 & WS 249 was replaced at 27,773 SFHRS.

Fleet inspections at this location have been undertaken by the USN and the RAAF with a total of six aircraft having cracks. These findings are summarised in Table A-4.

*Table A-4: FCA351-CDN-2 Fleet Inspection Results*

| **Fleet Findings (Nov 2005) within FCA351-CDN-2** | | | | | | |
|---|---|---|---|---|---|---|
| **Source** | **Aircraft Inspect.** | **Aircraft with Cracks** | **Length (inch)** | **Number of Cracks** | **Station** | **Time (AFHRS)** |
| **USN (3)** | 30 | 3 | $\leq 0.03$ | 3 | WS 155 | 12,854 – 20,587 |
| | | | | | | |
| **USN AEB (3)** | 41 | 3 | Small | 2 | WS 155 | Unknown |
| | | | Large | 1 | WS 155 | Unknown |
| | | | | | | |
| **RAAF S76 (0)** | 5 | 0 | - | 0 | - | - |

## A.3. FCA352-PDN-1

FCA352-PDN-1 pertains to the lower wing inboard fillet fairing DNHs on the inboard nacelle located at WS 160. This FCA does not include the first DNH which is common to the front spar cap, as this is covered by FCA351-CDN-2. The location of this FCA is shown in Figure A- 3.

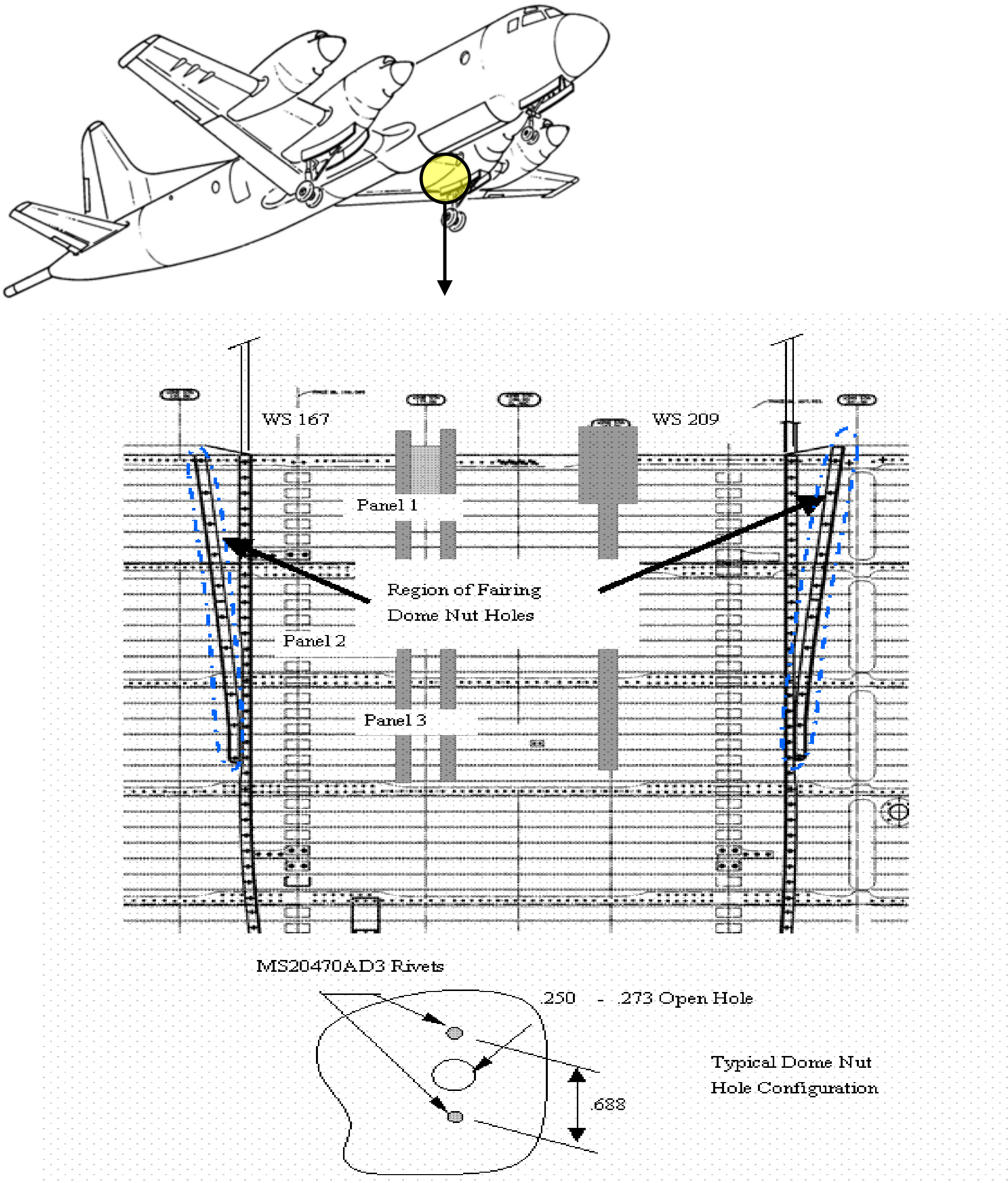


*Figure A- 3: Location of FCA352-PDN-1*

Extensive cracking in this region was discovered on the FSFT after 16,785 hours of testing. Cracking was discovered in both the LH and RH wings, with the RH wing having undergone 10,988 hours of pre-test usage, while the LH structure was new at the start of testing. A summary of the cracks detected is provided in Table A-5.

*Table A-5: FCA352-PDN-1 FSFT Results*

| Finding No. | FS | WS | Hole Dia. (inch) | Crack Length (inch) | Hours |
|---|---|---|---|---|---|
| 1362 | 576 | 157 L | 0.27 | 0.164 | 16,785 |
| 1363 | 596 | 160 L | 0.27 | 0.13 | 16,785 |
| 1350 | 576 | 157.5 R | 0.27 | 1.49 | 27,773 |
| 1351 | 580 | 157.7 R | 0.27 | 0.99 | 27,773 |
| 1352 | 584 | 158.2 R | 0.27 | 0.82 | 27,773 |
| 1353 | 588 | 158.7 R | 0.27 | 1.34 | 27,773 |
| 1354 | 592 | 159 R | 0.27 | 1.03 | 27,773 |
| 1355 | 596 | 159.4 R | 0.27 | 1.04 | 27,773 |

At this point in time, several of the larger DNH cracks on the RH wing were cut from the structure, and doubler/tripler repairs applied to the entire region of the inboard nacelle inboard fillet fairing. Force-tec retainers were installed in the RH DNHs and the satellite holes were split sleave cold worked. The cracks on the LH wing were stop-drilled, and repair doublers/triplers applied to the entire region. No further cracking was found during testing or teardown, however due to the extensive repairs applied, the loading on these fasteners was no longer representative of in-service structure.

Fleet inspections at the inboard nacelle DNHs have been undertaken by the USN and the RAAF. Significant findings of fatigue cracking have been recorded, and the results are summarised in Table A-6.

*Table A-6: FCA352-PDN-1 Fleet Inspection Results*

| **Fleet Findings (Nov 2005) within FCA352-PDN-1** | | | | | | |
|---|---|---|---|---|---|---|
| **Inspection program** | **Aircraft Inspect.** | **Aircraft with Cracks** | **Length (inch)** | **Number of Cracks** | **Station** | **Time (AFHRS)** |
| **USN (55)** | 64 | 28 | ≤ 0.03 | 2 | WS 155 – 161 | 4,435 |
| | | | ≤ 0.03 | 36 | WS 155 – 161 | 12,550 – 20,224 |
| | | | 0.04 - 0.06 | 8 | WS 156 – 167 | 13,409 – 19,020 |
| | | | 0.12 – 0.25 | 9 | WS 156 – 167 | 12,518 – 19,290 |
| | | | | | | |
| **USN AEB (94)** | 41 | 21 | Large | 12 | WS 156 | Unknown |
| | | | Small | 77 | WS 156 | Unknown |
| | | | X Small | 5 | WS 156 | Unknown |
| | | | | | | |
| **RAAF S76 (0)** | 5 | 0 | - | 0 | - | - |

## A.4. FCA375-PSS-2

FCA375-PSS-2 is concerned with cracking in lower wing panel 3 of the panel 2/3 splice between the inboard and outboard engine nacelles. Only cracks between WS 239 to 311 were considered. This location is shown in Figure A- 4.

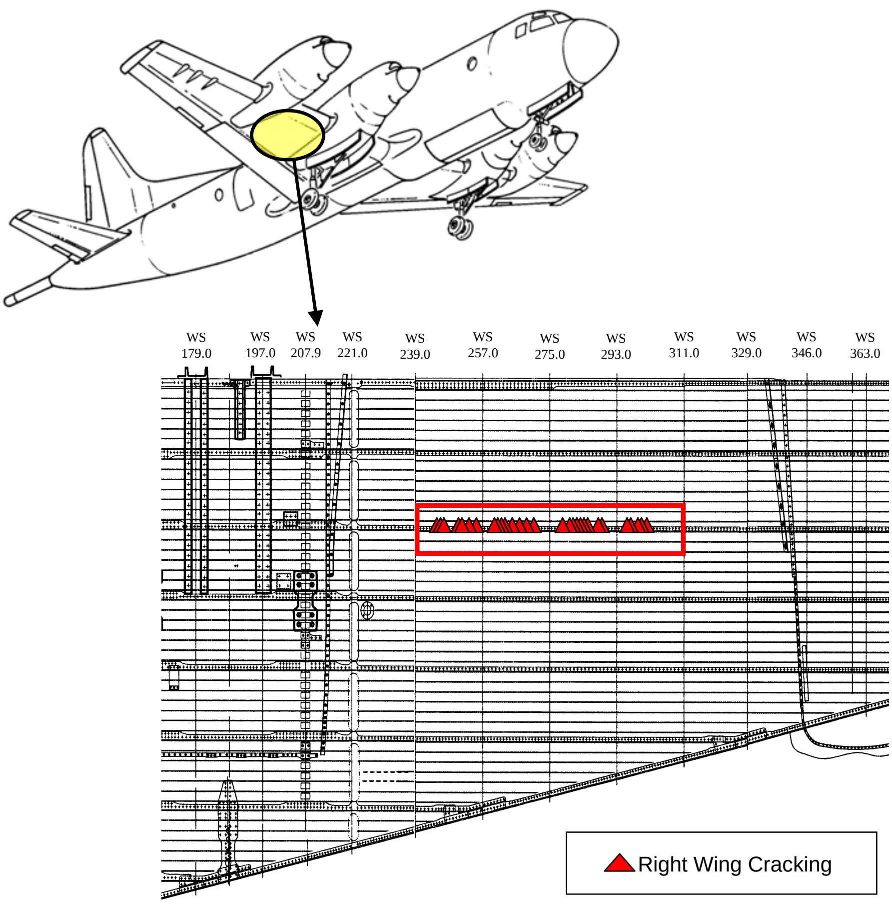


*Figure A- 4: Location of FCA375-PSS-2*

No cracks were discovered at this location during testing. On teardown, extensive cracking was found in the RH wing with a total of 31 cracks, ranging from 0.052" to 0.998". No cracks were discovered in the LH wing, which was not subjected to in-service usage. A summary of the FSFT cracks is included in Table A-7.

*Table A-7: FCA375-PSS-2 FSFT Results*

| Finding No. | FS | WS | Hole Dia. (inch) | Crack Length (inch) | Hours |
|---|---|---|---|---|---|
| 1096 | 600 | 243 R | 0.187 | 0.147 | 48,988 |
| 1097 | 600 | 244 R | 0.186 | 0.192 | 48,988 |
| 1098 | 600 | 245 R | 0.188 | 0.232 | 48,988 |
| 1099 | 600 | 249 R | 0.189 | 0.209 | 48,988 |
| 1510 | 600 | 301.5 R | 0.185 | 0.339 | 48,988 |
| 1511 | 600 | 300 R | 0.185 | 0.161 | 48,988 |
| 1512 | 600 | 299 R | 0.185 | 0.471 | 48,988 |
| 1513 | 600 | 297 R | 0.185 | 0.542 | 48,988 |
| 1514 | 600 | 296 R | 0.185 | 0.175 | 48,988 |
| 1516 | 600 | 289 R | 0.185 | 0.168 | 48,988 |
| 1517 | 600 | 288 R | 0.185 | 0.312 | 48,988 |
| 1519 | 600 | 285 R | 0.185 | 0.198 | 48,988 |
| 1520 | 600 | 284 R | 0.185 | 0.203 | 48,988 |
| 1521 | 600 | 283 R | 0.185 | 0.052 | 48,988 |
| 1522 | 600 | 282 R | 0.185 | 0.321 | 48,988 |
| 1523 | 600 | 282 R | 0.185 | 0.303 | 48,988 |
| 1524 | 600 | 281 R | 0.185 | 0.996 | 48,988 |
| 1525 | 600 | 280 R | 0.185 | 0.77 | 48,988 |
| 1526 | 600 | 278 R | 0.185 | 0.086 | 48,988 |
| 1528 | 600 | 270 R | 0.185 | 0.083 | 48,988 |
| 1529 | 600 | 270 R | 0.185 | 0.054 | 48,988 |
| 1532 | 600 | 268 R | 0.185 | 0.157 | 48,988 |
| 1534 | 600 | 266 R | 0.185 | 0.259 | 48,988 |
| 1536 | 600 | 264 R | 0.185 | 0.159 | 48,988 |
| 1538 | 600 | 262 R | 0.185 | 0.484 | 48,988 |
| 1539 | 600 | 261 R | 0.185 | 0.132 | 48,988 |
| 1541 | 600 | 260 R | 0.185 | 0.285 | 48,988 |
| 1543 | 600 | 259 R | 0.185 | 0.348 | 48,988 |
| 1546 | 600 | 254 R | 0.185 | 0.154 | 48,988 |
| 1549 | 600 | 252 R | 0.185 | 0.381 | 48,988 |
| 1551 | 600 | 250 R | 0.185 | 0.238 | 48,988 |

A total of 12 USN aircraft have had the panel 2/3 splice inspected in this region as part of teardown or replaced part inspections. Four of these aircraft had cracks reported. However, all of these cracks were minor crack indications measuring 0.03″ or less. A summary of the cracking reported is in Table A-8.

*Table A-8: FCA375-PSS-2 Fleet Inspection Results*

| Fleet Findings (Nov 2005) within FCA375-PSS-2 | | | | | | |
|---|---|---|---|---|---|---|
| **Source** | **Aircraft Inspect.** | **Aircraft with Cracks** | **Length (inch)** | **Number of Cracks** | **Station** | **Time (AFHRS)** |
| **USN (19)** | 12 [1] | 4 | ≤ 0.03 | 19 | WS 240 – 307 | 16,905 – 20,224 |

[1] Note that one aircraft only had one wing inspected and another aircraft was only inspected up to WS 293.

## A.5. FCA811-1

FCA811-1 is a structural detail, including fastener holes, in the vertical stabiliser front spar cap at the root, see Figure A- 5 and Figure A- 6.

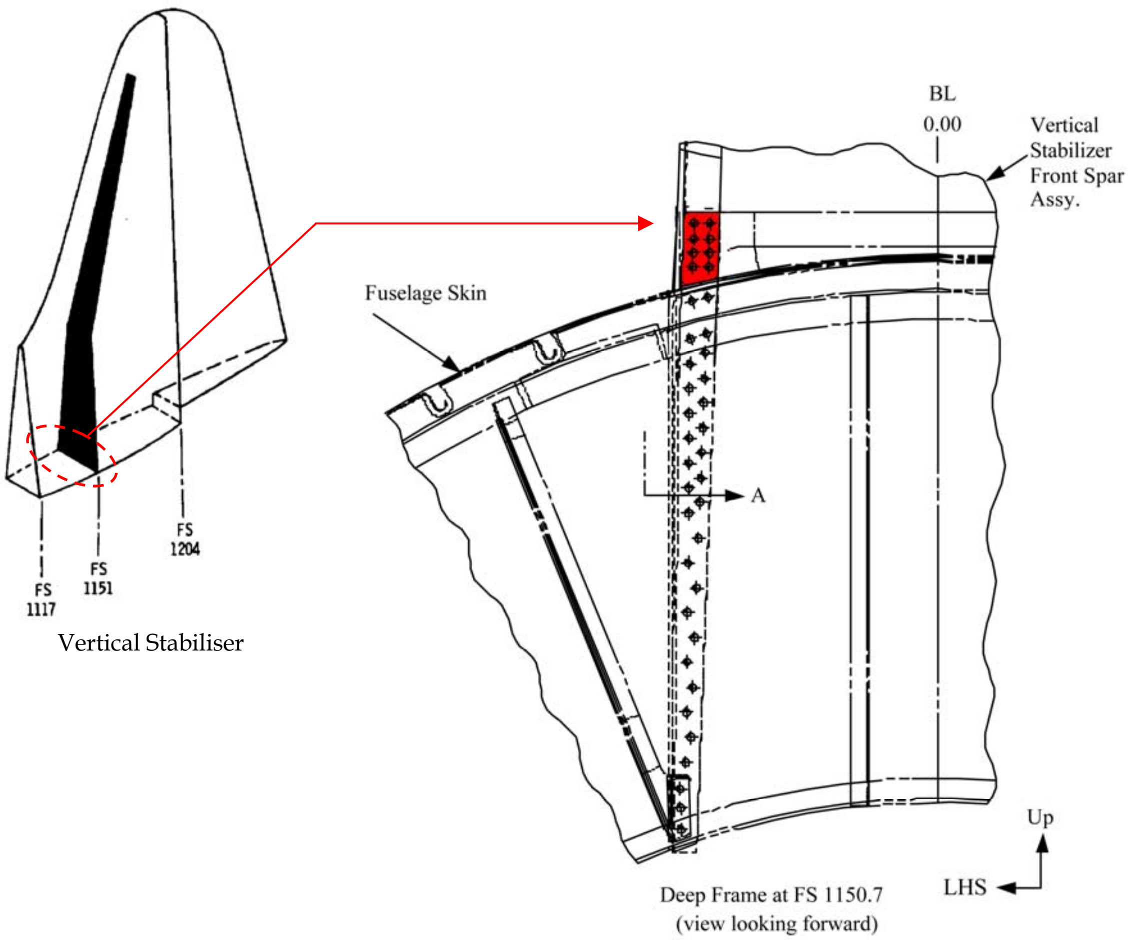


*Figure A- 5: Location of FCA811-1*

There was no cracking detected on the USN test article in this region. Cracking was detected on the Australian test article, and the details are presented in Table A-9.

*Table A-9: FCA811-1 FSFT Results*

| Defect No. | FS | BL | Hole Dia. (inch) | Crack Length (inch) | Hours |
|---|---|---|---|---|---|
| 52 | 1150.7 | 11 R | n/a | 0.59 [1] | 45,000 |
| 53 | 1150.7 | 11 R | n/a | 0.1 | 60,000 |

[1] Crack was 1.65”after 46,478 hours of testing.

There have been no reported inspections of this location for fatigue cracks by any of the P-3 SLAP partners.

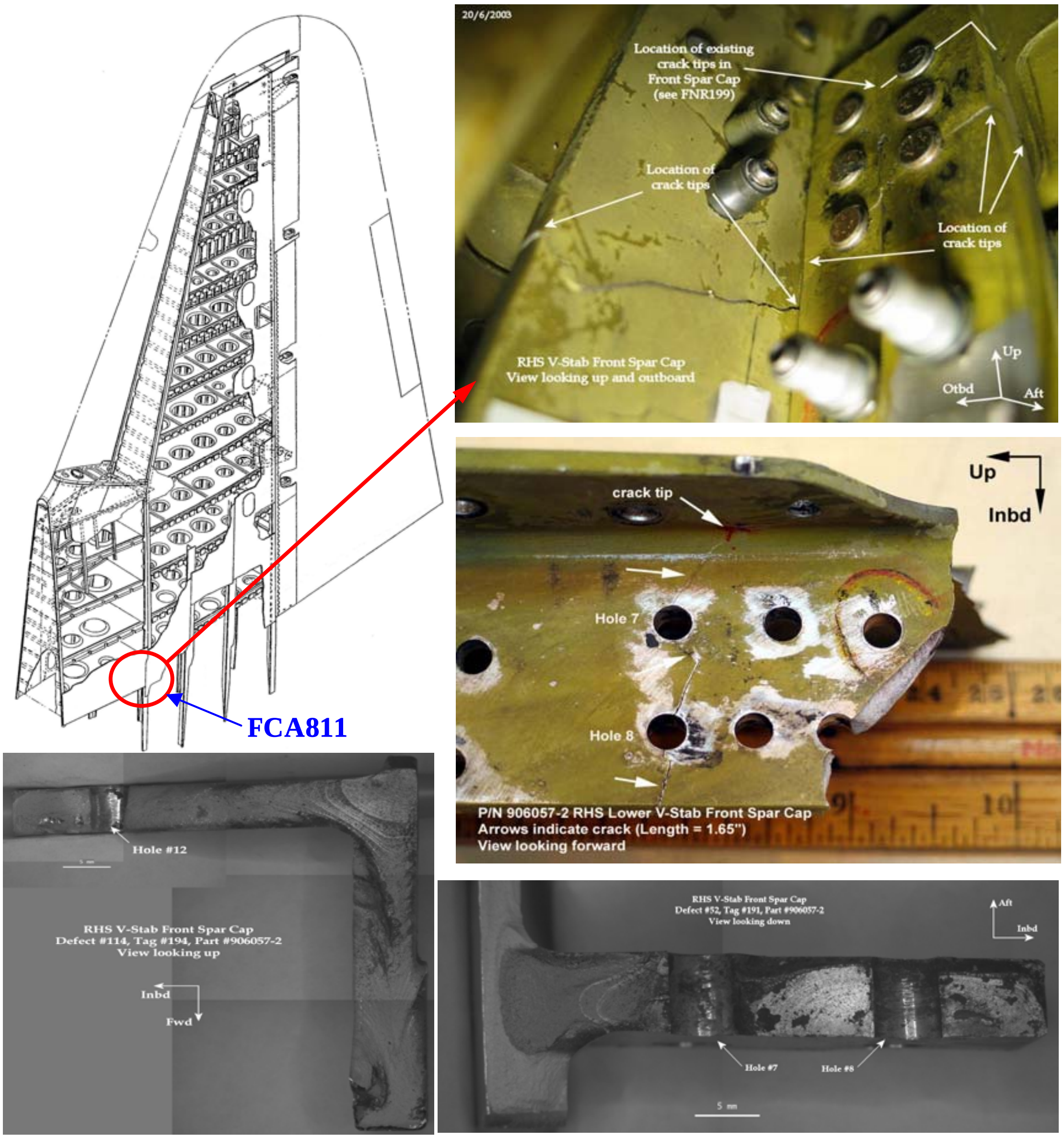


*Figure A- 6: Photographs of the cracking discovered at FCA811 (both 811-1 and -2)*

## A.6. FCA811-2

FCA811-2 details the vertical stabiliser front spar cap at the aft flange runout radius, see Figure A- 7.

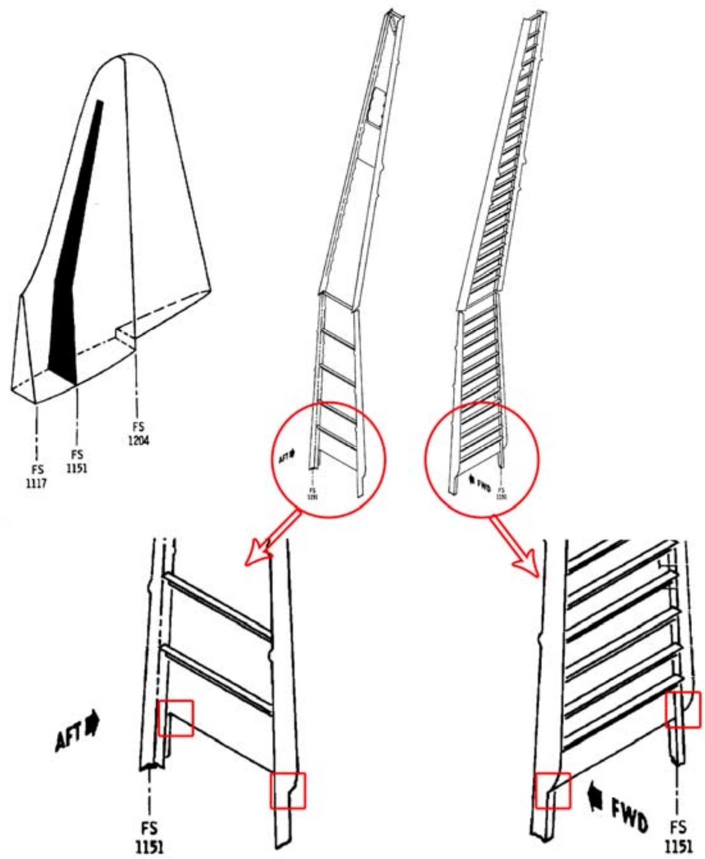


*Figure A- 7: Location of FCA811-2*

There was no cracking detected on the USN FSFT article at this location. Two cracks were found on the Australian test article with the details presented in Table A-10.

*Table A-10: FCA811-2 FSFT Results*

| Defect No. | FS | BL | Hole Dia. (inch) | Crack Length (inch) | Hours |
|---|---|---|---|---|---|
| 114 | 1150.7 | 11 R | n/a | 3.5 (severed) | 46,478 |
| 56 | 1150.7 | 11 L | n/a | 0.21″ | 60,000 |

There have been no reported inspections of this location for fatigue cracks by any of the P-3 SLAP partners.

## A.7. FCA886

FCA886 is located at the root of the RH horizontal stabiliser upper rear spar cap. FCA885 is located at the same point, but on the LH side. Due to the different loading, these locations were identified separately. This location is shown in Figure A- 8.

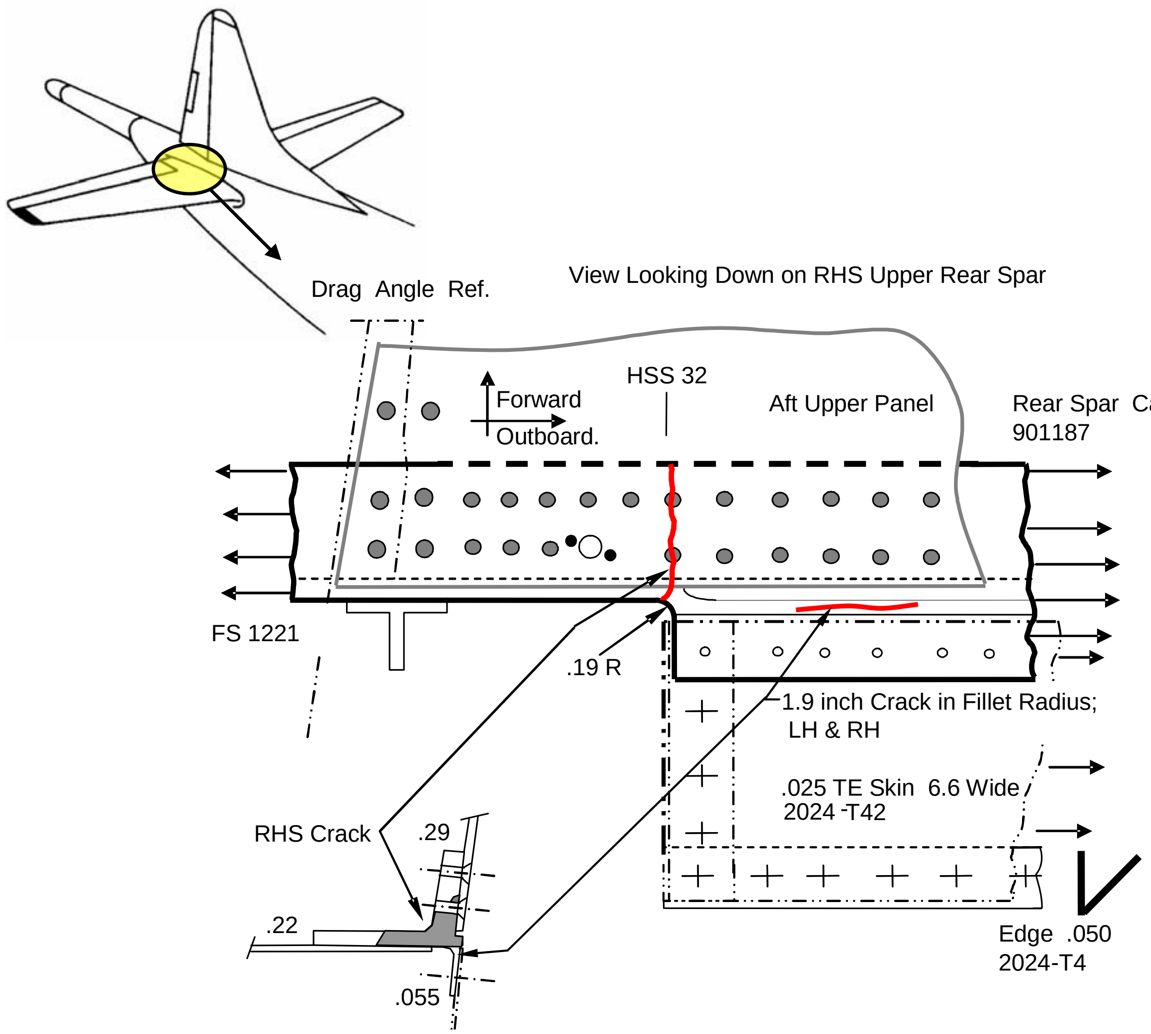


*Figure A- 8: Location of FCA886*

No cracks were detected at this location during cycling of the USN and Australian empennage FSFTs. However, during the RST of the USN FSFT article, a failure occurred at this FCA. The details of this crack are provided in Table A-11. No cracking was found at this location on the Australian FSFT, even though it was tested to 60,000 SFHRS with an augmented spectrum.

*Table A-11: FCA886 FSFT Results*

| Finding No. | FS | HSS | Hole Dia. (inch) | Crack Length (inch) | Hours |
|---|---|---|---|---|---|
| 1061 | 1221 | 32.75 R | n/a | 1.9 | 38,000 |

An examination of the upper rear spar caps of the USN and Australian test articles revealed a significant structural configuration difference at the failure location. As can clearly be seen in Figure A- 9, the Australian spar cap has a blended runout radius, while the USN spar cap has a sharp runout radius. Both configurations are within the tolerances on the drawing. Investigations as part of the DSTO TI have shown this has a significant effect on the localised stresses at this detail which in turn has a significant effect on the life of the component.

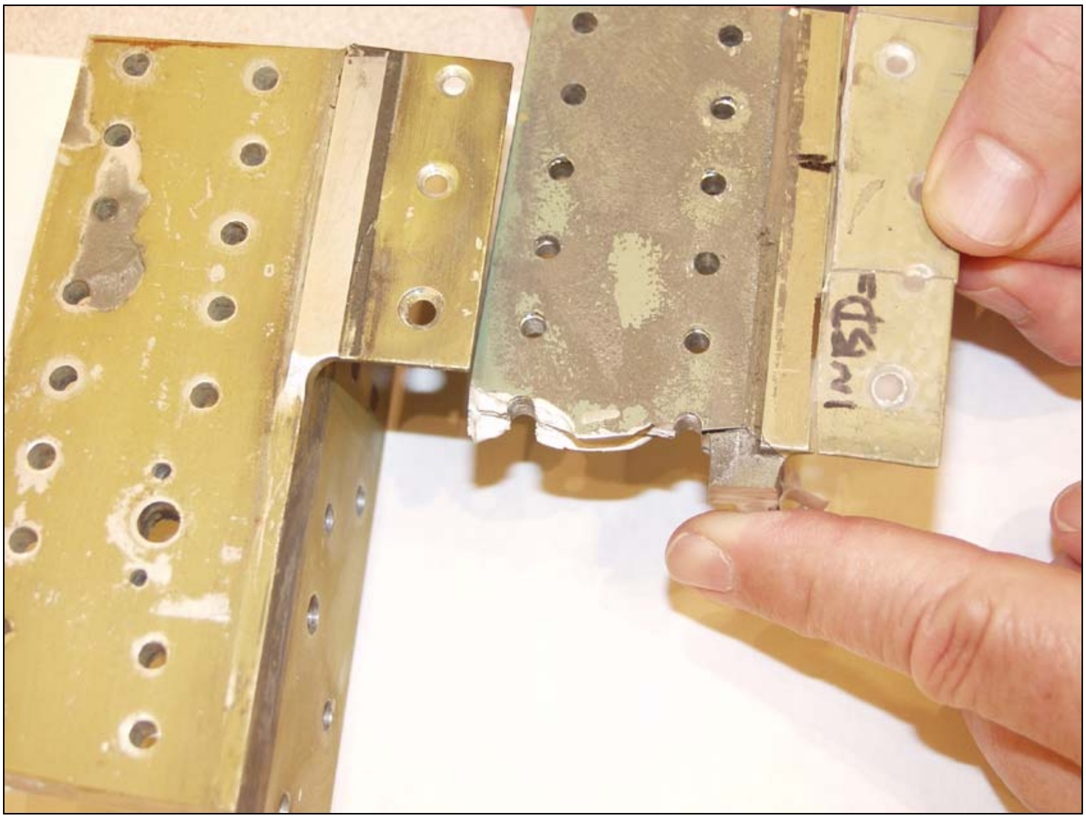


*Figure A- 9: Difference between the Australian (left) and USN (right) Upper Rear Spar Caps*

There have been no reported inspections of this location for fatigue cracks by any of the P-3 SLAP partners.

# Appendix B: DCPD Calibration of P-3 Coupons

Prior to commencing the P-3 coupon test program, two coupons were used to validate/calibrate the DCPD system as per [12]. The validation process involved checking the DCPD crack growth against fractographic crack growth results after application of an F/A-18 sequence (the FT55 "m512" spectrum which is described in [12]). An F/A-18 sequence was selected over a P-3 sequence as the resulting fracture surface is much easier to read fractographically. Note that the process of validation/calibration which checks/determines the relationship between voltage and crack length, is independent of sequence for a given coupon configuration. Figure B. 1 and Figure B. 2 present plots of crack growth from fractography, DCPD using the Johnson Equation and DCPD using the multi-part polynomial derived in [12] for coupons P-3C-03 and P-3C-04 respectively. Crack length is measured from the centre-line of the coupon. As can be seen, the crack growth from the Johnson Equation provides a poor match with the fractographic data while the multi-part polynomial is better, but could be improved for crack lengths less than 5 mm.

As a result, a calibration using the data from coupon P-3C-04 was performed following the process outlined in [12]. Figure B. 3 shows a plot of a/W (fractographic crack length divided by coupon width) versus U (ratio of active coupon voltage divided by reference coupon voltage – see [12] for more details) for a/W values greater than 0.248. Note that here 'a' represents the total crack length including the notch. A 3$^{rd}$ order polynomial was fitted through this data and is included in the plot. Figure B. 4 shows a plot of a/W versus U for a/W values less than 0.248. Note that for a/W values less than 0.23, the U values tended to fluctuate. Consequently, these data points were removed and an initial point representative of an uncracked coupon was inserted at a/W = 0.2 and U = 1. This point represents the total notch length divided by the coupon width while U should equal 1 at the start of cycling. A 3$^{rd}$ order polynomial was then fitted through this data and is shown in Figure B. 4. The transition point between the two polynomials is set at U = 1.0175. Therefore, the new multi-part polynomial is as follows:

1. U < 1.0 — a = notch length
2. 1.0 ≤ U < 1.0175 — a = (11228.21U3 – 34096.74U2 + 34515.63U – 11646.9) × W
3. U ≥ 1.0175 — a = (0.4196U3 – 2.0292U2 + 3.6353U – 1.7866) × W

The performance of this new multi-part polynomial was checked against the fractographic crack growth data for coupons P-3C-04 and P-3C-03 in Figure B. 5 and Figure B. 6 respectively. The crack length represented by the multi-part polynomial in these plots is the total crack length which includes the notch. As can be seen, the new multi-part polynomial is an improvement over the Johnson Equation and the old multi-part polynomial provided in [12]. Therefore, the new multi-part polynomial was used to convert DCPD voltages to crack lengths for the P-3 coupon test results provided in Section 9.

Finally, the minimum crack size measurable by the DCPD system was evaluated in Figures B.7 and B.8 where the fractographic and DCPD crack lengths were compared on a log scale. The crack length in these plots represents the left hand side crack plus the right hand side crack only (i.e. the notch is not included). As can been, the new DCPD multi-part polynomial is able to measure 'total' crack lengths down to about 0.8 mm (0.031") which is equivalent to a 0.4 mm (0.016") crack on both sides of the notch if the cracking was symmetrical. These values are significantly less than the coupon thickness of 3.048 mm (0.12").

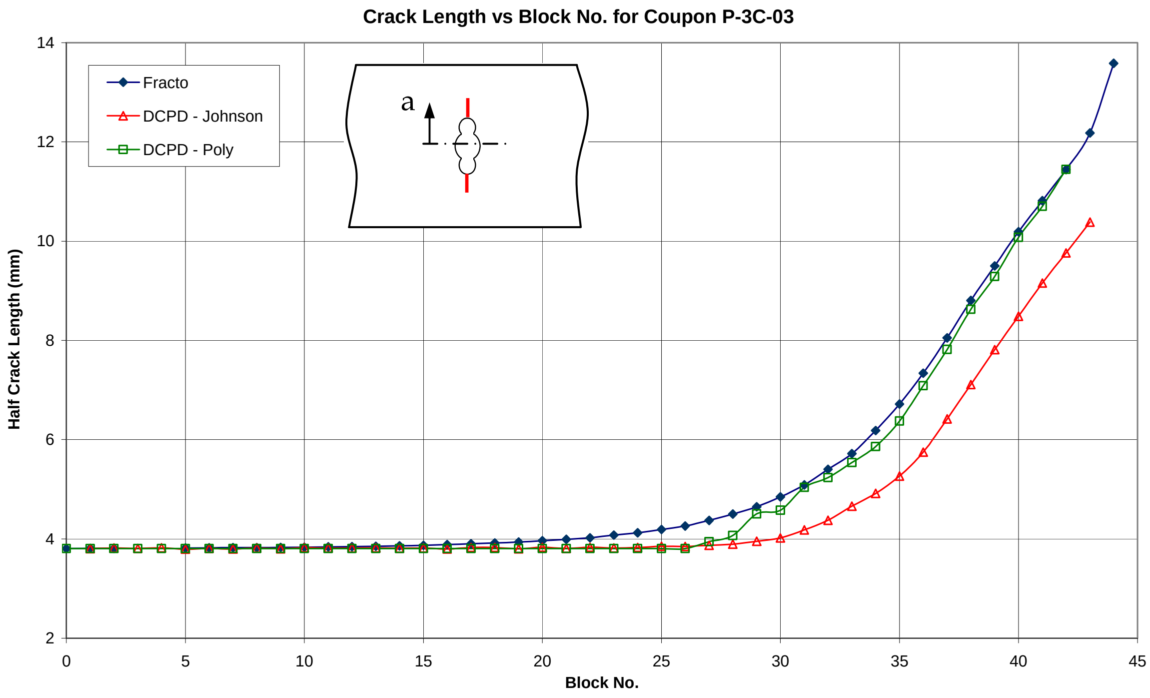


*Figure B. 1: Crack Length versus Block Number for Coupon P-3C-03*

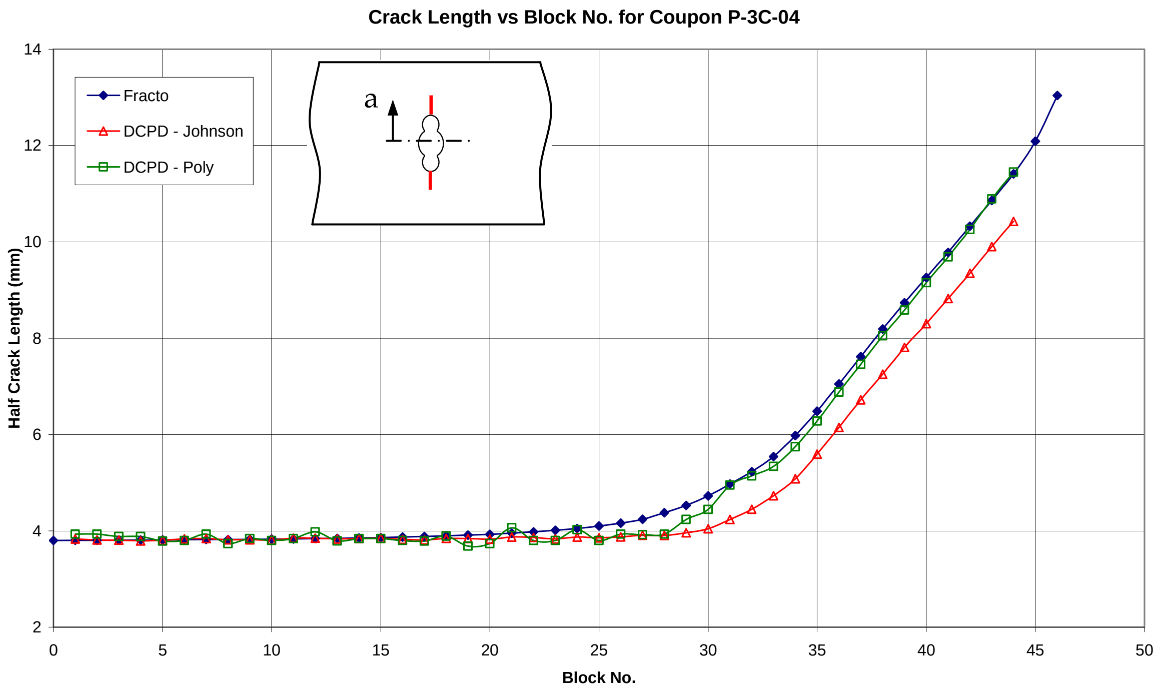


*Figure B. 2: Crack Length versus Block Number for Coupon P-3C-04*

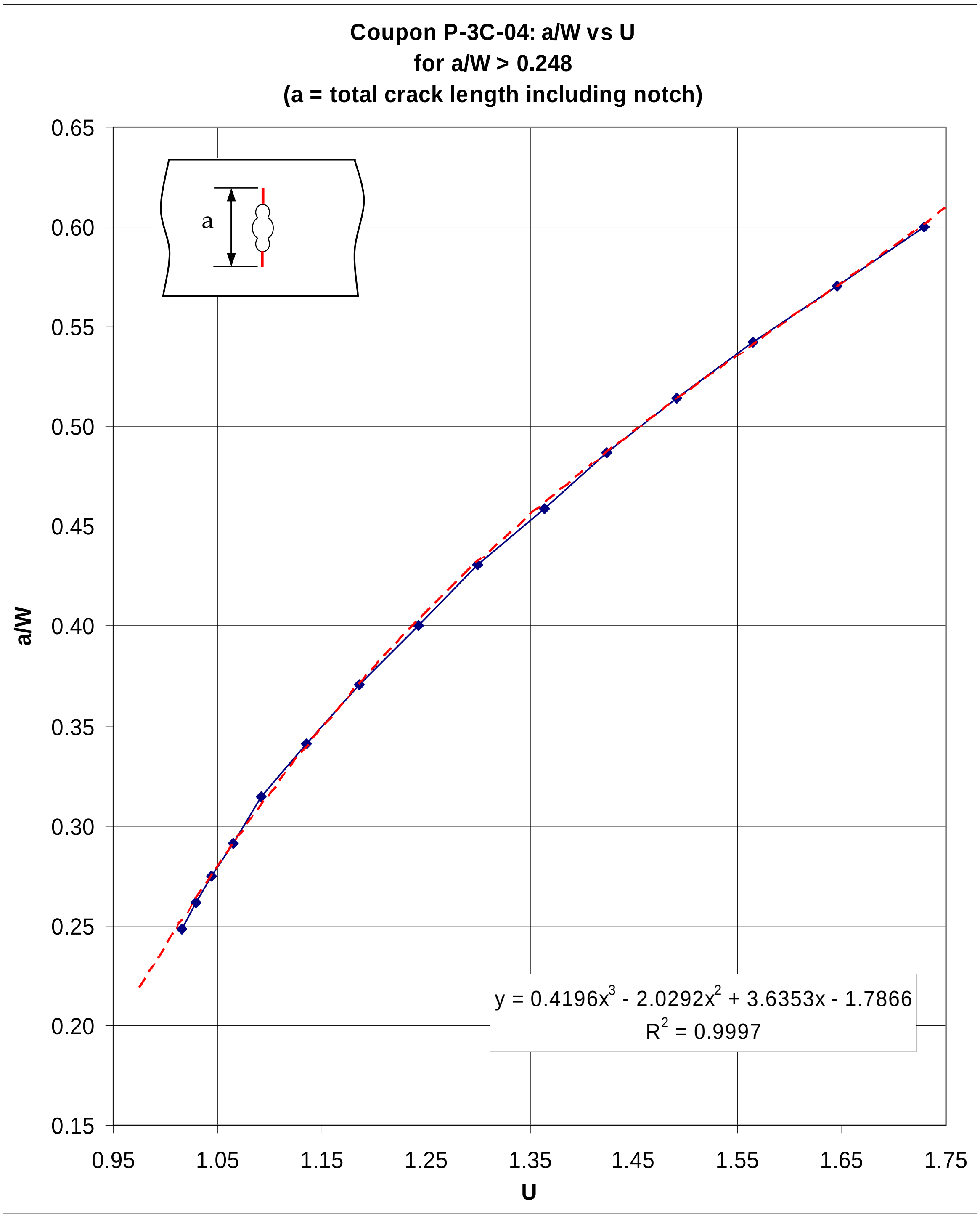


*Figure B. 3: DCPD Calibration of Coupon P-3C-04 for a/W > 0.248*

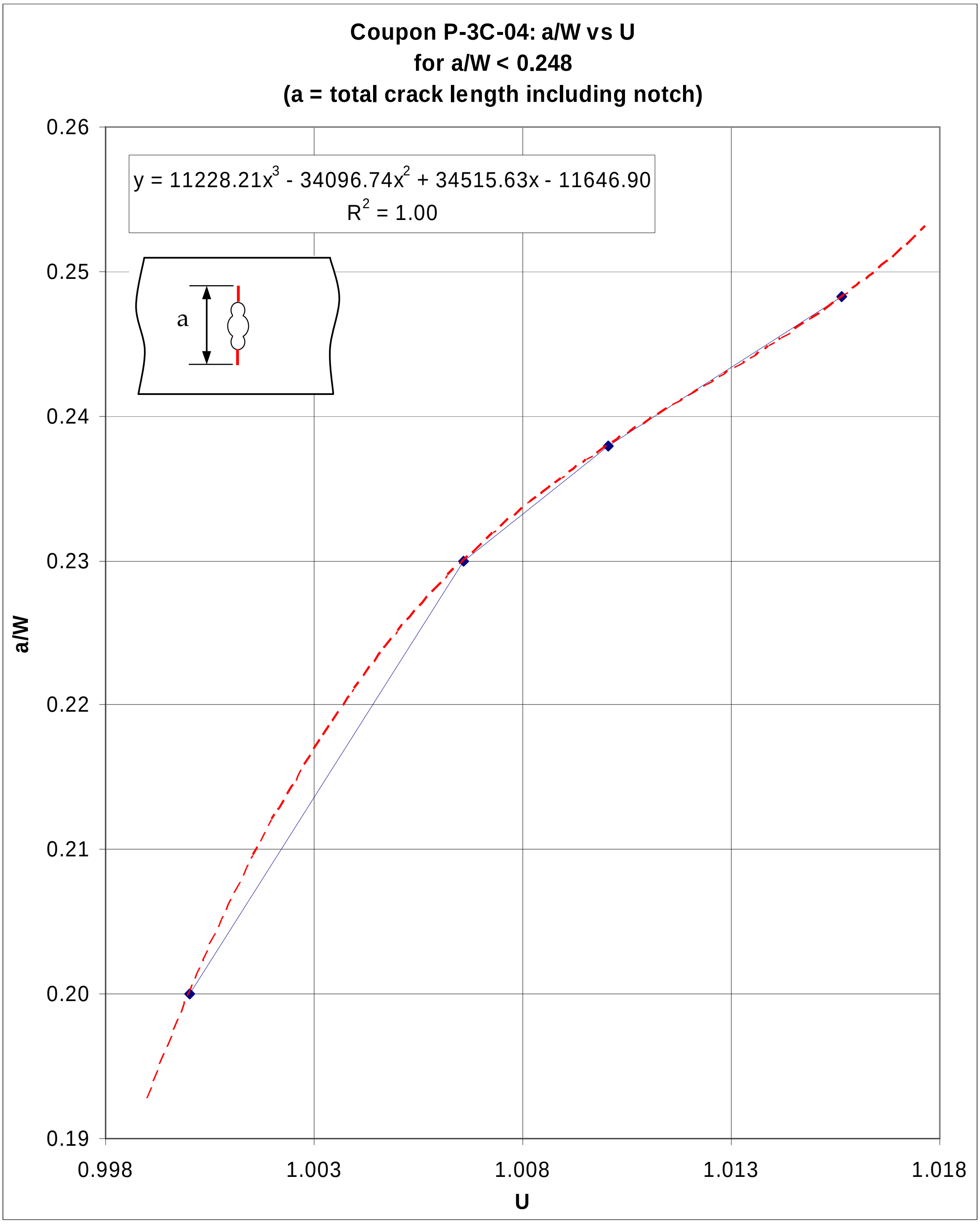


*Figure B. 4: DCPD Calibration of Coupon P-3C-04 for a/W < 0.248*

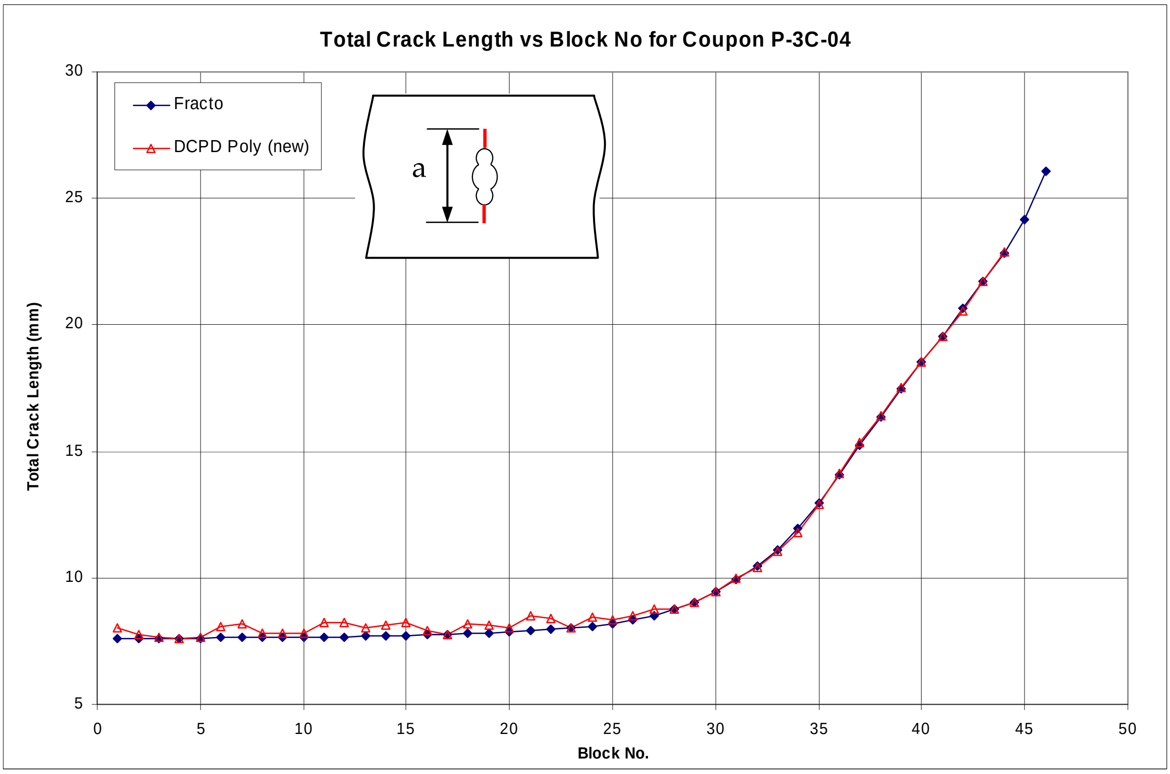


*Figure B. 5: Total Crack Length versus Block Number for Coupon P-3C-04 (New Polynomial)*

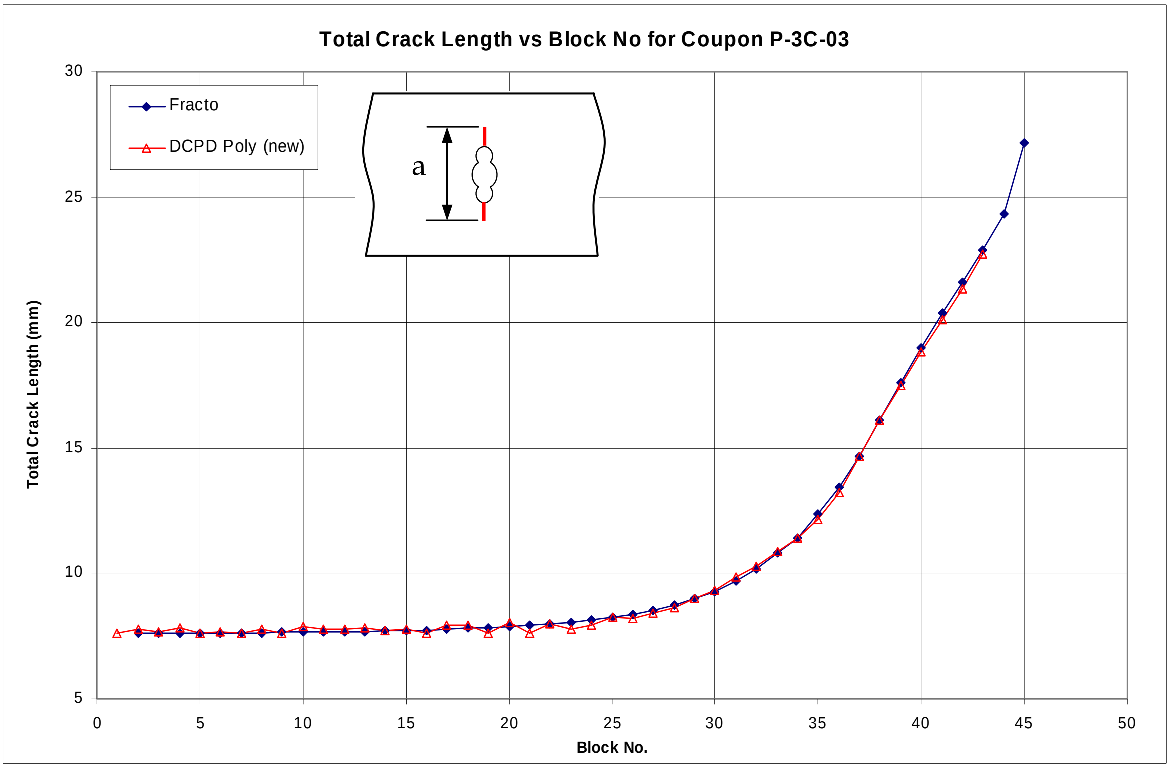


*Figure B. 6: Total Crack Length versus Block Number for Coupon P-3C-03 (New Polynomial)*

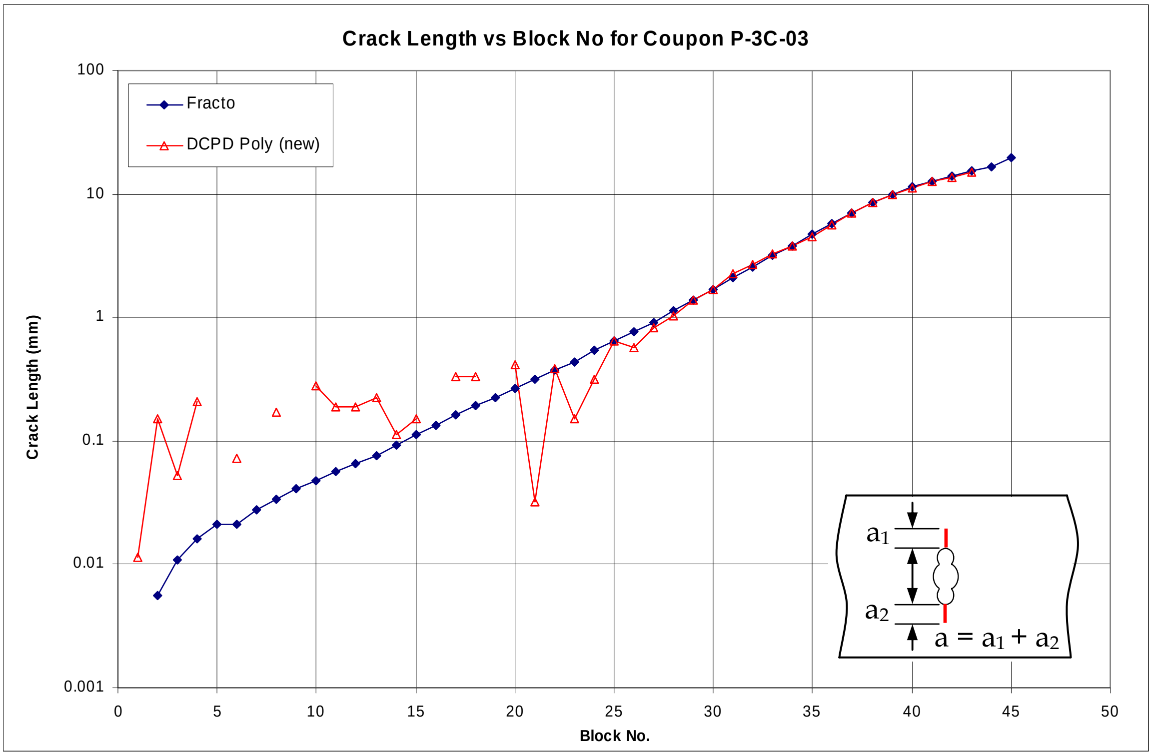


*Figure B. 7: Crack Length versus Block Number for Coupon P-3C-03 (New Poly) – Log Scale*

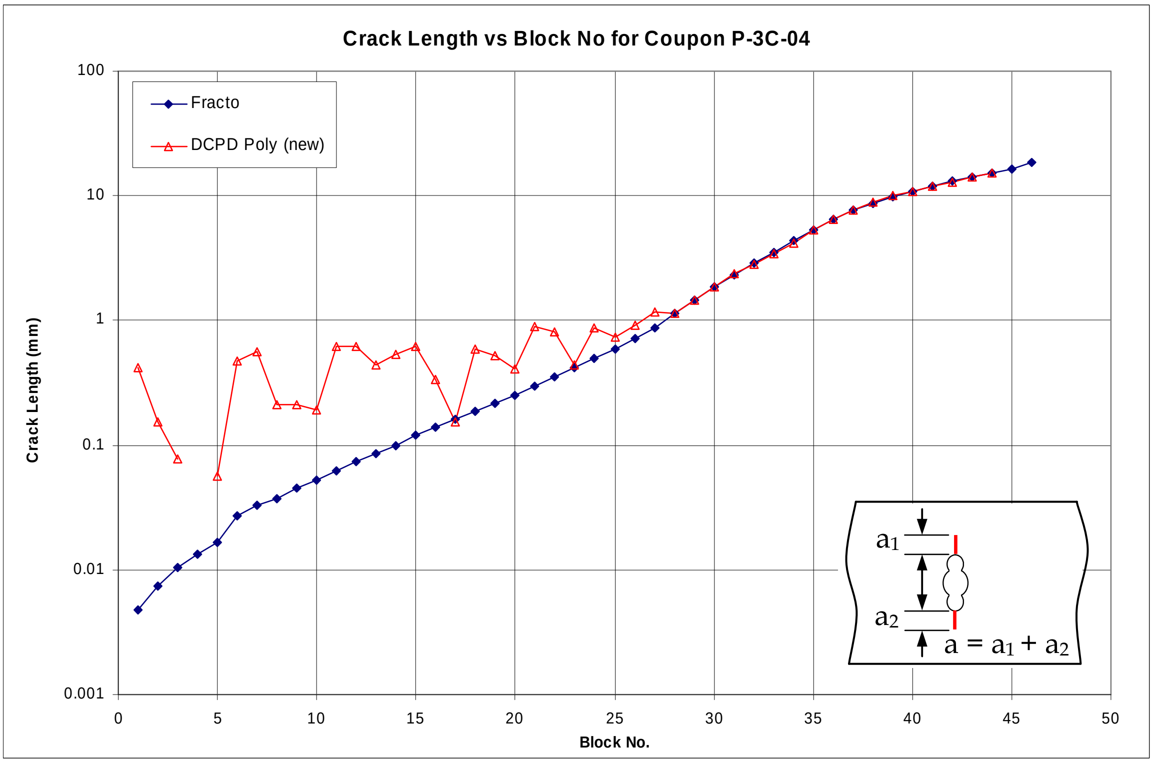


*Figure B. 8: Crack Length versus Block Number for Coupon P-3C-03 (New Poly) – Log Scale*

# Appendix C: Stress Intensity Solution for Ktg = 5 Double Ear Coupon

| Crack Size (inch) | Beta Factor |
|---|---|
| 0.0001 | 2.91 |
| 0.00290625 | 2.27896 |
| 0.00532811 | 2.25689 |
| 0.00823433 | 2.20592 |
| 0.011625 | 2.11709 |
| 0.0178344 | 2.05649 |
| 0.0263682 | 1.94055 |
| 0.0370343 | 1.89306 |
| 0.0498429 | 1.81172 |
| 0.0634315 | 1.7287 |
| 0.0783811 | 1.77695 |
| 0.0936213 | 1.76152 |
| 0.104767 | 1.71826 |
| 0.12143 | 1.66265 |
| 0.147413 | 1.62448 |
| 0.178175 | 1.60052 |
| 0.213716 | 1.57787 |
| 0.252091 | 1.59258 |
| 0.291398 | 1.63224 |
| 0.328806 | 1.69872 |
| 0.368797 | 1.83063 |
| 0.411374 | 1.98067 |

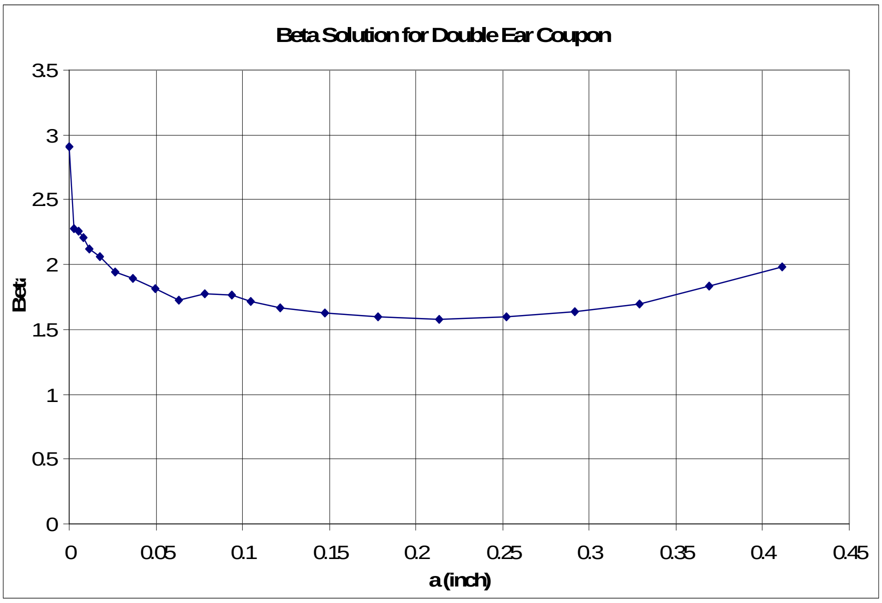

# Appendix D: Coupon Test Program Specimen Design

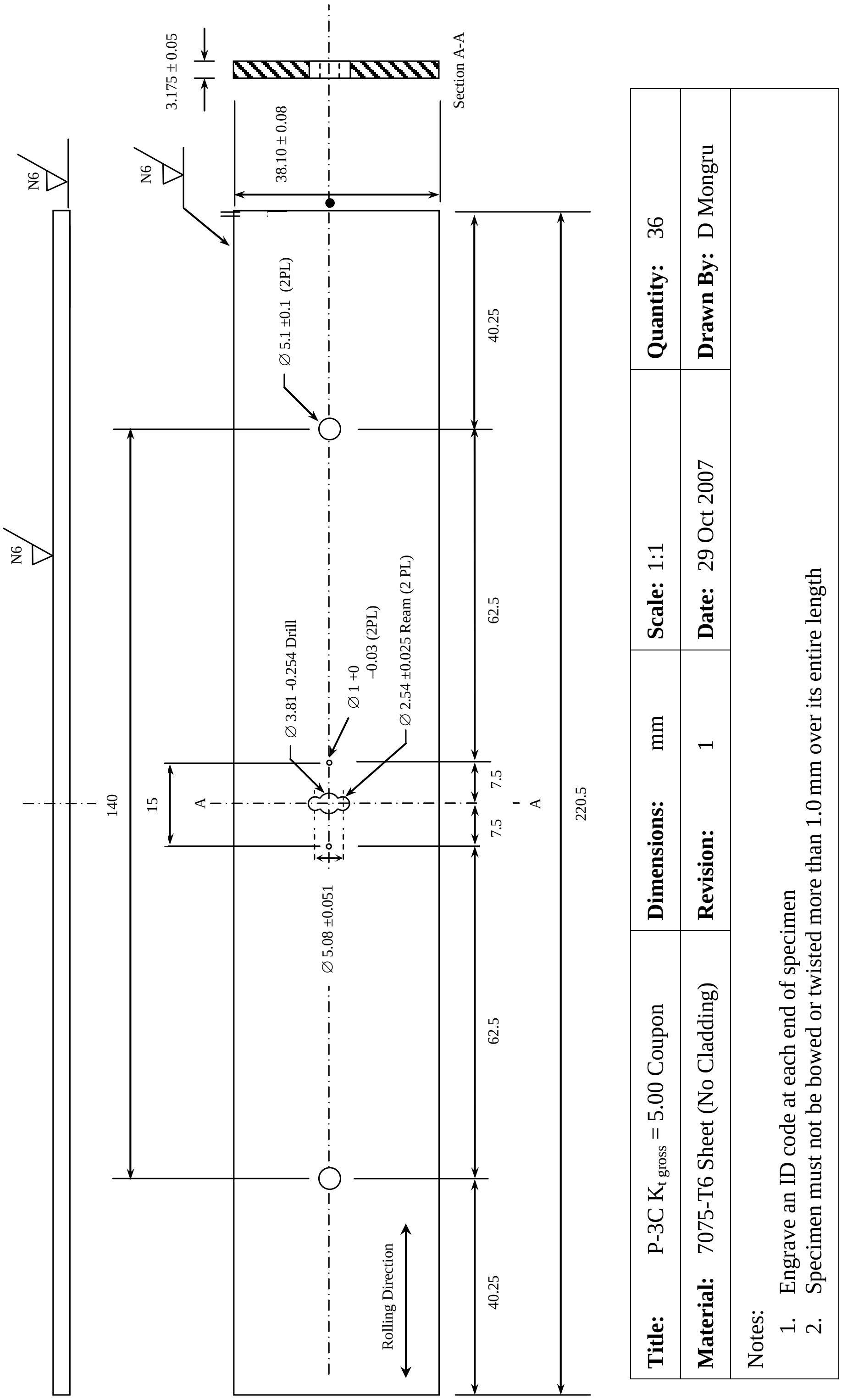


*Figure D-1: Notched Coupon Geometry*

**DEFENCE SCIENCE AND TECHNOLOGY ORGANISATION**
**DOCUMENT CONTROL DATA**

1. PRIVACY MARKING/CAVEAT (OF DOCUMENT)

| 2. TITLE | 3. SECURITY CLASSIFICATION (FOR UNCLASSIFIED REPORTS THAT ARE LIMITED RELEASE USE (L) NEXT TO DOCUMENT CLASSIFICATION) |
|---|---|
| Evaluation of Alternative Life Assessment Approaches Using P-3 SLAP Test Results | Document (U)<br>Title (U)<br>Abstract (U) |

| 4. AUTHOR(S) | 5. CORPORATE AUTHOR |
|---|---|
| David Mongru, Phil Jackson, Kai Maxfield and Chris Wallbrink | DSTO Defence Science and Technology Organisation<br>506 Lorimer St<br>Fishermans Bend Victoria 3207 Australia |

| 6a. DSTO NUMBER | 6b. AR NUMBER | 6c. TYPE OF REPORT | 7. DOCUMENT DATE |
|---|---|---|---|
| DSTO-TR-2418 | AR-014-780 | Technical Report | June 2010 |

| 8. FILE NUMBER | 9. TASK NUMBER | 10. TASK SPONSOR | 11. NO. OF PAGES | 12. NO. OF REFERENCES |
|---|---|---|---|---|
| 2009/1100614 | 07/283 | DGTA | 93 | 22 |

| 13. URL on the World Wide Web | 14. RELEASE AUTHORITY |
|---|---|
| http://www.dsto.defence.gov.au/corporate/reports/DSTO-TR-2418.pdf | Chief, Air Vehicles Division |

15. SECONDARY RELEASE STATEMENT OF THIS DOCUMENT

*Approved for public release*

OVERSEAS ENQUIRIES OUTSIDE STATED LIMITATIONS SHOULD BE REFERRED THROUGH DOCUMENT EXCHANGE, PO BOX 1500, EDINBURGH, SA 5111

16. DELIBERATE ANNOUNCEMENT

No Limitations

17. CITATION IN OTHER DOCUMENTS Yes

18. DSTO RESEARCH LIBRARY THESAURUS http://web-vic.dsto.defence.gov.au/workareas/library/resources/dsto_thesaurus.shtml

Airworthiness standards, fatigue life

19. ABSTRACT
The effect of selecting different airworthiness standards and lifing methodologies on in-service structural life assessments is examined by using the full scale test results from the P-3 Service Life Assessment Program (P-3 SLAP). The effect on structural inspection thresholds and intervals is determined by applying the methods advanced by major international military and civilian airworthiness standards. Different life prediction models are also compared against the P-3 SLAP results and against results from DSTO coupon tests.